



SMART FUNCTIONAL NANOENERGETIC MATERIALS

Overview

2012 Joint Office of Naval Research (ONR)/Air
Force Office of Scientific Research Advanced
Energetic Materials Program Review
7-10 August 2012



AFOSR/MURI

Report Documentation Page

Form Approved
OMB No. 0704-0188

Public reporting burden for the collection of information is estimated to average 1 hour per response, including the time for reviewing instructions, searching existing data sources, gathering and maintaining the data needed, and completing and reviewing the collection of information. Send comments regarding this burden estimate or any other aspect of this collection of information, including suggestions for reducing this burden, to Washington Headquarters Services, Directorate for Information Operations and Reports, 1215 Jefferson Davis Highway, Suite 1204, Arlington VA 22202-4302. Respondents should be aware that notwithstanding any other provision of law, no person shall be subject to a penalty for failing to comply with a collection of information if it does not display a currently valid OMB control number.

1. REPORT DATE AUG 2012	2. REPORT TYPE	3. DATES COVERED 00-00-2012 to 00-00-2012		
4. TITLE AND SUBTITLE Smart Functional Nanenergetic Materials Overview		5a. CONTRACT NUMBER		
		5b. GRANT NUMBER		
		5c. PROGRAM ELEMENT NUMBER		
6. AUTHOR(S)		5d. PROJECT NUMBER		
		5e. TASK NUMBER		
		5f. WORK UNIT NUMBER		
7. PERFORMING ORGANIZATION NAME(S) AND ADDRESS(ES) Purdue University, West Lafayette, IN, 47907		8. PERFORMING ORGANIZATION REPORT NUMBER		
9. SPONSORING/MONITORING AGENCY NAME(S) AND ADDRESS(ES)		10. SPONSOR/MONITOR'S ACRONYM(S)		
		11. SPONSOR/MONITOR'S REPORT NUMBER(S)		
12. DISTRIBUTION/AVAILABILITY STATEMENT Approved for public release; distribution unlimited				
13. SUPPLEMENTARY NOTES				
14. ABSTRACT				
15. SUBJECT TERMS				
16. SECURITY CLASSIFICATION OF:			17. LIMITATION OF ABSTRACT	
a. REPORT unclassified	b. ABSTRACT unclassified	c. THIS PAGE unclassified	Same as Report (SAR)	18. NUMBER OF PAGES 88
				19a. NAME OF RESPONSIBLE PERSON

A Brief History of Nanoenergetic Materials

● 1st Generation

- Nanometer-sized Al powder/conventional propellants
- Some performance gain, variable results

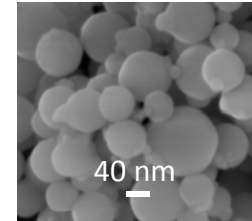
● 2nd Generation

- Coated nanometer-sized metal powders
- Controlled oxidation, improved storage lifetime
- Quasi-ordered nanometer-sized inclusions in energetic matrix
- Cryo-Gel/Sol-Gel processing

● 3rd Generation

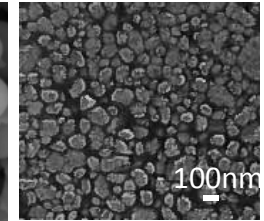
- 3-dimensional nanoenergetics
- Structured/ordered
- Controlled reactivity
- Improved manufacturability/processing

nAl



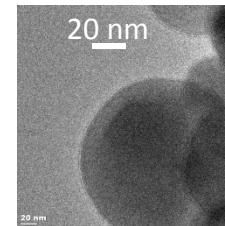
Nanotechnology

RESS nRDX



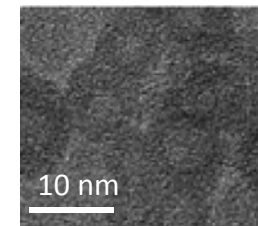
A. Cortopassi, T. Wawiernia, J. T. Essel, P. Ferrara, K. K. Kuo, and R. M. Doherty, 8-ISICP, 2009

L-ALEX



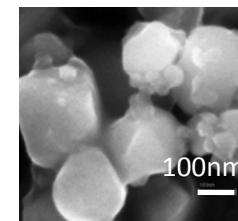
T. Sippel and S.F. Son, TEM of palmitic acid coated ALEX

Fe₀-AOT



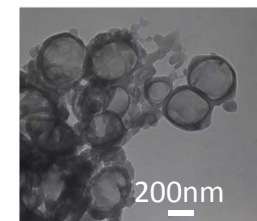
C.E. Bunker and J.J. Karnes, JACS 126, 10852, 2004

Al-C₁₃F₂₇COOH



R.J. Jouet, A.D. Warren, D.M. Rosenberg, V.J. Bellitto, K. Park, and M.R. Zachariah, Chem. Mater. 17 (2005) 2987-2996.

CL-20/NC Cryogel



T. B. Brill, B. C. Tappan and J. Li (2003). MRS Proceedings, 800, AA2.1doi:10.1557/PROC800AA2.1



AFOSR/MURI
August 9, 2012

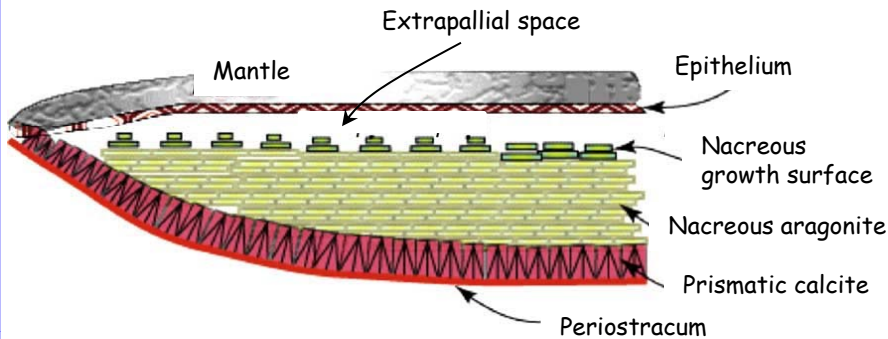
Integrated Multiscale Organization of Energetic Materials

- Many biological and physical objects derive their unique properties through an integrated multilength scale organization of their constituent nano and microscale structures.
- Such multiscaled structures are being exploited to engineer devices such as adhesives mimicking spatulae of a gecko, porous silicon drug delivery systems, to adaptive porous materials that mimic the multifunctionality of bone.
- A common feature in all these structures is that nanoscale units are all integrated into micron to macro scale structures and are accessible as individual modules for rapid response.
- Such design principles are crucial to the goals of our proposed work.



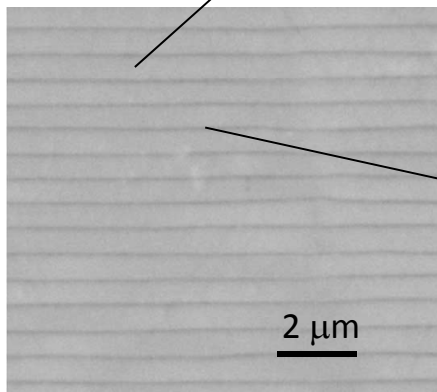
Structure of the Abalone Shell

Abalone Shell



Structure of the nacre:
95 wt.% inorganic material
5 wt.% organic material

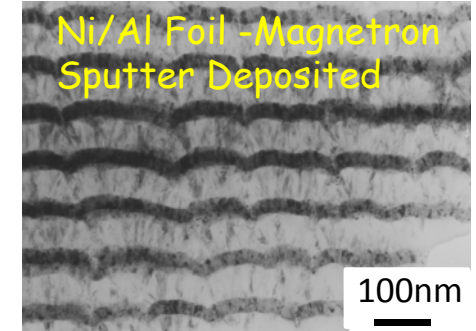
inorganic layers: CaCO_3 - aragonite



organic layers

A. Lin and A. Meyers, *Mat. Sci. Eng. A* 390, 27-41, 2005.

Example of Reactive Material



From Tim Weihs, The Johns Hopkins University

NanoFoil® Properties

Size - thickness	40-150 μm
Composition Before Reaction	Alternating layers of Ni and Al
Composition After Reaction	$\text{Ni}_{50}\text{Al}_{50}$
Foil Density	5.6-6.0 g/cm^3
Heat of Reaction	1050-1250 J/g
Reaction Velocity	6.5-8 m/s
Maximum Temperature	1350°-1500°C
Thermal Conductivity	35-50 W/mK
RoHS Compliant	Pb-free



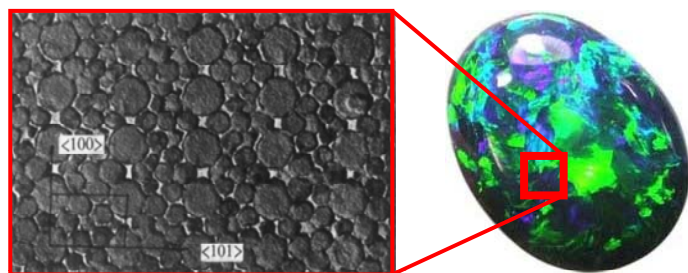
Indium Corporation – formerly Reactive Nanocomposites
<http://www.indium.com/nanofoil/#ixzz1xQC55jc>



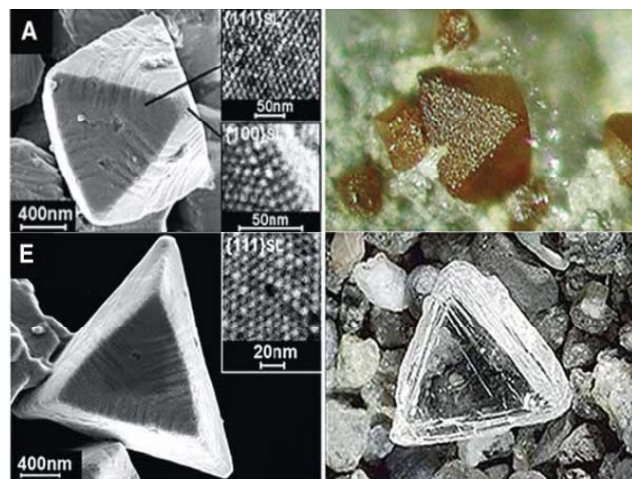
AFOSR/MURI
August 9, 2012

Nanoparticle Self-Assembly

Opel Gem - an example of particle self assembly

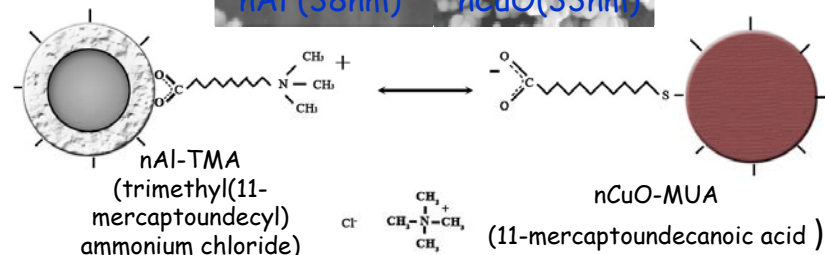
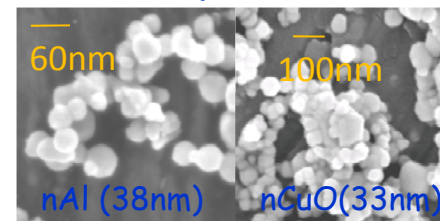


Sanders, J. V., Murray, M. J., *Nature* v275, 1978.

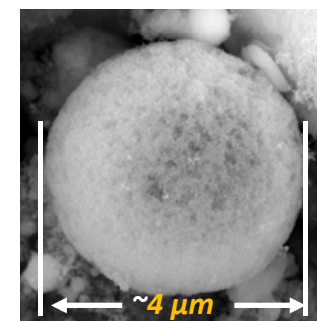


Kalsin, A. M., Fialkowski, M., Paszewski, M., Smoukov, S. K., Bishop, K. J., Grzybowski, B. A., *Science* v312, 2006

Self-Assembled Nanoscale Thermite Microspheres



- Create SAM on surface of individual particles
- Monolayers contain a functionalized group at tail end (either + or - charged)
- When mixed in a diluted and slightly elevated temperature they form macroscale structures with nanoscale constituents



Malchi, J., Foley, T., Yetter, R.A., *ACS Applied Mat. & Interfaces*, 1, 11, 2420, 2009

F. Severac, P. Alphonse, A. Estève, A. Bancaud, and C. Rossi, High Energy Al/CuO Nanocomposites obtained by DNA-Directed Assembly, *Adv. Functional Materials*, 22, 323, 2012

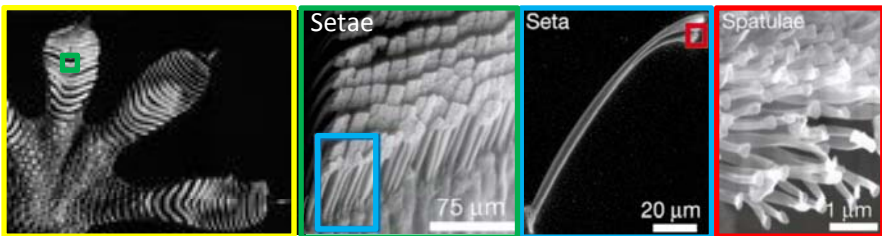


AFOSR/MURI
August 9, 2012

Multiscale Structures

Gecko foot-hair micro/nano-structures

- Compliant micro- and nanoscale high aspect ratio beta-keratin structures at their feet to adhere to any surface with a pressure controlled contact area
- Adhesion is due mainly to molecular forces (van der Waals forces)



Gecko foot

Rows of setae from a toe

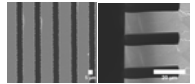
Single seta

Finest terminal branch of seta called spatulae

- Foot hairs start from the micrometer scale (stalks or seta) and go down to 100-200 nm diameter (spatular stalks) by branching.
- Each foot has ~ 500k setae, each 30-130 μm long with 100's of spatular stalks.
- At the ends of the spatular stalks are oriented caps (spatulae) with diameters of 300-500 nm.

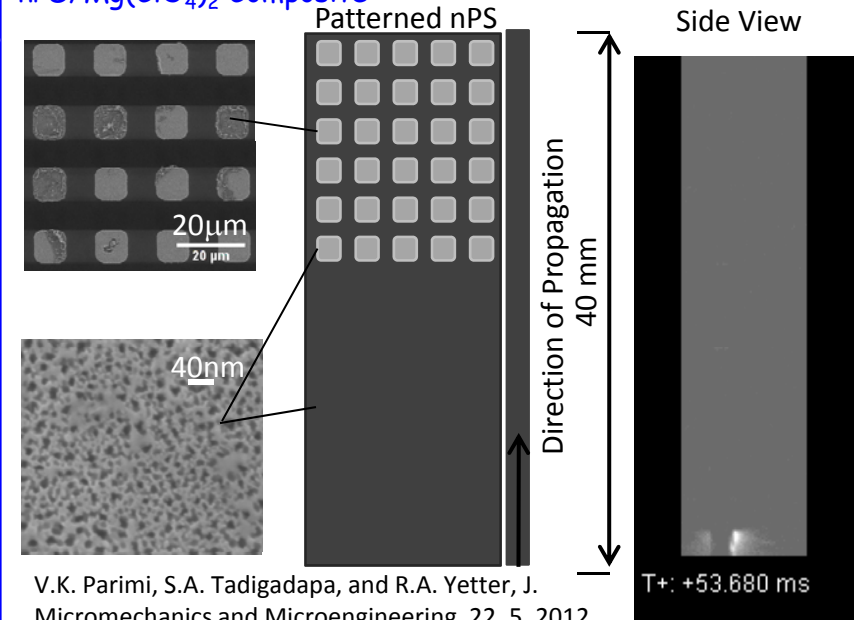
Autumn, K., *et al.*, Nature, 405, 681-684, 2000

Multiscale Energetic Composites Fabricated on pSi Substrates



- Si wafers (highly doped p-type) were photo lithographically patterned using thick layers of photo-resist
- RF RIE process was used to etch pillared structures
- Photo-resist was stripped and nanopores were etched using an electrochemical process
- The pillars were ~ 35 μm tall and have 8 μm square bases separated by ~8 μm. The pore diameters on the pillars and the substrate are ~ 20nm and filled with Mg(ClO₄)₂

Example of Reaction Propagation through Patterned nPS/Mg(ClO₄)₂ Composite



V.K. Parimi, S.A. Tadigadapa, and R.A. Yetter, J. Micromechanics and Microengineering, 22, 5, 2012



AFOSR/MURI
August 9, 2012

Objectives

- Develop new macroscale (micron-sized or larger) energetic materials with nanoscale features that provide *improved performance and ease of processing and handling, managed energy release, reduced sensitivity, and potential for internal/external control and actuation.*
- Obtain fundamental understanding of the relationship between the integrated multi-length scale design of newly developed energetic materials and their reactive and mechanical behaviors.



Critical Technology Issues

- Supramolecular chemistry and integrated multiscale organization of energetic materials have lagged far behind chemistries in other disciplines (such as pharmaceuticals, microelectronics, microbiology).
- There is no fundamental understanding of what type of nano and micron scale hierarchical structures provide desirable performance in combustion, mechanical, and hazard characteristics.



AFOSR/MURI
August 9, 2012

Probing Questions

- How can we make smaller length scale materials?
- In what form can they be assembled to be utilized effectively?
- What are the desirable shapes and sizes of the nanostructures?
- What structures allow us to control the rate of energy release over a wide range of conditions?
- What structures allow us to control ignition criteria
- What structures lead to reduced sensitivity?
- What structures lead to focused or directional energy release?
- Can the structures be made to be responsive, smart?
- How best to couple the output of the nanoenergetics to usable functions?



AFOSR/MURI
August 9, 2012

An Integrated, Systematic Approach

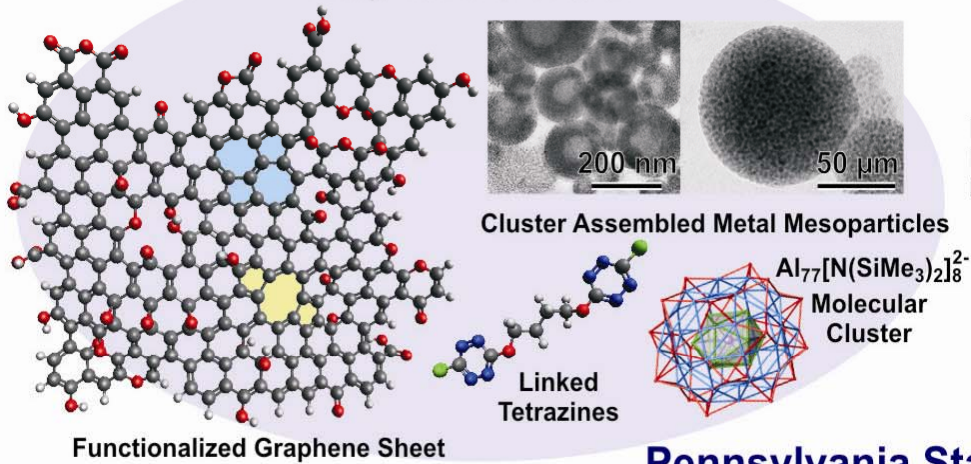
- Four major inter-related areas:
 - (a) processing of nanoenergetic materials such as metal nanoclusters and graphene
 - (b) multiscale processing to enable the insertion of nanoenergetic materials into larger units - bottom-up approach, and comparison to top-down approaches
 - (c) atomistic to mesoscale modeling and design, and
 - (d) experimental analysis and performance characterization for propulsion.



Program Organization

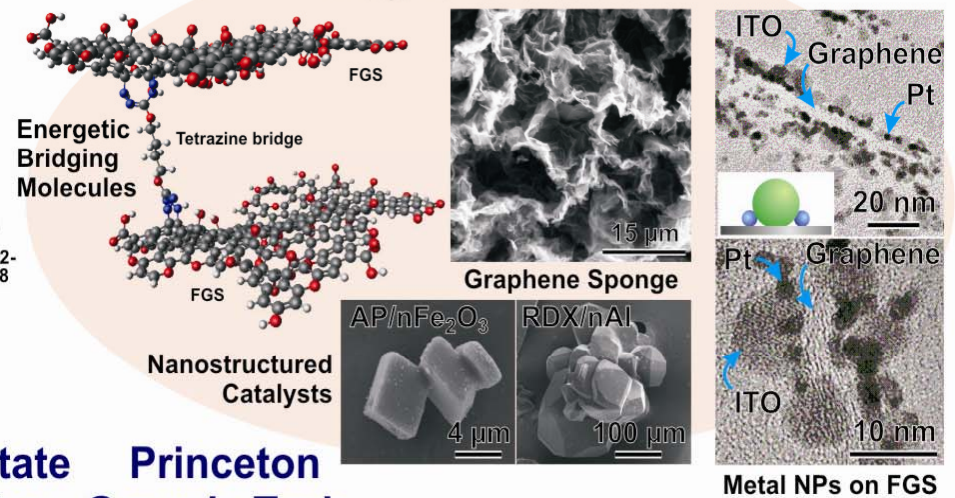
(a) Processing Nanoenergetic Materials

Aksay, Eichhorn, Zachariah

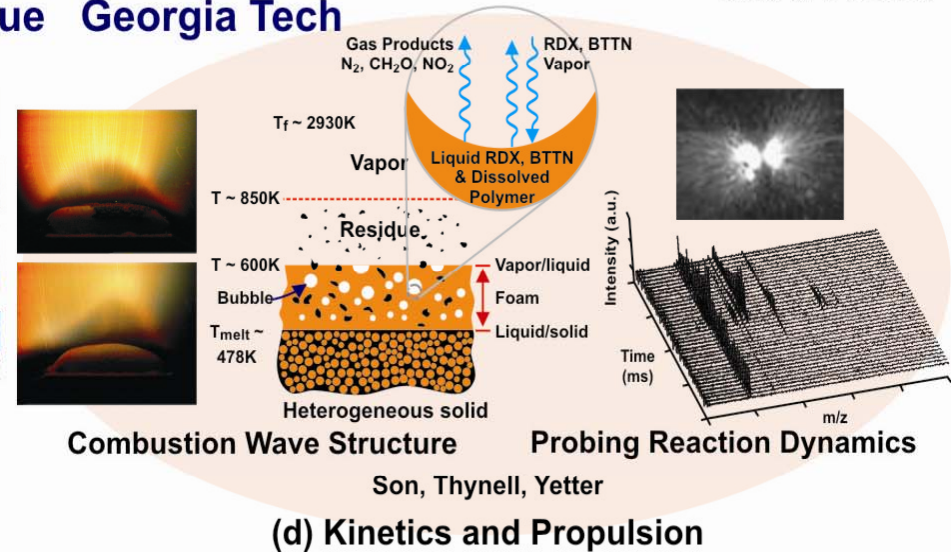
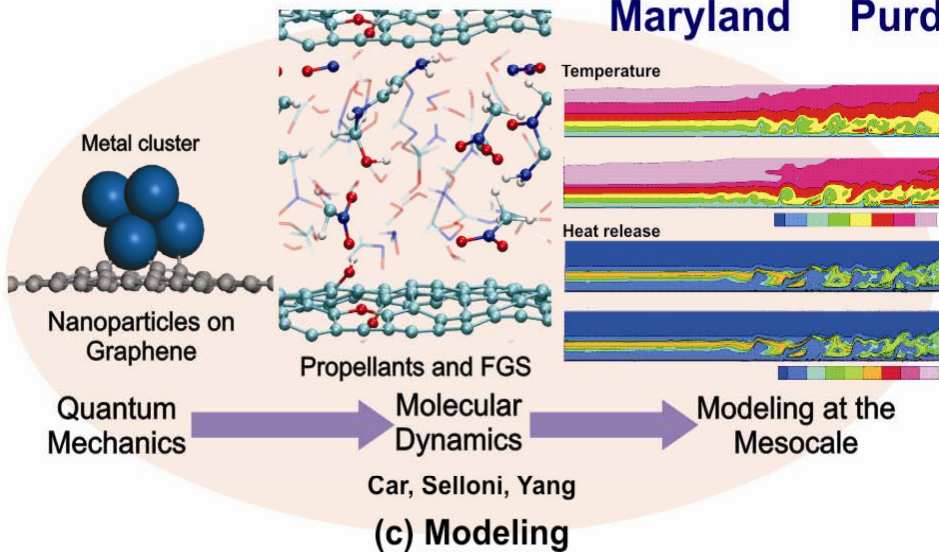


(b) Multiscale Processing

Aksay, Eichhorn, Zachariah



Pennsylvania State University
Maryland
Purdue University
Princeton University
Georgia Tech



AFOSR/MURI
August 9, 2012

Materials Research Emphasis

- Bottom up approaches boosting the energetics of functionalized graphene using the addition of nitrogen via chemisorption of nitrogen-containing molecules and/or replacing carbon atoms in the network with nitrogen atoms
- Metal-based cluster composites with energetic organic ligands (such as high nitrogen molecules)
- Decorated graphene with nano metal-based composites
- Analogous systems produced through top down approaches via porous materials and encapsulation.



Impact

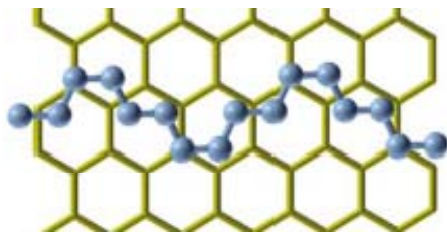
- New storable energetic propellants, additives, or catalysts to achieve on-demand, on-time, tailorable, and affordable propulsion and munition capabilities not currently available.
- Methodologies to create smart and functional nanoenergetics for incorporation into various systems ranging from MEMs devices to rocket propellants to explosives that permit new functions to be performed ultimately enhancing the performance of the system.



Example of polymeric nitrogen chains in a graphene matrix as a nanoenergetic material

Abou-Rachid, H., et al., *Phys. Review Letters*, 100, 196401, 2008. Christe, K.O., *PEP* 32, 3, 2007, 194. T. Manning, A. Lahamer and Z. Iqbal, Electrochemical Functionalization of Carbon Nanotubes with Nitrogen Clusters, *9-ISICP*, July 2012

- High nitrogen material of interest because of large energy difference between single N-N or double N=N and triple N≡N bonds.
- Potential to stabilize polymeric nitrogen in carbon based materials (Timoshevskii et al., *Phys Review B* 80, 115409, 2009)



Examples of conventional propellant performance with small quantities of graphene nitrogen composite additives (examples have not been optimized for performance)

Propellant	Isp (s)	Condensed Phase Products
Baseline AP/HTPB (85wt% AP / 15wt% HTPB)	243	None
AP/HTPB/G-N(C/N~1.25) (Baseline AP/HTPB with 6wt% G-N)	252	None
Baseline AP/HTPB/Al (68wt% AP / 12wt% HTPB / 20wt% Al)	265	0.101% Al ₂ O ₃
AP/HTPB/Al/G-N(C/N ~1.25) (Baseline AP/HTPB/Al with 6wt% G-N)	267	0.09% Al ₂ O ₃

Future non-metalized propellants that approach performance of current metalized propellants



AFOSR/MURI
August 9, 2012

Participating MURI Team Members

- Ilhan A. Aksay, Chemical and Biological Engineering, Princeton University (iaksay@princeton.edu)
- Roberto Car, Chemistry, Princeton University (rcar@princeton.edu)
- Bryan Eichhorn, Chemistry and BioChemistry, University of Maryland (eichhorn@umd.edu)
- Annabella Selloni, Chemistry, Princeton University (aselloni@princeton.edu)
- Steven F. Son, Mechanical Engineering, Purdue University (sson@purdue.edu)
- Stefan T. Thynell, Mechanical and Nuclear Engineering, The Pennsylvania State University (thynell@psu.edu)
- Vigor Yang, Aerospace Engineering, Georgia Institute of Technology (vigor@gatech.edu)
- Richard A. Yetter, Mechanical and Nuclear Engineering, The Pennsylvania State University (rayetter@psu.edu)
- Michael R. Zachariah, Mechanical Engineering and Chemistry, University of Maryland (mrz@umd.edu)



Program Interactions

- Thomas M. Klapötke (Visiting Professor, UMD)
- Alex Gash and Thomas Lagrange (LLNL)
- Dave Adams and Robert Reeves (SNL)
- Chris Bunker (AFRL, Propulsion Directorate, Wright-Patterson Air Force Base)
- Seeking collaborations with other government research laboratories and scientists



AFOSR/MURI
August 9, 2012

Meeting Presentations

- **10:45-10:55 MURI Program Overview**
Rich Yetter, Pennsylvania State University
- **10:55-11:25 Metallic Clusters, Mesoscopic Aggregates, and their Characterization**
Bryan Eichhorn/Mike Zachariah, University of Maryland
- **11:25-11:55 Graphene as a Reactive Material and Carrier of Energetic Materials**
Ilhan Aksay/Annabella Selloni, Princeton University
- **11:55-12:15 Decomposition, Ignition, and Combustion Studies on Nanoenergetic Composite Ingredients and Mixtures**
Steve Son, Purdue University/Rich Yetter, Pennsylvania State University



AFOSR/MURI
August 9, 2012



Metallic Clusters, Mesoscopic Aggregates and their Reactive Characterization

Bryan Eichhorn and Michael R. Zachariah



MURI: SMART FUNCTIONAL NANOENERGETIC MATERIALS



AFOSR/MURI

It Is Well Known That Going Smaller Results In Faster Chemistry

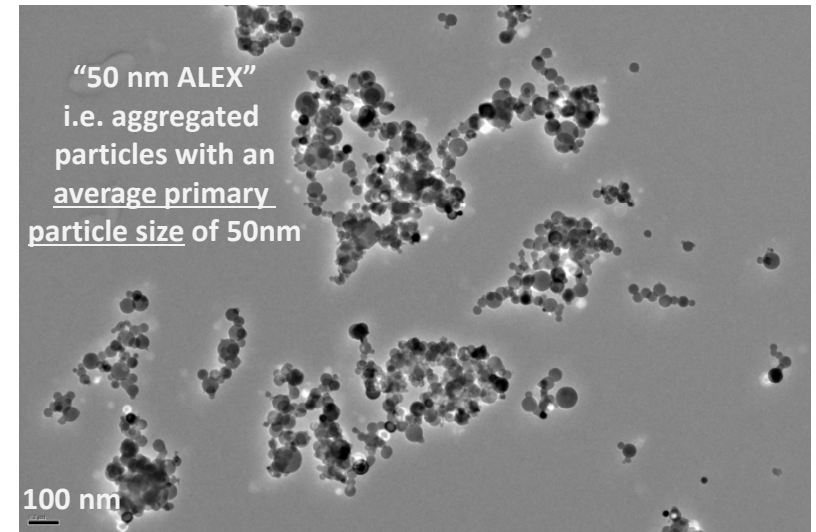
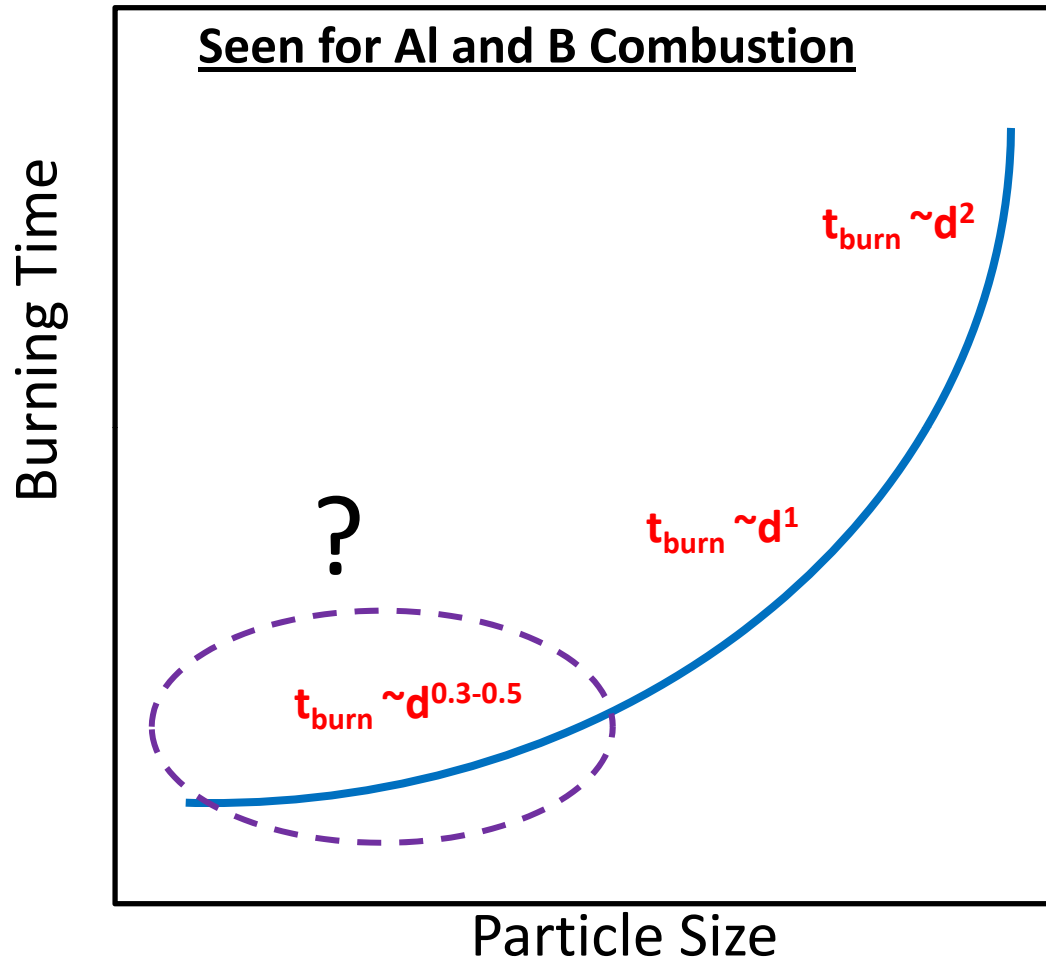
However this poses two challenges:

- a. How can we make smaller length scale materials ?
- b. In what form can they be assembled to be utilized effectively?



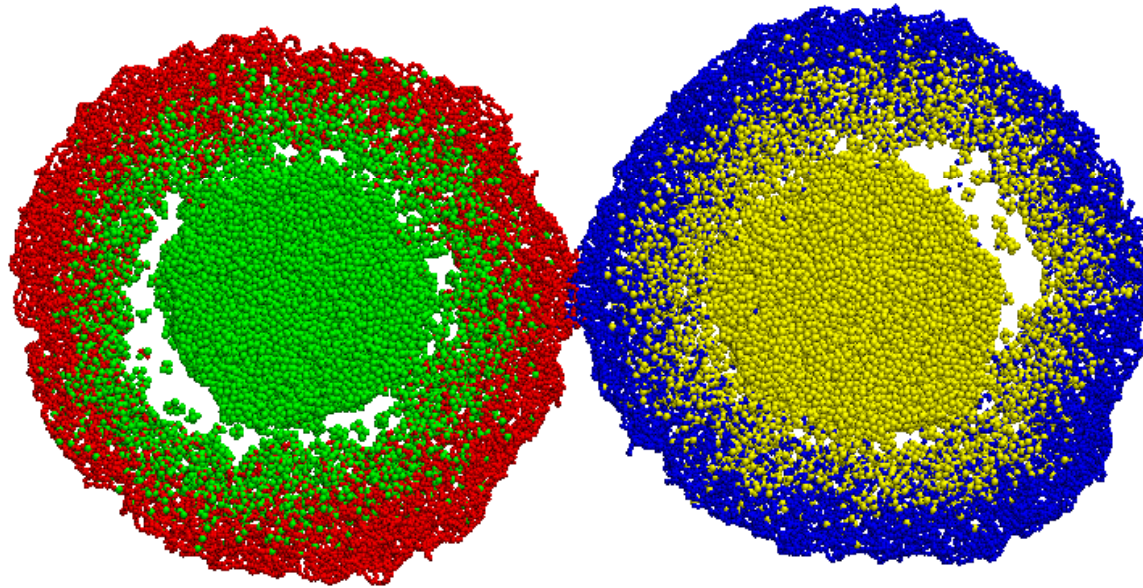
AFOSR/MURI
August 9, 2012

Going smaller helps, but it appears not as much as it should !



AFOSR/MURI
August 9, 2012

Sintering of 16 nm core with 2 nm oxide coating



Green/Yellow – core Al atoms
Red/Blue – shell atoms (both Al and O)
Total ~ 400,000 atoms (8nm particles)

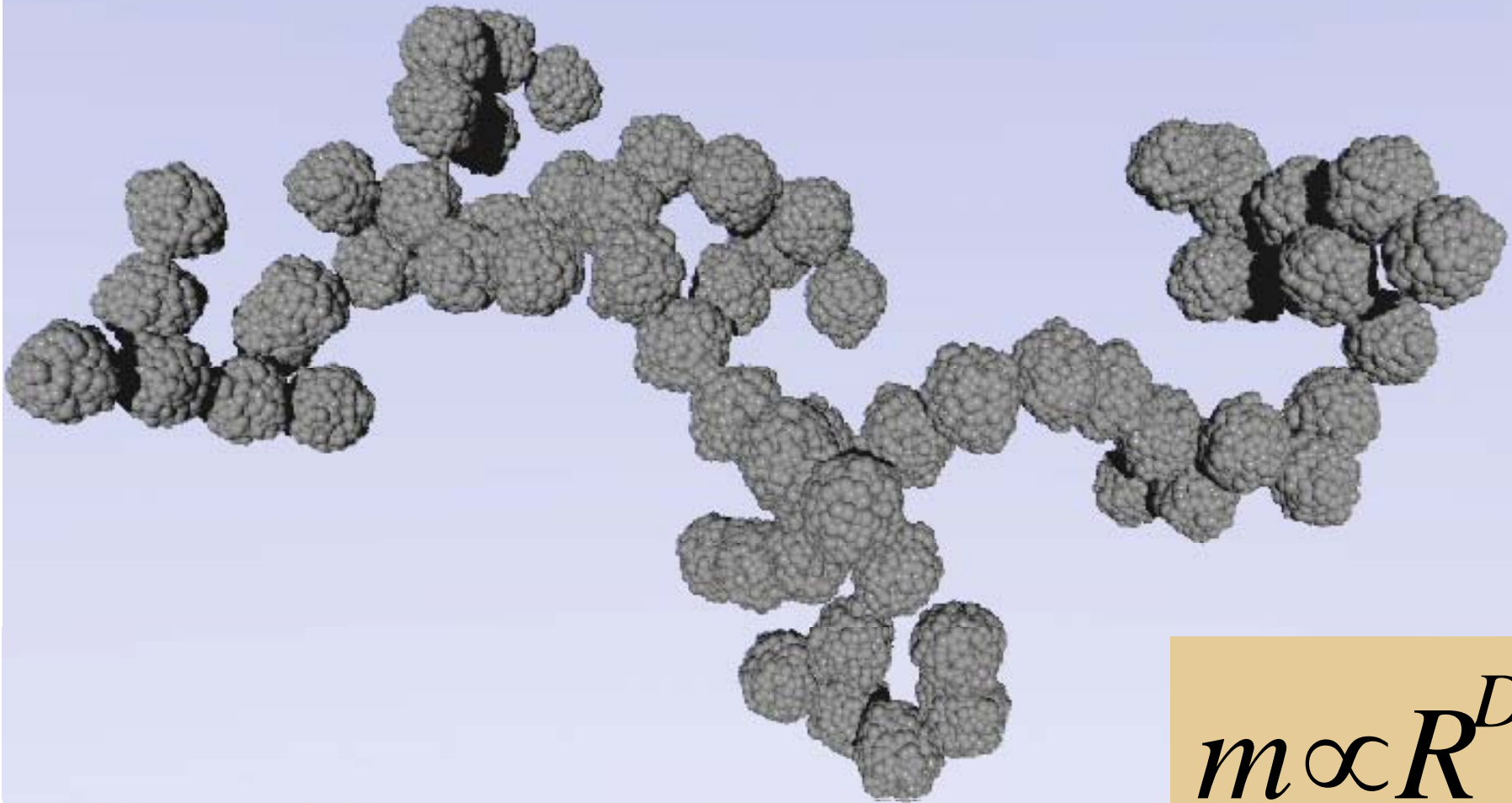
- Two particles are heated from 500 K to 2000 K @ 10^{13} K/s

Temperature is subsequently held at 2000 K



AFOSR/MURI
August 9, 2012

Fractal Aggregate ($D_f = 1.9$)



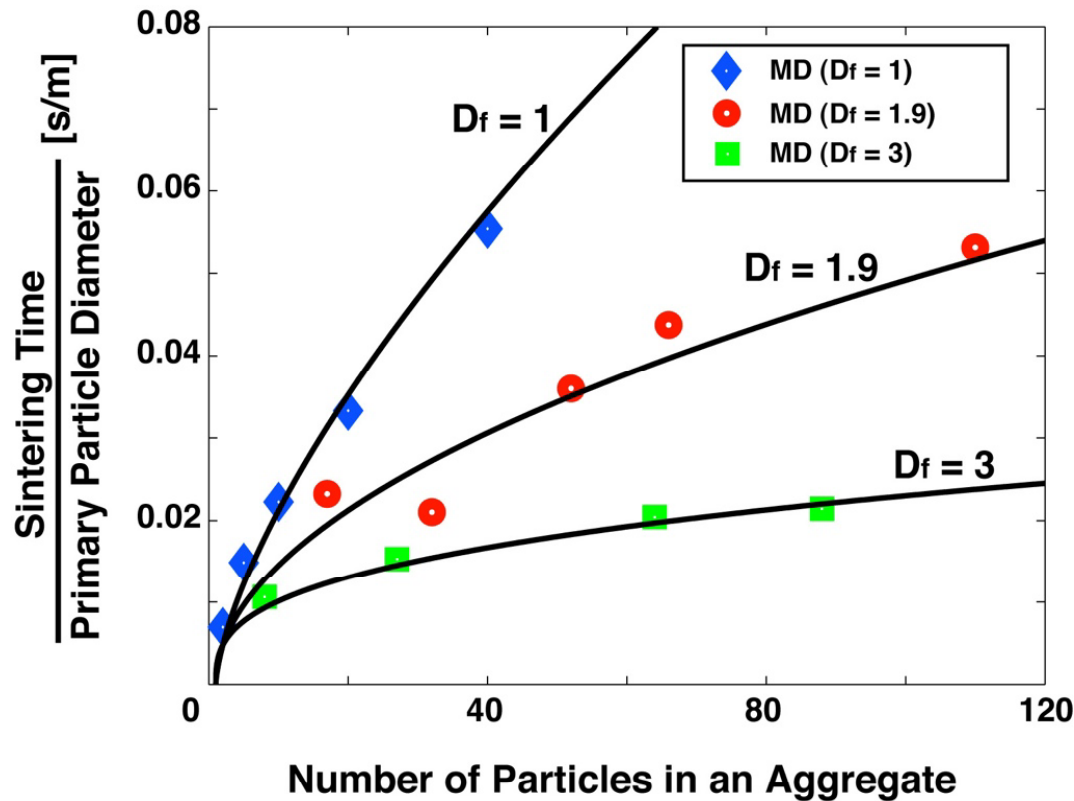
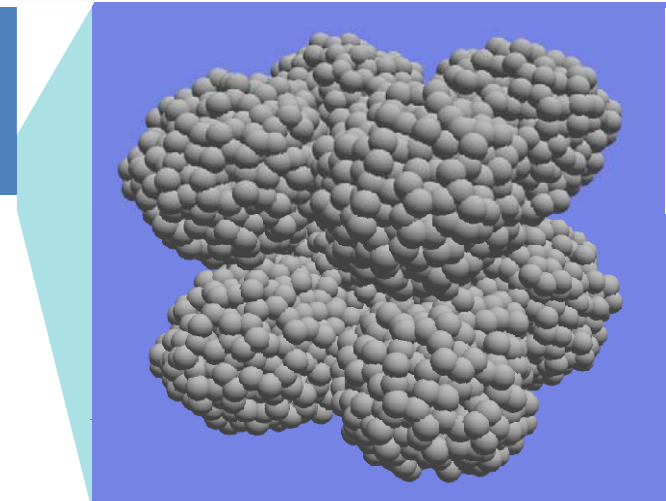
$$m \propto R^{D_f}$$

Sintering time for Fractal Aggregate

Fractal Dimension, D_f

$$m \propto R^{D_f}$$

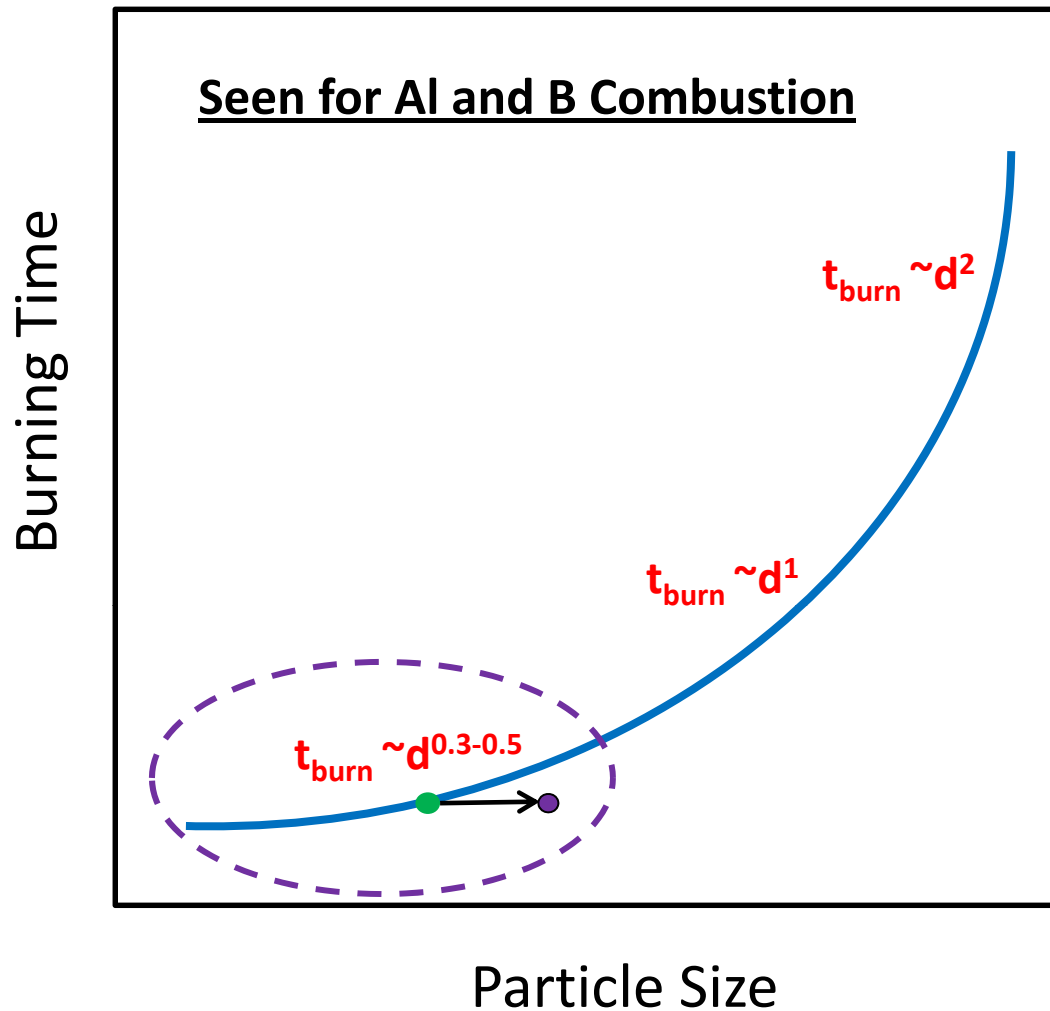
$D_f = 1$: wire
 $D_f = 1.9$: aerosol aggregates
 $D_f = 3$: compact



$$t = \frac{\eta d_p}{\sigma} (N-1)^{0.68^{D_f}}$$



AFOSR/MURI
 August 9, 2012



Sintering of Fractal Aggregates

$$t = \frac{\eta d_p}{\sigma} (N-1)^{0.68^{D_f}}$$

Example:

$$D_f = 1.8$$

$$d_p = 50 \text{ nm}$$

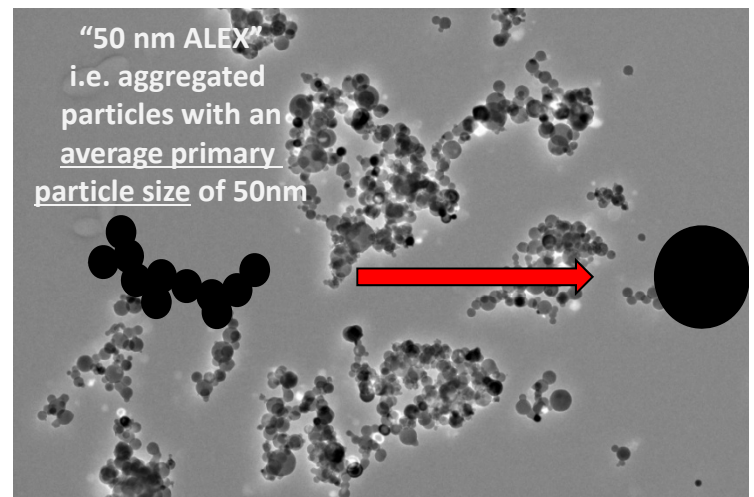
$N = 100$ primary particle in agg.

Fusion time + heating time $< 15 \mu\text{s}$

Characteristic Reaction Time = $10 \mu\text{s}$,
an experimentally-measured pressure
rise time

An aggregate of 100, 50 nm primaries when
sintered yields a 230 nm sphere.

Characteristic pressurization time \sim Sintering time.



This is Bad News:

These results imply that simply going smaller has diminishing returns because sintering (i.e. loss of surface area) competes with reaction.

i.e. Sintering times and Reaction times are sufficiently close that the nanostructure is lost before it can be effectively utilized.

We need an approach that enables us too:

1. Go to smaller length scales.
2. Disables sintering

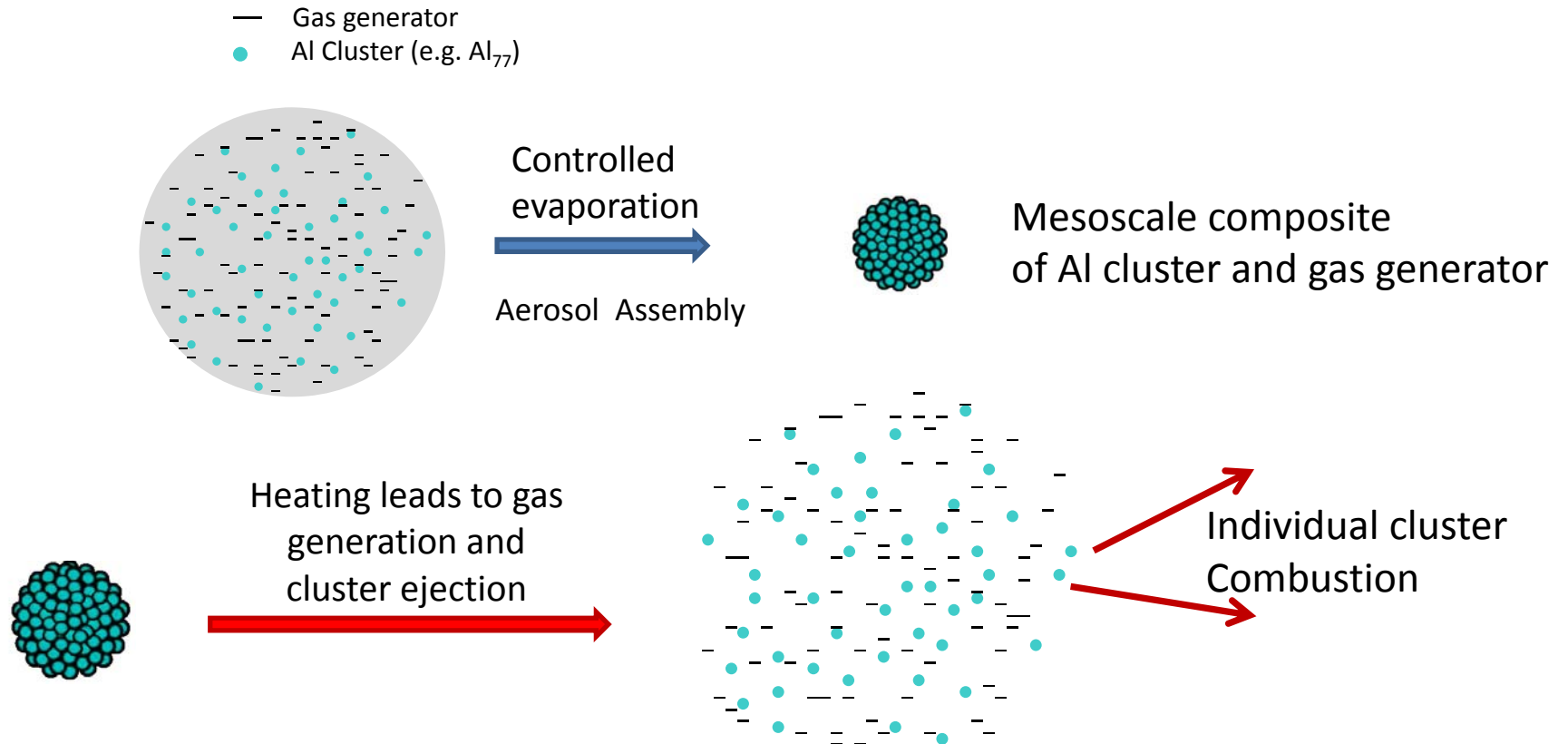


AFOSR/MURI
August 9, 2012

Strategy for this Project:

Develop a mesoparticle comprised of ultra-small nanostructures that can be rapidly disassembled releasing highly reactive nanostructures.

1. Develop very small energetic clusters < 2 nm that are surface passivated.
2. Assemble these clusters into a meso-scale particle with gas generators.
3. Study and optimize mesoparticle disassembly and cluster combustion.



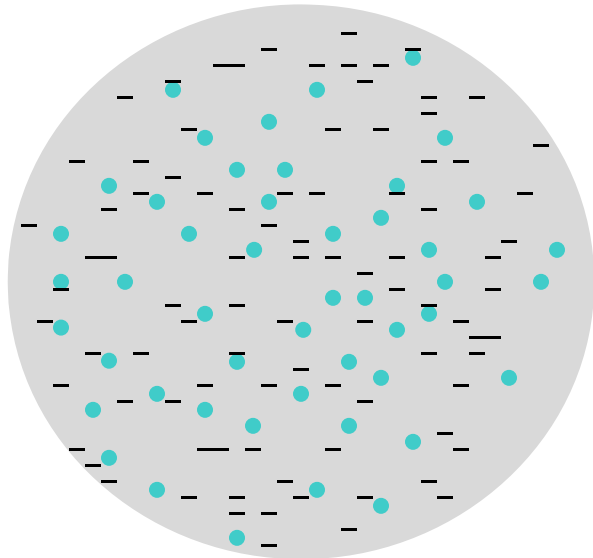
Aerosol-Based Self-Assembly: *A bulk manufacturing process.*

Atomizer containing clusters dispersed in solvent



Spray containing droplets

- Gas generator
- Al Cluster (e.g. Al₇₇)

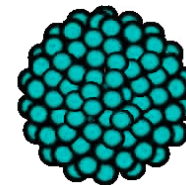


Mesoscale composite
of Al cluster and gas generator

Controlled evaporation

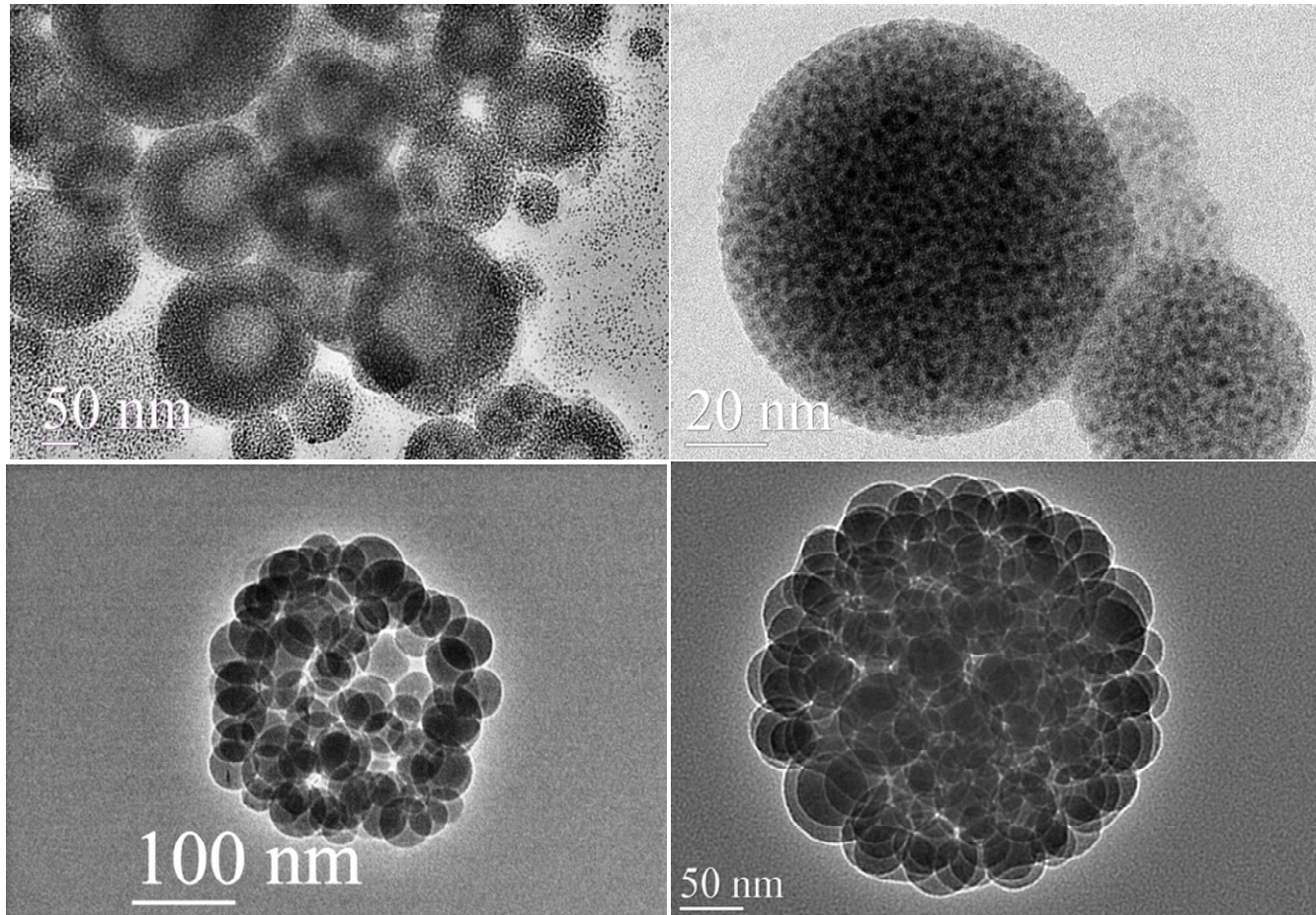


Aerosol Assembly



AFOSR/MURI
August 9, 2012

Proof of Principle: Aerosol-Based Self-Assembly

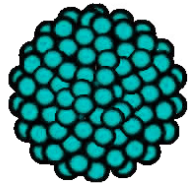


TEM images of hollow and compact structured Fe_3O_4 (A and a) and SiO_2 (B and b) assemblies

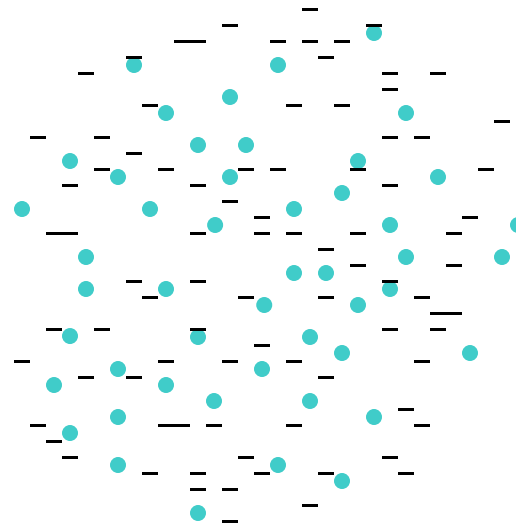


AFOSR/MURI
August 9, 2012

Disassembly



Heating leads to
gas generation and
cluster ejection



AFOSR/MURI
August 9, 2012

Characterization of Disassembly and Reactivity

- T-Jump TOF Mass Spectrometry
- Rapid Heating e-Microscopy
- ion-mobility spectrometry

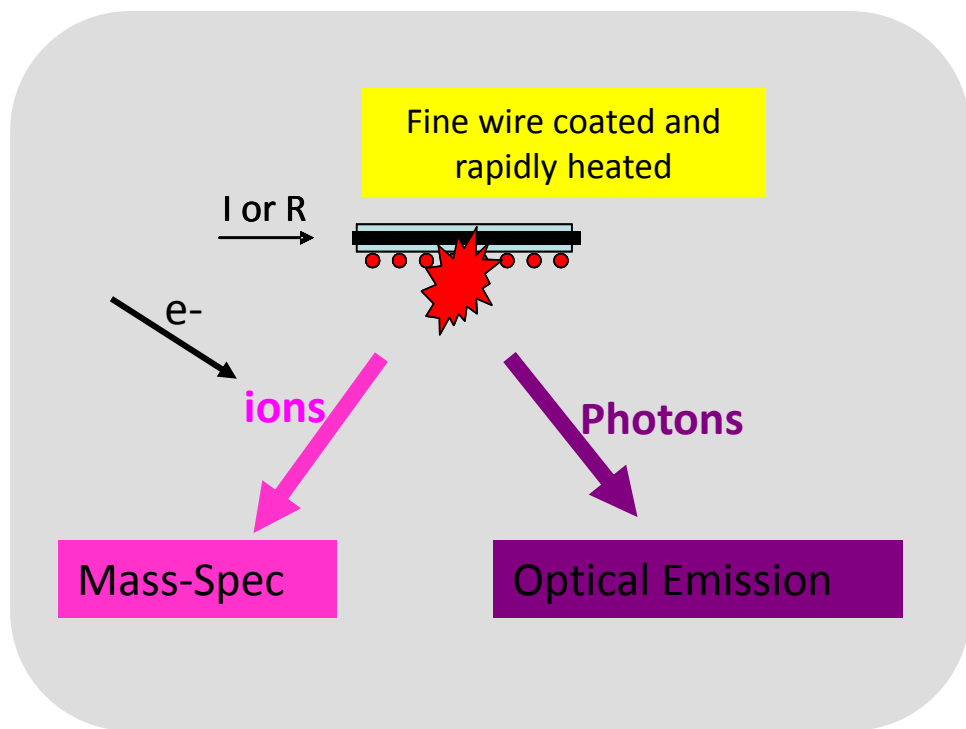


AFOSR/MURI
August 9, 2012

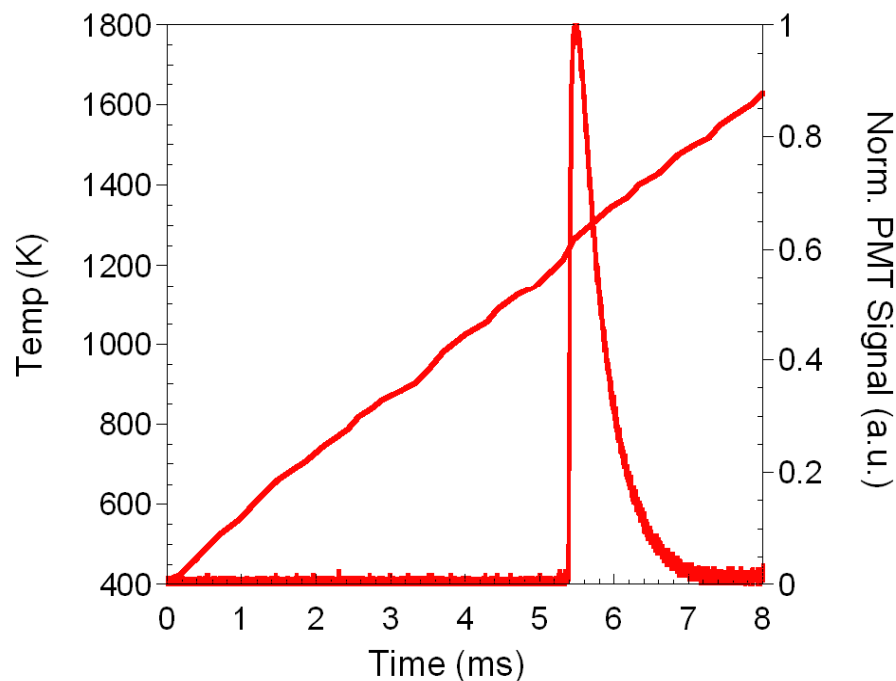
How to characterize the reactivity of a Mesoparticle?

T-Jump Mass Spectrometry/Optical Emission

Basic Approach:

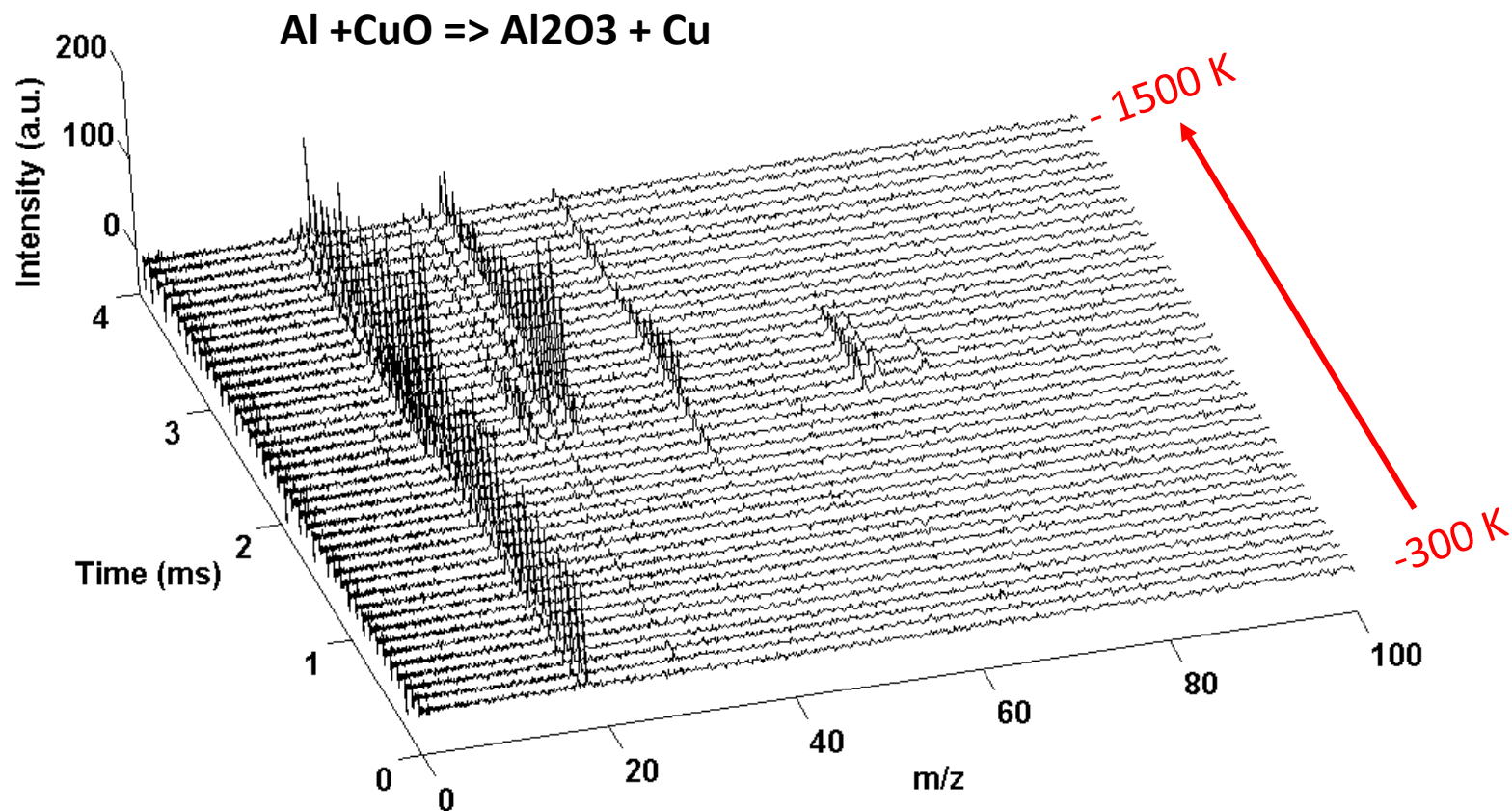


Example of heating rate of 1.7×10^5 C/s



Time Resolved Mass-Spectrum

Stoichiometric Al/CuO- one spectrum every 100 μ s.



Al/CuO nanocomposite under heating rate 8.8×10^5 K/s

Zhou *et al.*, J. Physical Chemistry C. 114, 14269 (2010)



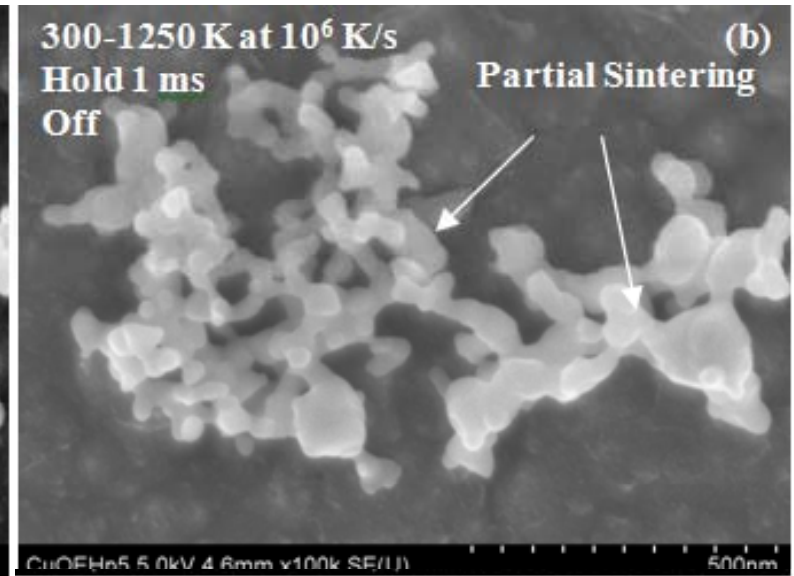
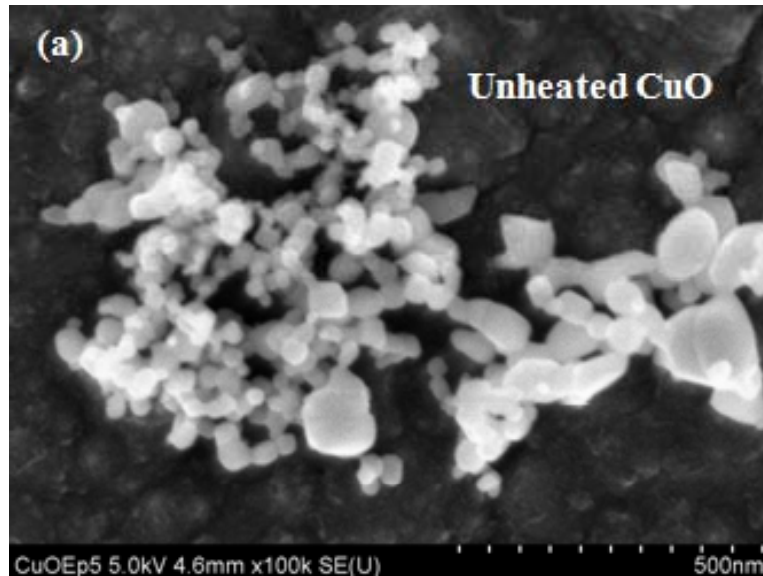
AFOSR/MURI
August 9, 2012

Rapid Heating Microscopy

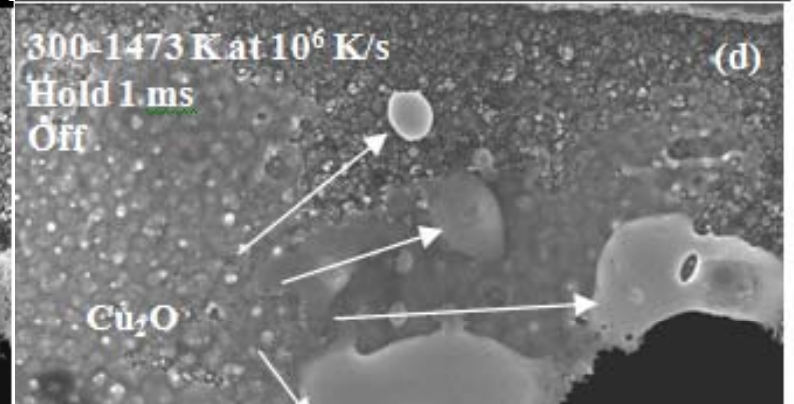
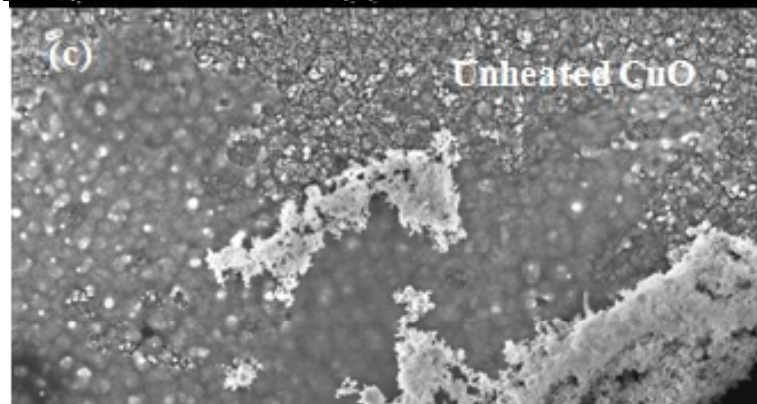
Before

After

300 => 1250K



300 => 1473K

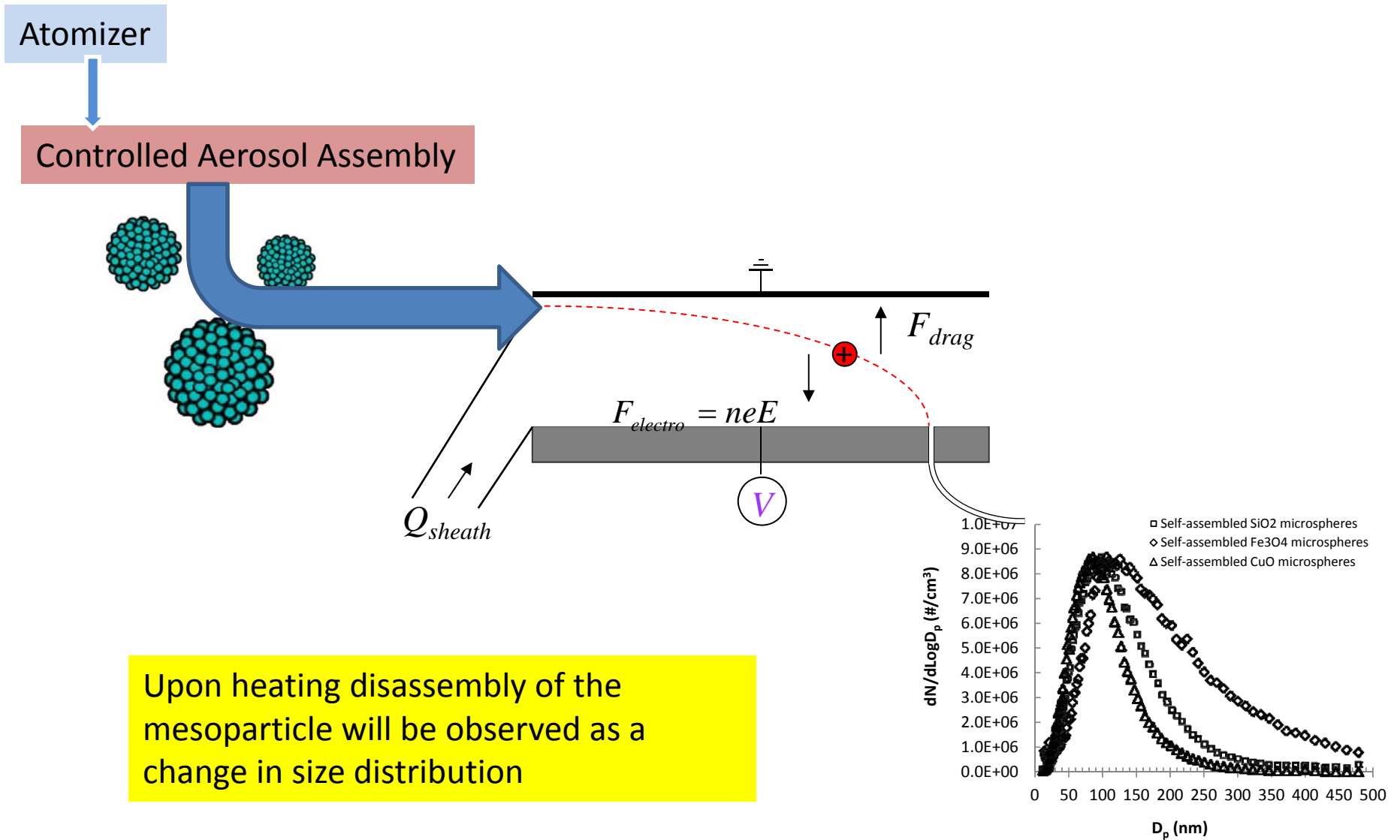


The ability to use heating rate of up to 10^6 K/sec will offer the ability to observe mesoparticle disintegration and subsequent reaction



AFOSR/MURI
August 9, 2012

Ion-mobility Characterization of Assembly - Disassembly



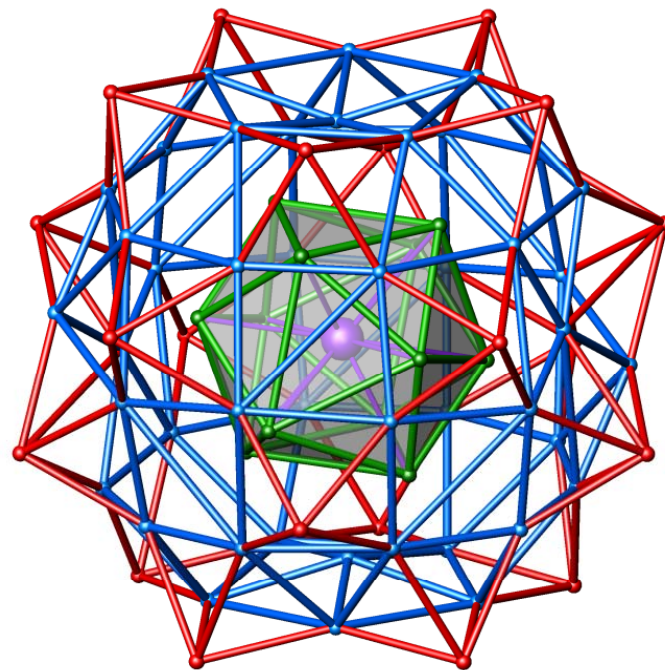
Upon heating disassembly of the mesoparticle will be observed as a change in size distribution

Size distributions of Fe₃O₄, SiO₂ and CuO self-assembled mesospheres



What are the components of the mesoparticle

E.g. Al₇₇

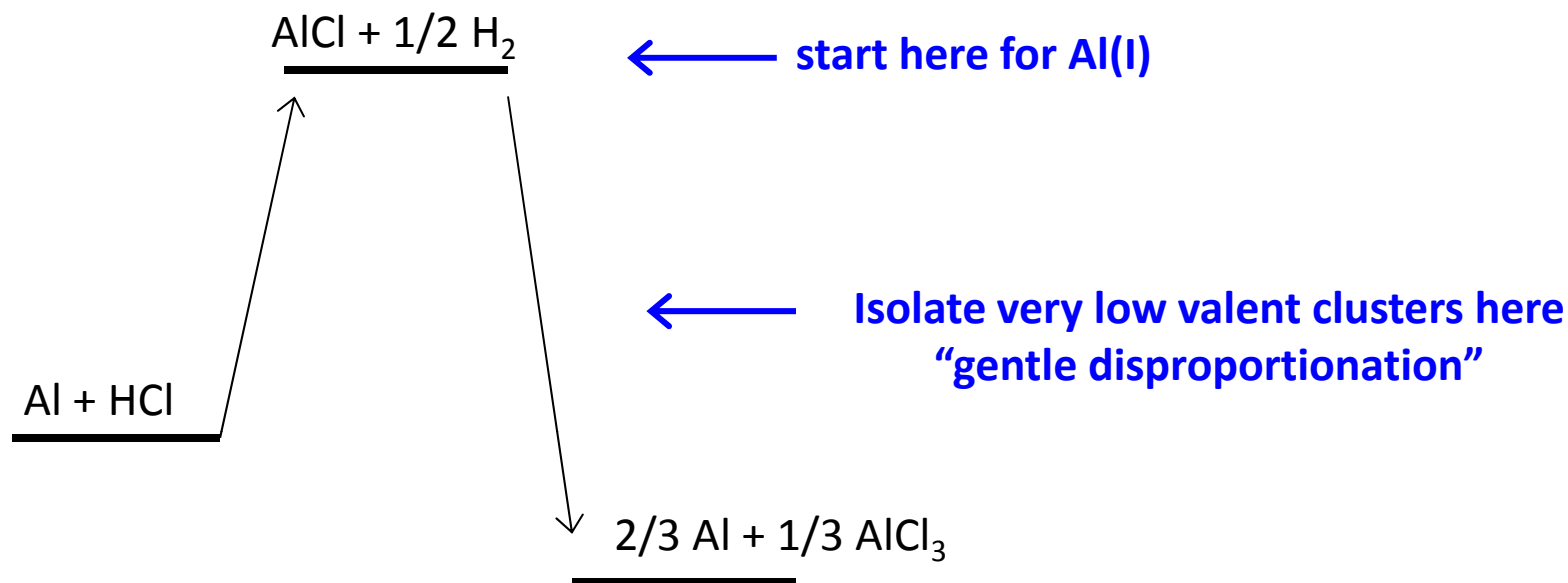


~ 1 nm



AFOSR/MURI
August 9, 2012

Schnöckel Concept In Aluminum Cluster Chemistry

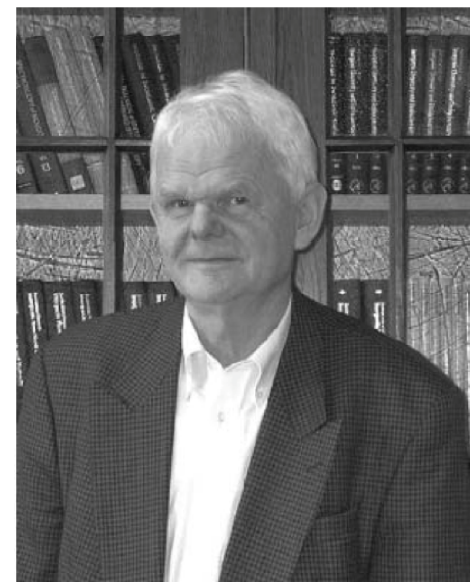


Metalloid Al Clusters: contain more M-M bonds than M-L bonds
- the interface between very large clusters and small nanoparticles

Al metalloid clusters have low oxidation states (< 1) with metallic cores.

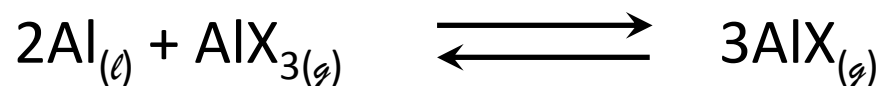
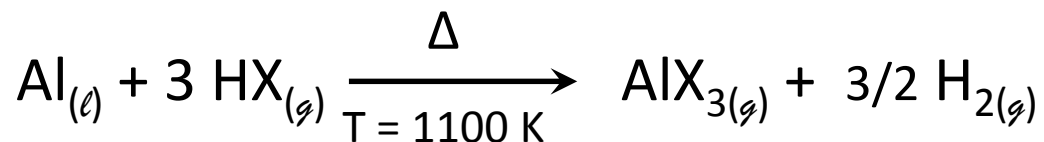
Clusters are protected by ligands and particles sizes are less than 2 nm

Schnöckel, H. "Structures and Properties of Metalloid Al and Ga Clusters"
Chem Rev., **110**, 4125 (2010)

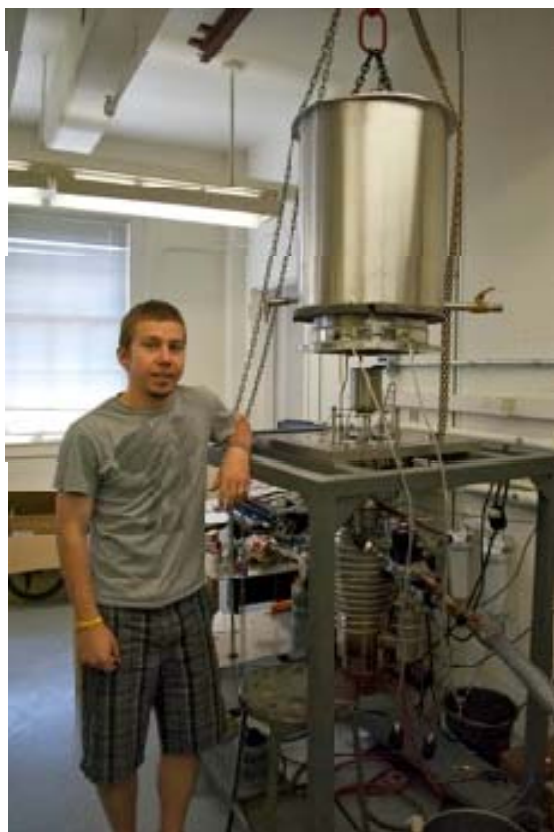


H. Schnöckel

AIX Precursors from Gas Phase Condensation



X = Cl, Br, I



The Schnöckelator!

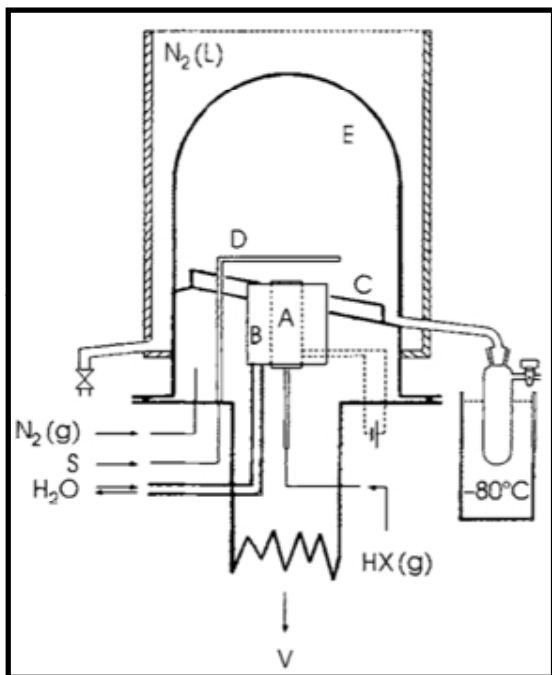
- Modeled after H.G. Schnöckel's co-condensation reactor in Karlsruhe, Germany
- Constructed by Kit Bowen (Johns Hopkins) with funding from DTRA, NSF and AFOSR support
- Collaborators: Schnöckel, Bowen, and IHD scientists – Lightstone, Horn, Stoltz, Mayo

Dohmeier *et. al.* *Angew. Chem. Int. Edit.* **1996**, 35, 2, 129-149

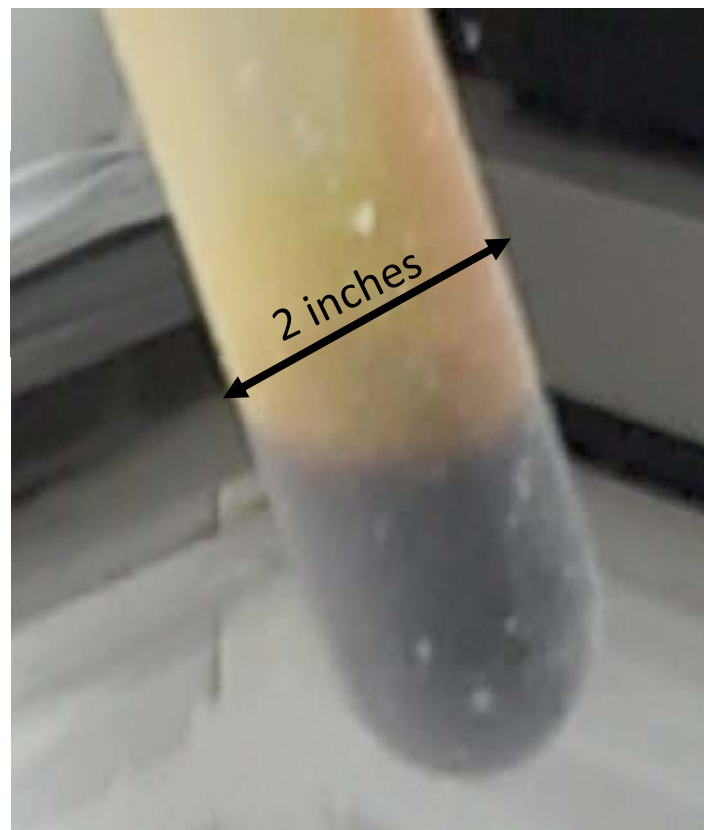


AFOSR/MURI
August 9, 2012

AIX precursors (X = Cl, Br, I)



- A. Graphite block containing Al
- B. Cooling block
- C. Drainage channel
- D. Solvent inlet
- E. Stainless deposition surface

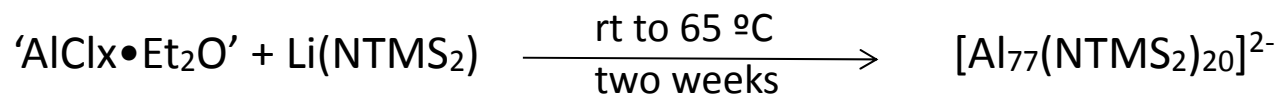


~60 mmol AIX generated in 3 hours
Metastable AIX can be stored for weeks



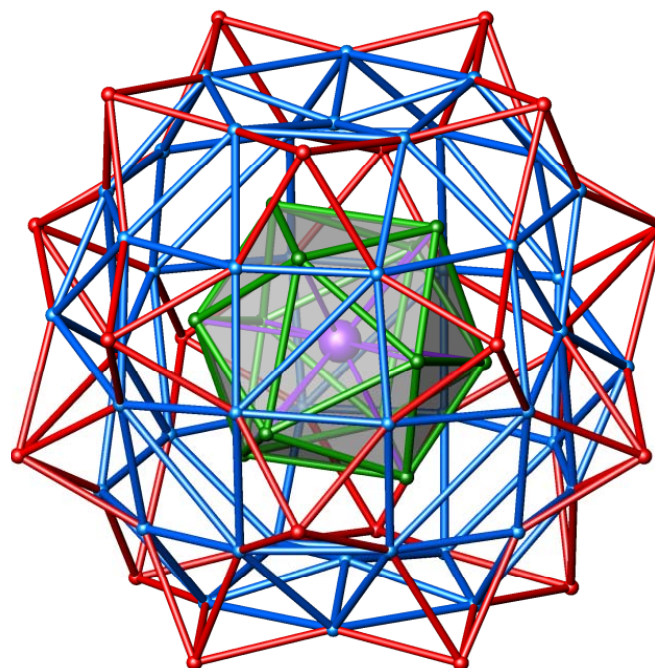
AFOSR/MURI
August 9, 2012

Reproducible Al₇₇ Cluster



X = 1.1, 1.2, 1.8

- Reproduced six times from AlCl (vs. AlI).
- X-ray structures suggest variable oxidation states
- This Al₇₇ core is stabilized by 20 organic ligands (NTMS₂).



different cluster shells of Al₇₇: 1(purple, central atom) +12 (green, distorted icosahedron), 44 (blue), 20 (red)

Ecker, A.; Weckert, E.; Schnöckel, H. *Nature* 1997, 387, 379.

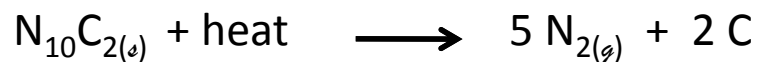
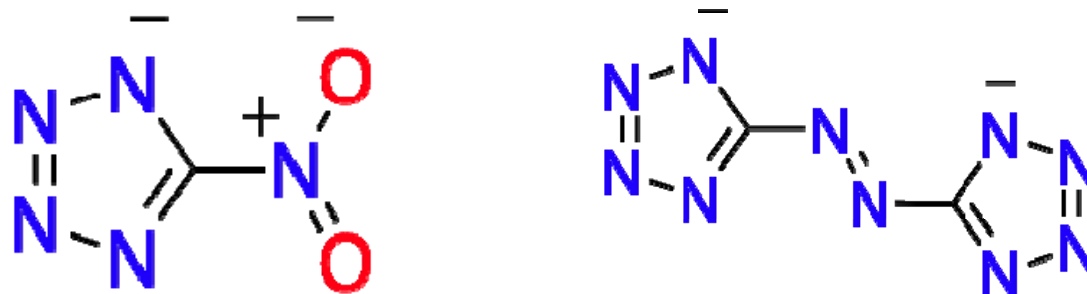


AFOSR/MURI
August 9, 2012

Potential Gas Generators for Cluster Dispersion: Klapötke Compounds

“Simple” stable high-nitrogen-content salts

- Energetic ligands with large ΔH of combustion
- generates large volumes of gas (primarily N_2) without consuming significant oxygen
- counter ions can be varied to optimize H-bonding, inter-particle interactions and solubility to optimize mesoparticle formation



T. M. Klapötke, et al. *Inorg. Chem.* **2008**, 47, 6014

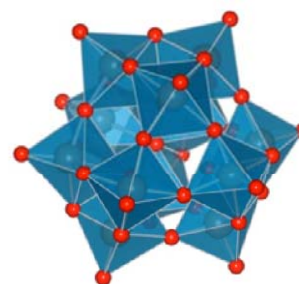


AFOSR/MURI
August 9, 2012

Target Clusters for Mesoparticle Formation

Initial studies with polyoxometallates and C_{60}

- air stable, chemically tunable
- size and mass similarities to Al clusters
- charge and hydrophobicity control



α -Keggin
 $[PMo_{12}O_{40}]^{3-}$

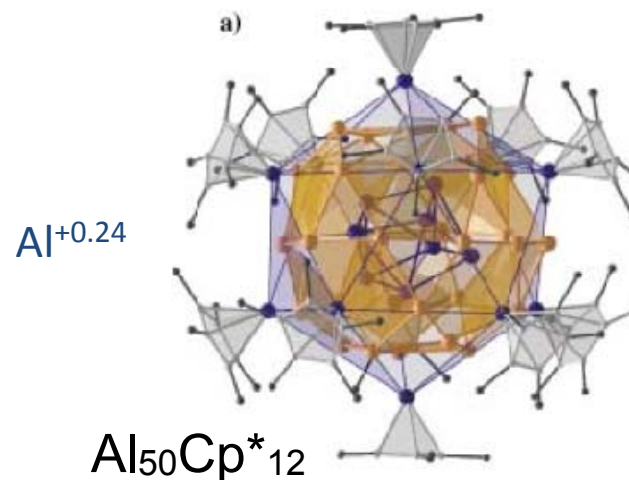
P. Putaj, et al., *Coordination Chemistry Reviews* 255 (2011) 1642–1685

Phase 2 – Al metalloids – Al_{77} and Al_{50} type clusters

- high energy content
- known synthetic procedures

Phase 3 – New Ti and Sc clusters?

- high energy content?
- new territory



$Al_{50}Cp^*_{12}$

Schnöckel, H. *Chem Rev.*, **110**, 4125 (2010)



AFOSR/MURI
August 9, 2012



Smart Functional Nanoenergetic Materials

AFOSR/MURI: Smart, Functional, Nanoenergetics
Design from the Atomistic/Molecular Scale
through the Mesoscale

Graphene as a Reactive Material and Carrier of Energetic Materials

I. A. Aksay, A. Selloni, R. Car, D. M. Dabbs
Chemical and Biological Engineering and Chemistry
Princeton University, Princeton, NJ 08544

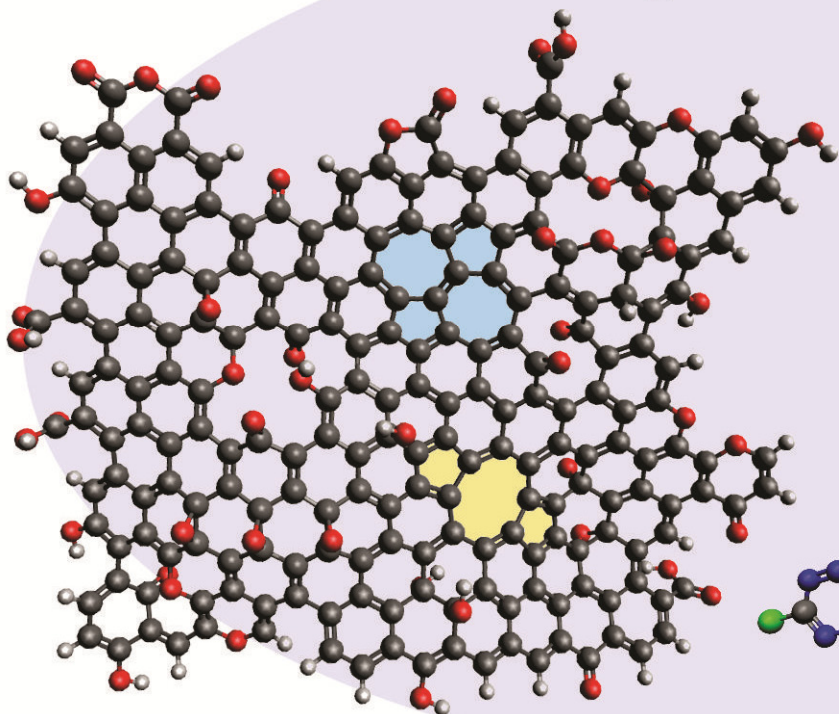


AFOSR/MURI

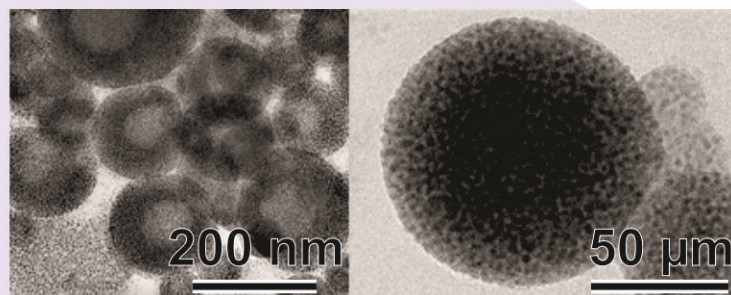
Smart Functional Nanoenergetic Materials

Processing Nanoenergetic Materials

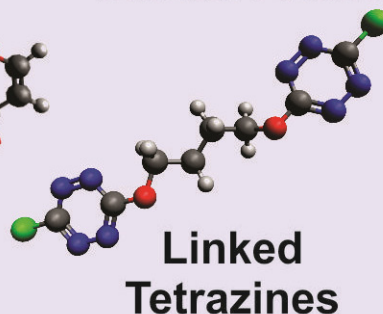
Aksay, Eichhorn, Zachariah



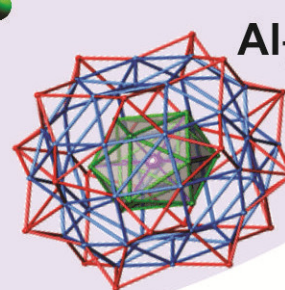
Functionalized Graphene Sheet



Cluster Assembled Metal Mesoparticles



Linked
Tetrazines



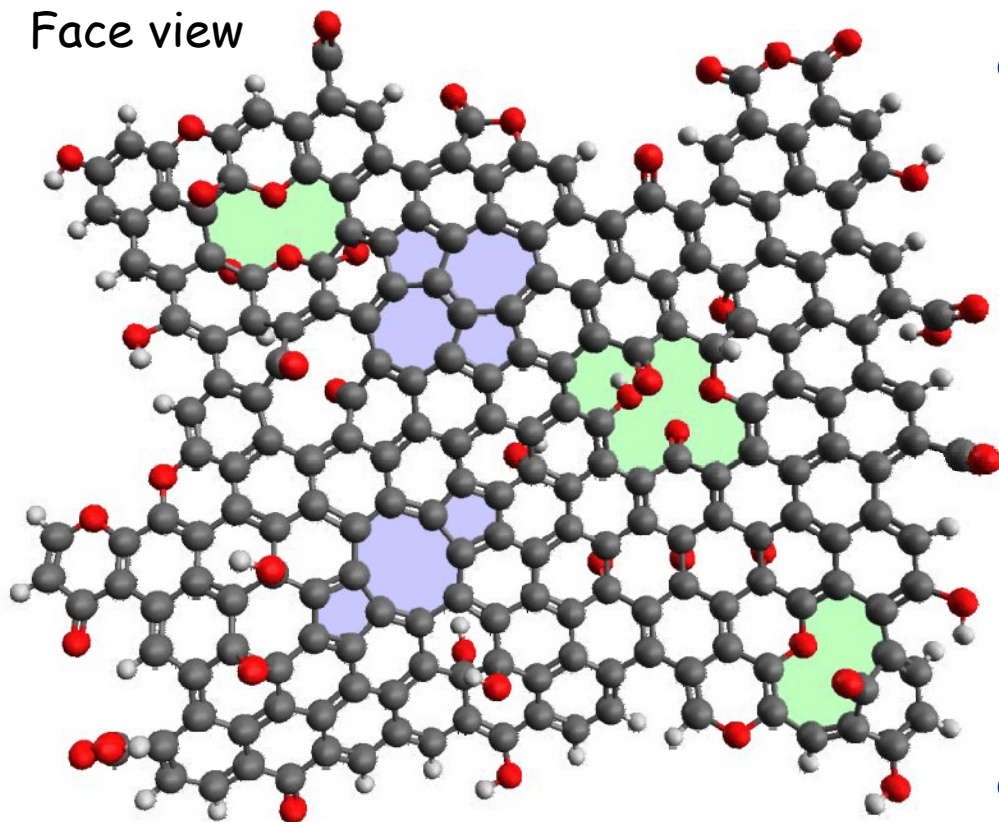
$\text{Al}_{77}[\text{N}(\text{SiMe}_3)_2]_8^{2-}$
Molecular
Cluster



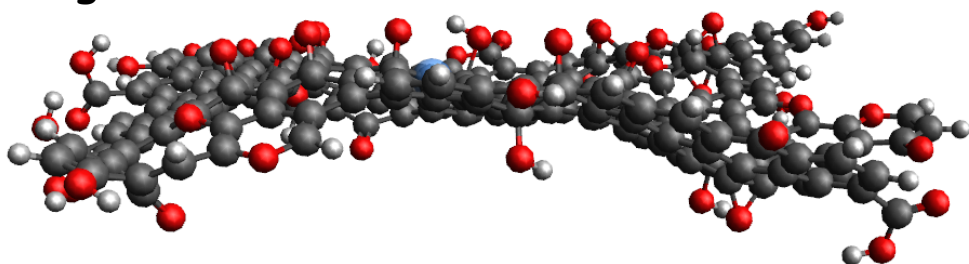
AFOSR/MURI
August 9, 2012

Functionalized Graphene Sheets

Face view



Edge view

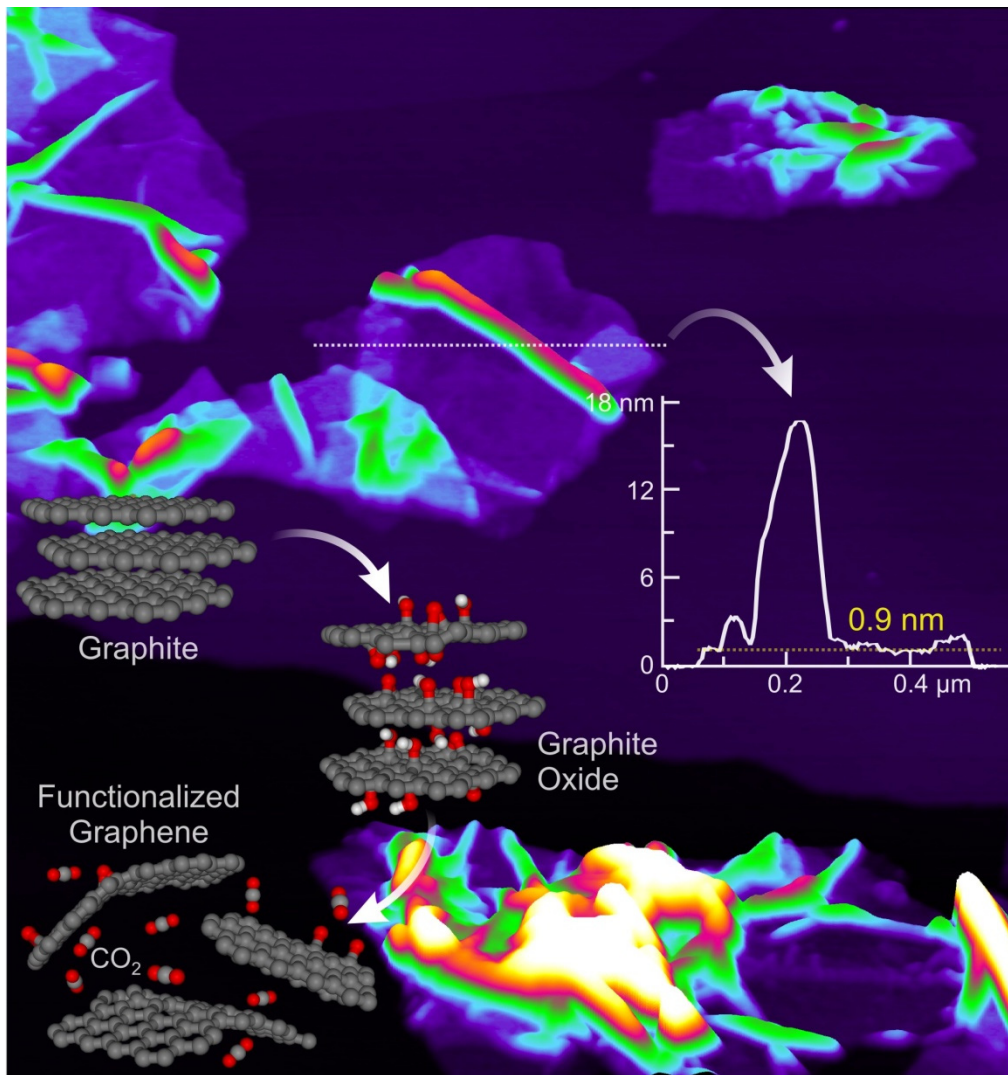


- **FGS: functionalized graphene sheet**
 - Large ($>2\mu\text{m}$ diameter) polyaromatic hydrocarbon
 - Commercial production of single sheets (Vorbeck Materials, Jessup, MD)
 - Wrinkling inhibits restacking, maintains surface area
- **Topological and lattice defects**
 - Carbon vacancies
- **Oxygen-containing groups**
 - Epoxides, hydroxides, carboxyls



AFOSR/MURI
August 9, 2012

Splitting of Graphite into Single Sheets



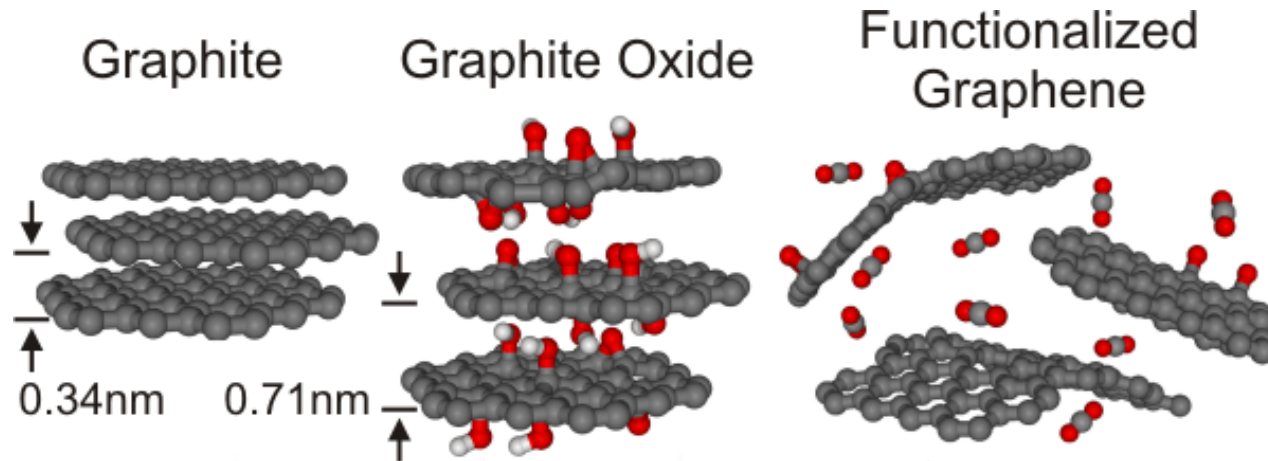
M.J. McAllister et al., *Chem. Materials* (2007)

- Graphite Oxide by Staudenmaier method (1898) - 4 fold volume expansion
- Thermal expansion (>500 fold) at 1050°C - Böhm (1962)
- SA ~850 m²/g by BET and >1800 m²/g by methylene blue adsorption in solvents
- Disappearance of graphite peaks after oxidation and elimination of all peaks after expansion
- >80% single sheet highly wrinkled functionalized graphene



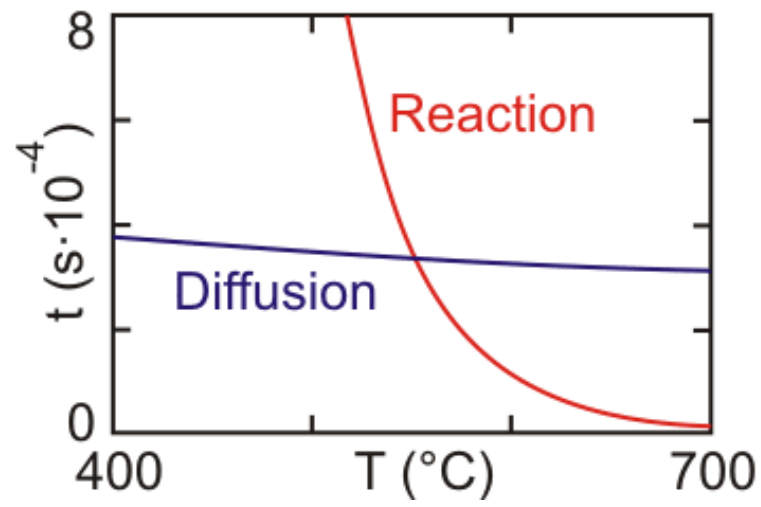
AFOSR/MURI
August 9, 2012

Graphite Exfoliation



HNO_3
 H_2SO_4
 KClO_3
 96 Hours

Δ



M.J. McAllister et al., *Chem. Materials* (2007)



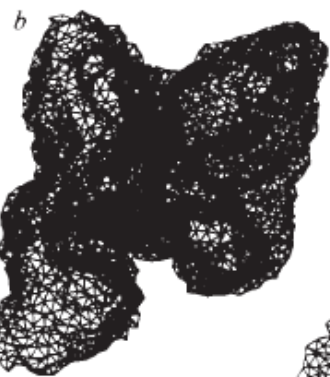
AFOSR/MURI
August 9, 2012

FGS Conformation and Compatibility

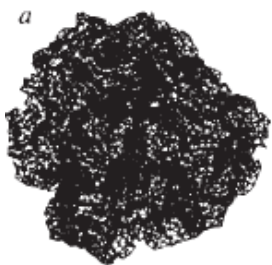
Poor to good dispersing medium

- Compatilization through grafting

Crumpled

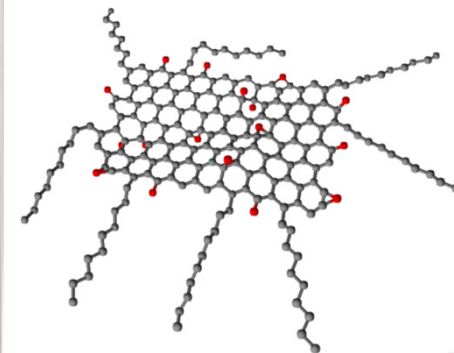
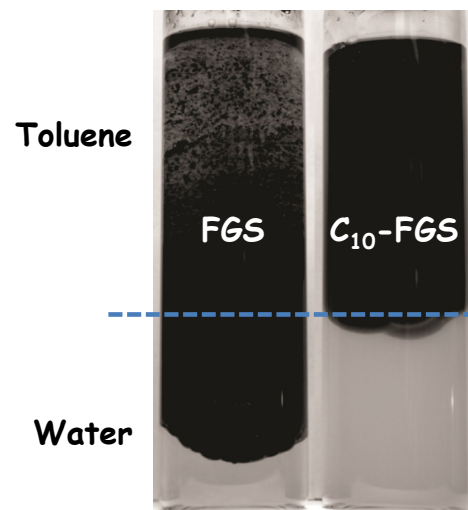


Wrinkled



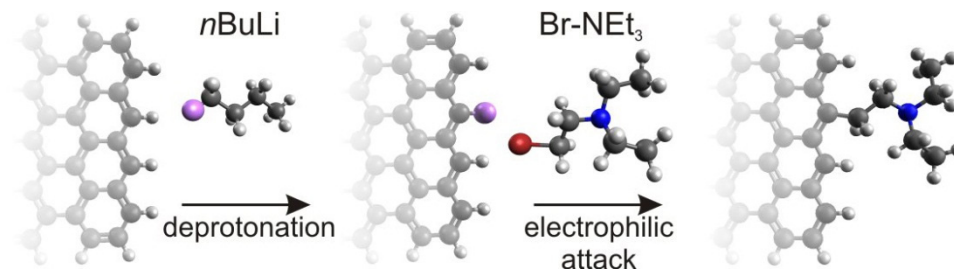
Collapsed

Wen, Tanaka, *Nature* (1992)



C_{10} -grafted FGS

Grafts at edges and on basal plane



Tessonnier, Barteau *Langmuir* (2012)



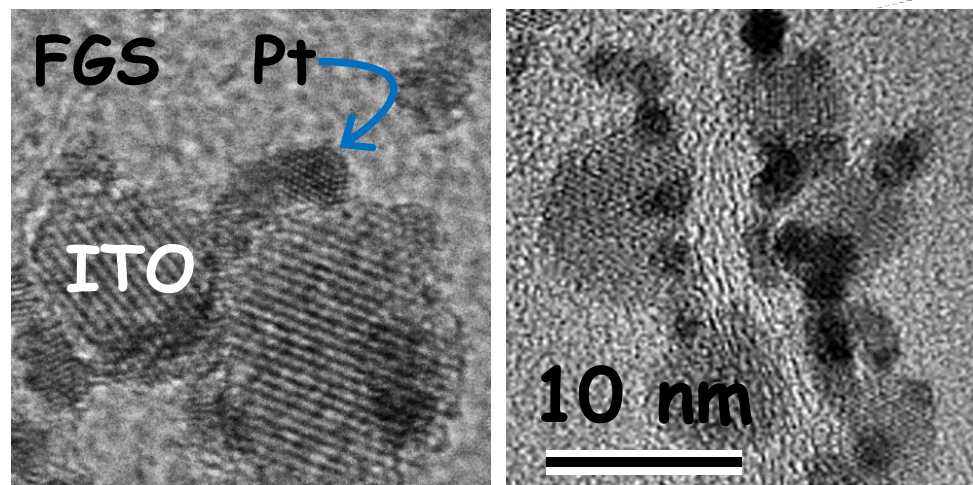
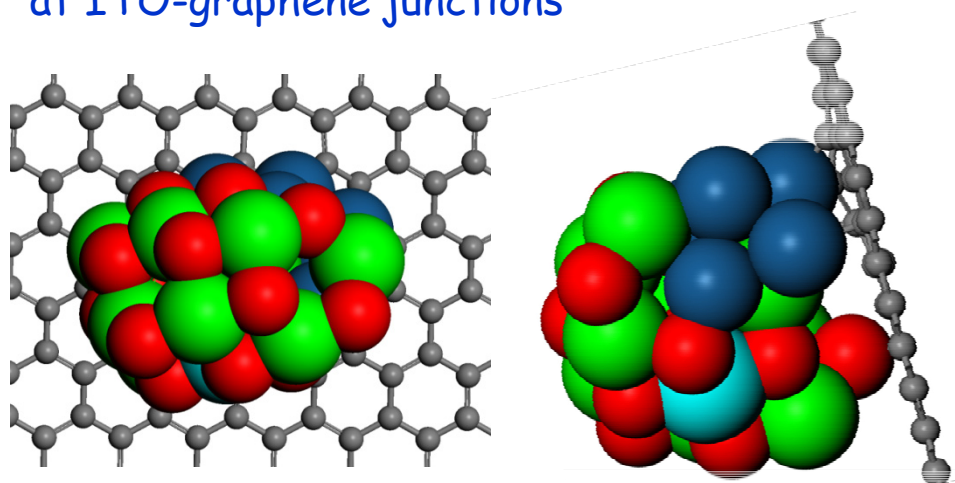
AFOSR/MURI
August 9, 2012

Stabilization of Pt Particles at ITO-graphene Junctions

- Graphene templates nanoparticle nucleation.
- ITO nanoparticles stabilized on FGS lattice defect sites
- Pt nanoparticles are stabilized at ITO-graphene junctions
- Coarsening/sintering of Pt nanoparticles arrested due to pinning at ITO-graphene junctions
- Expandable to other oxide/metal junctions on graphene templates

In collaboration with PNNL:

DFT models: Pt nanoparticles stabilized at ITO-graphene junctions



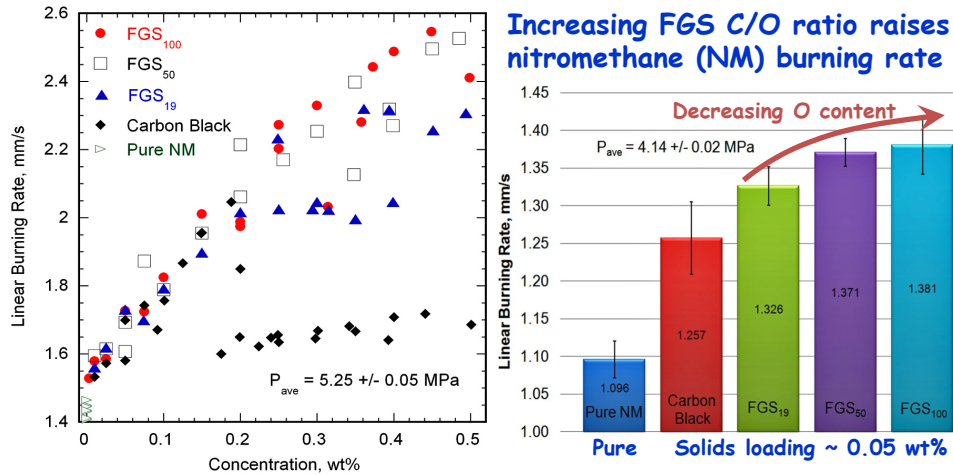
Kou, et al. *J. Am. Chem. Soc.* (2011)



AFOSR/MURI
August 9, 2012

FGS as Catalyst in Propellants and Fuels

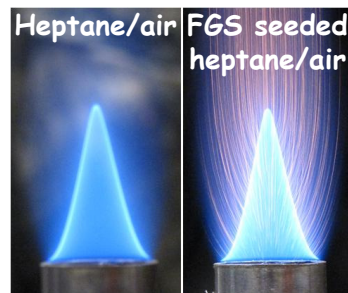
Catalysis of Propellants and Fuels



- **Liquid Strand Burner: NM gas-phase chemistry well understood; liquid-phase chemistry not important at low pressures**
 - More reduced FGS is a better accelerant than carbon black or FGS of low C/O (mol/mol).
 - Lower deflagration pressure-limit with carbon additives.
 - Reduced performance of carbon black and FGS₁₉ at ~0.2wt% may be due to particle aggregation at liquid/vapor interface, preventing passage of particles into vapor phase.
 - The role of FGS in liquid and vapor phases is under study.

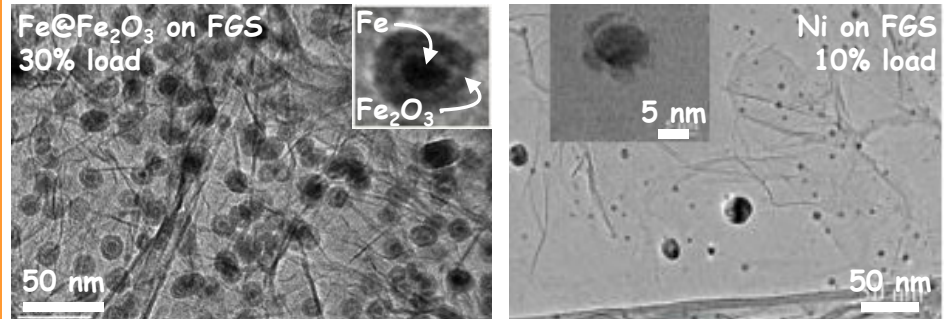
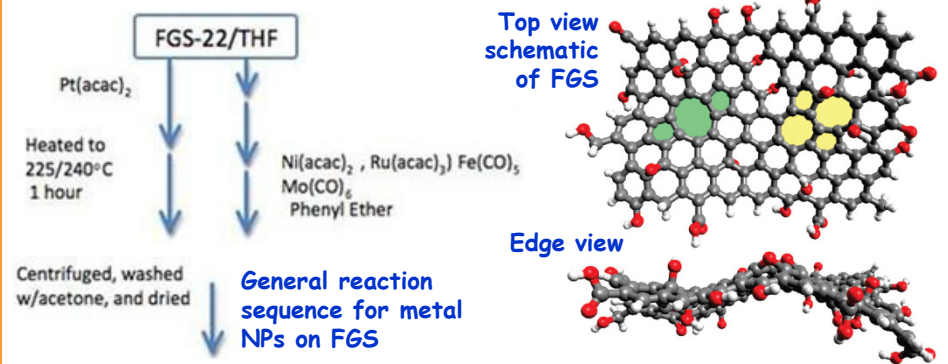
Laminar Burning Rate Measurements on Vaporized Hydrocarbons

- Dry seeding of propane with FGS increases burning rate by 10-15%
- Neat FGS poorly disperses in nonpolar liquid hydrocarbons (LHCs):
 - aggregates present in vapor visible as incandescent particles in flame
 - improved dispersion requires modifying FGS with dispersing molecules such as n-decane



FGS as Catalyst Substrate

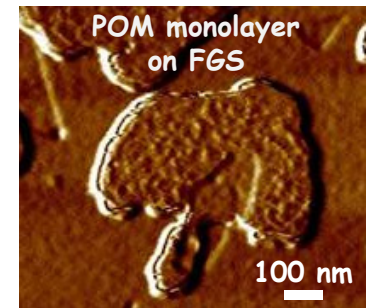
Surfactant and Template for Metal Nanoparticles (NPs)



- FGS substrate provides high loadings and stable dispersion of metal NPs (Fe, Ru, Ni, Pt) with narrow particle size distribution
 - Functionalization of FGS needed to disperse in non-polar LHCs

Surfactant and Template for Polyoxometallates (POMs)

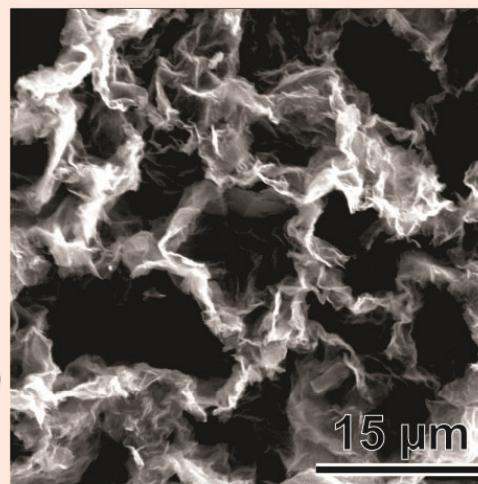
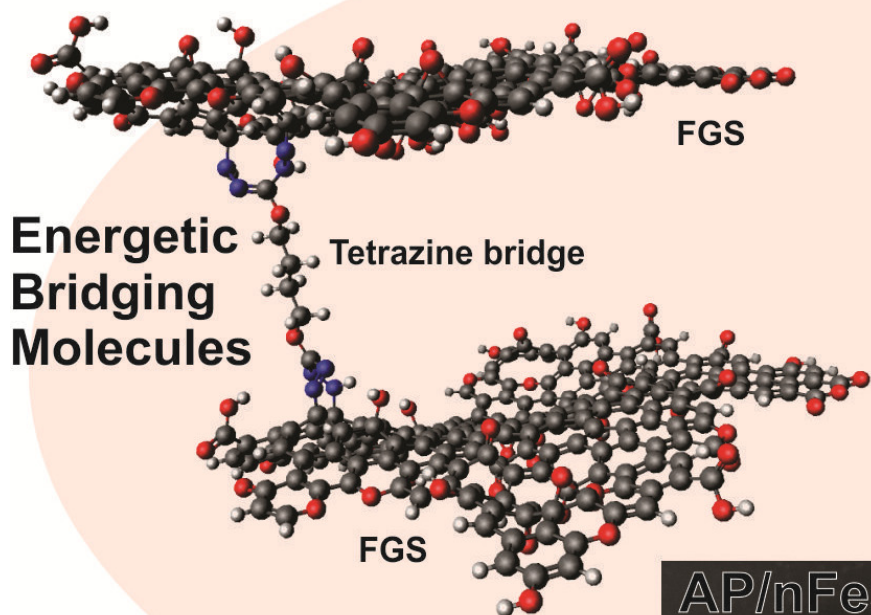
- POMs are transition metal oxygen-anion heteropolyanion clusters with wide range of architectures, charge densities, chemical and electronic properties.
 - Activity as oxidation catalysts can be easily tuned.
 - From solution, POM deposition occurs preferentially on FGS.



AFOSR/ARRA

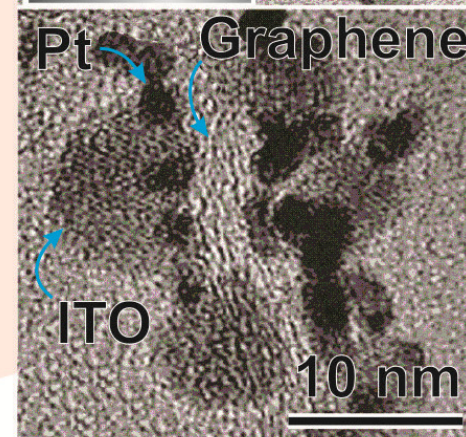
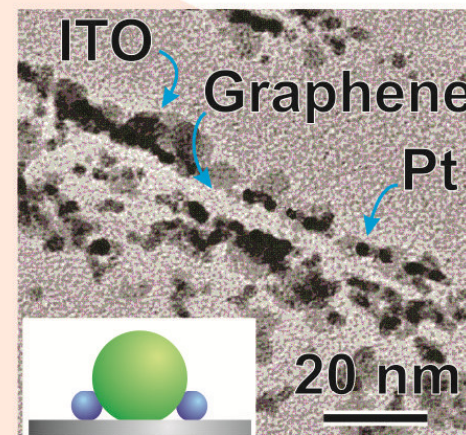
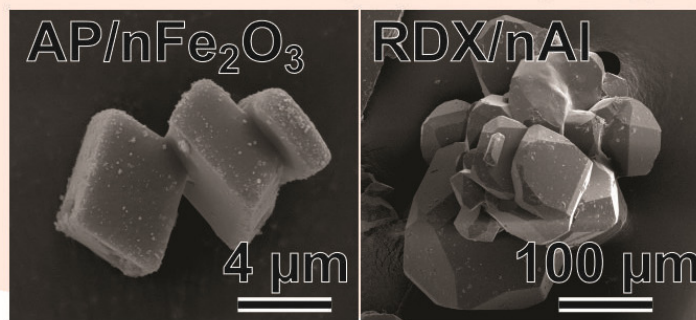
Multiscale Processing

Aksay, Eichhorn, Zachariah



Graphene Sponge

Nanostructured Catalysts



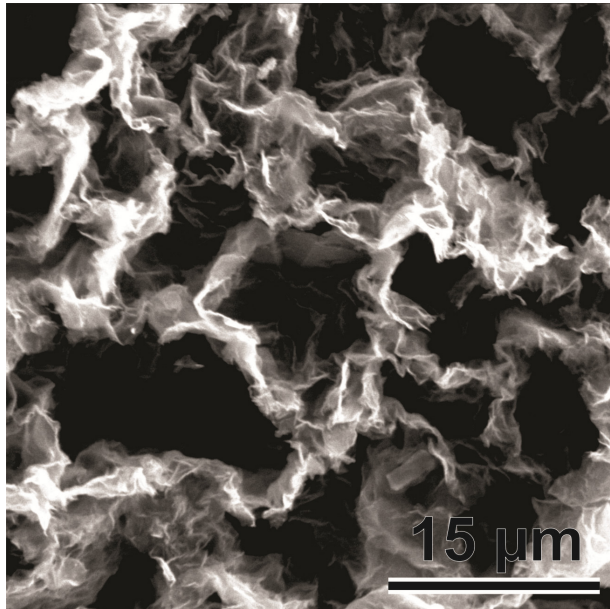
Metal NPs on FGS



AFOSR/MURI
August 9, 2012

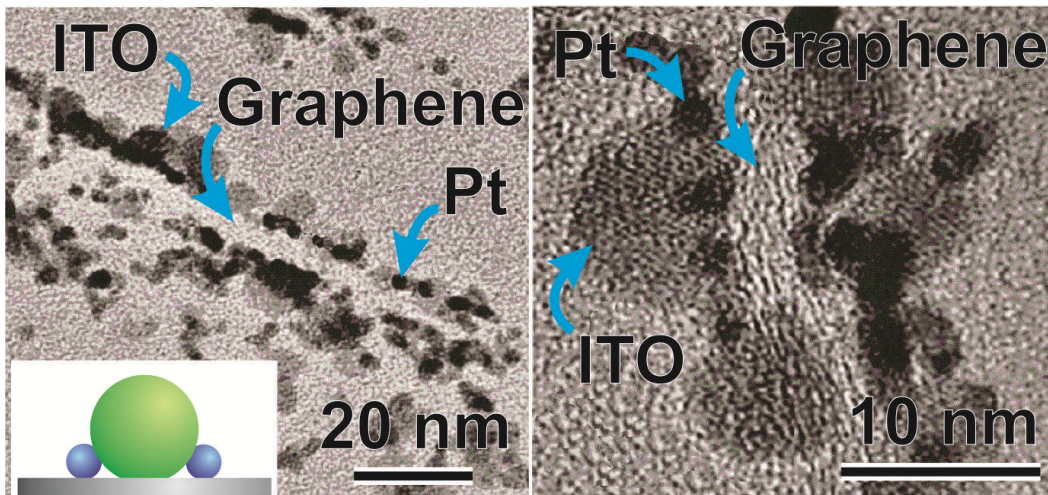
FGSs as Nanoenergetic Materials

FGS
sponge



Princeton
University
(2011)

- **Constructing a system**
 - Effective stabilizer for metal and polyoxometalate nanoparticles
 - High surface area porous matrices
- **Nanopropellant**
 - High C-fuel source
 - Intimate contact with oxidizers
 - Incorporation of high nitrogen compounds



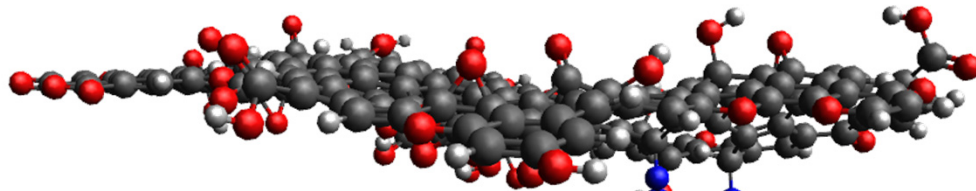
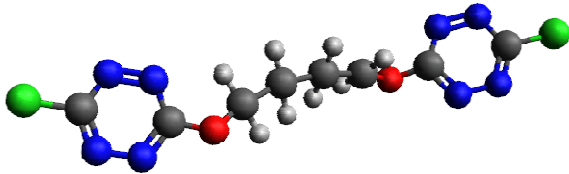
Kou, et al. *J. Am. Chem. Soc.* (2011)



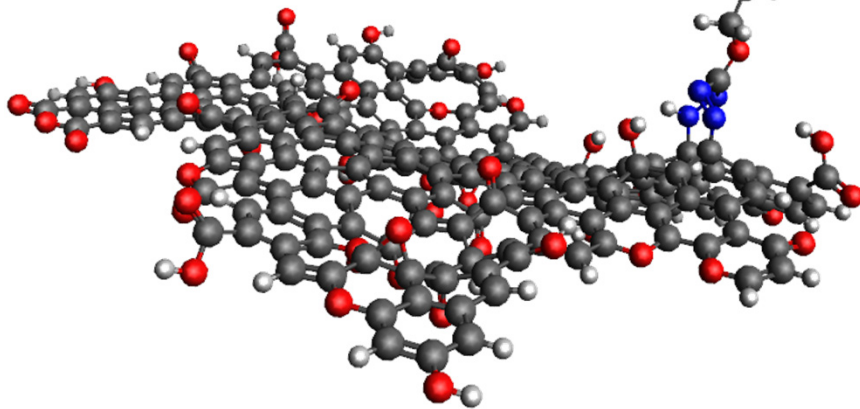
AFOSR/MURI
August 9, 2012

Energetic Scaffolding

Linked tetrazine



Tetrazine bridge



- **Chemical modification of FGSs**

- Basal plane and edge chemistries for attaching dispersants or binders
- Joining of FGSs for porous structures

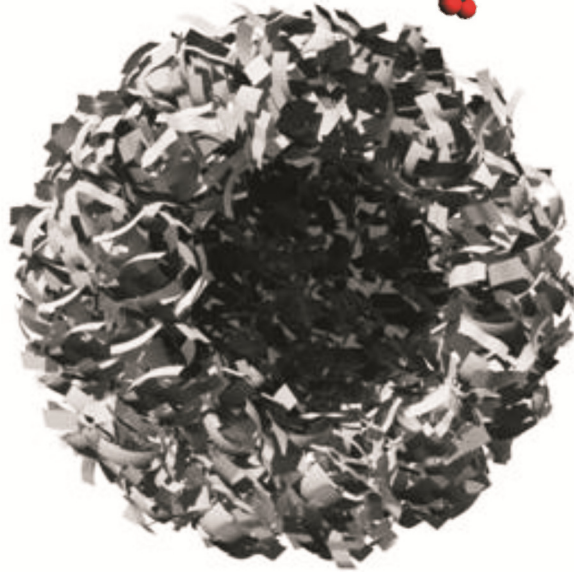
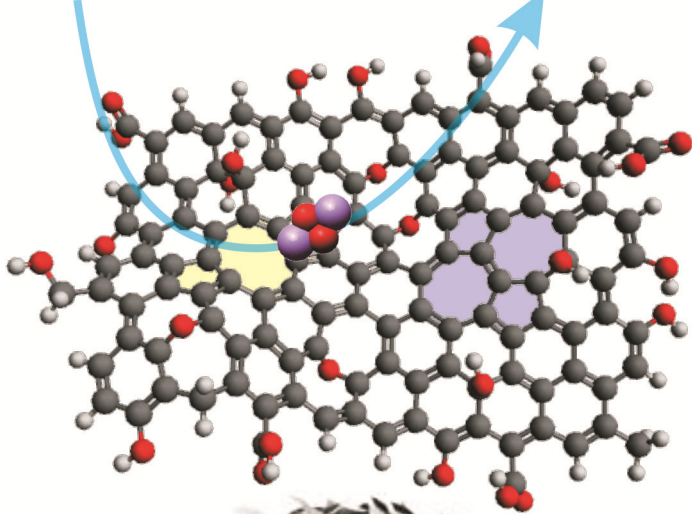
- **Spacers**

- Long chain, rigid molecules
- Nanoparticles (metals, polyoxometalates, carbon)
- "Click chemistry"



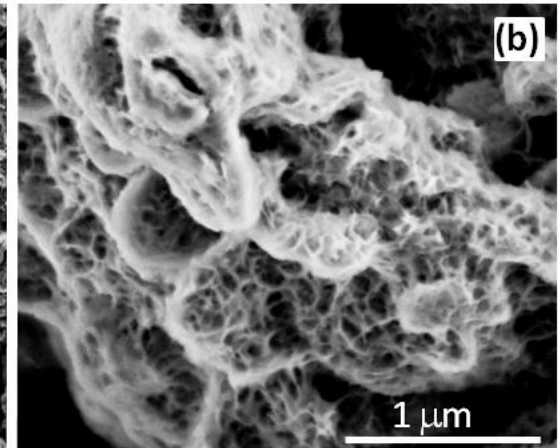
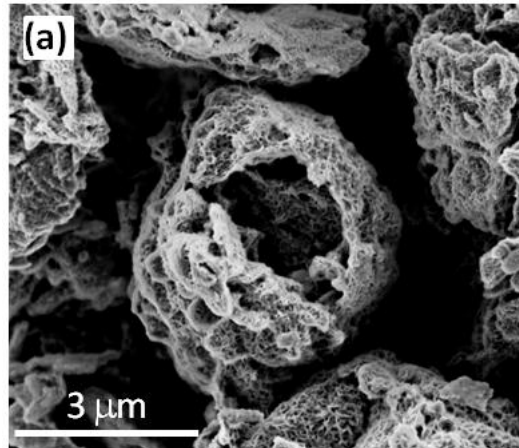
AFOSR/MURI
August 9, 2012

Hierarchically Porous FGS



In collaboration with PNNL:

Hierarchically structured porous FGS scaffolds for use in lithium air batteries

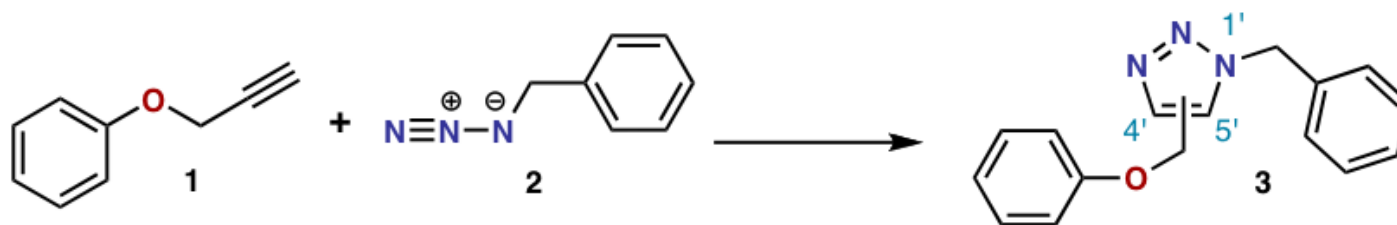


J. Xiao et al., *Nano Lett.*, 2011



AFOSR/MURI
August 9, 2012

Click Chemistry for Bridging Molecules



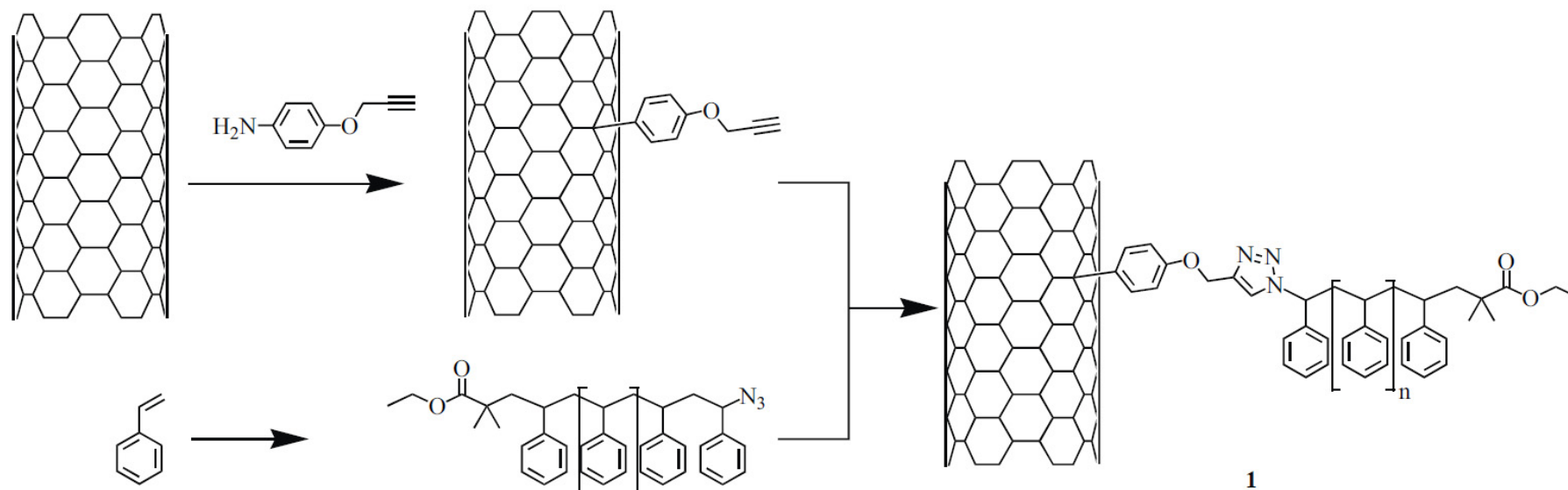
Terminal alkyne

Azide

1,2,3-triazole

H. C. Kolb, et al. *Angew. Chem.-Intern. Ed.* (2001)

Demonstrated on CNTs



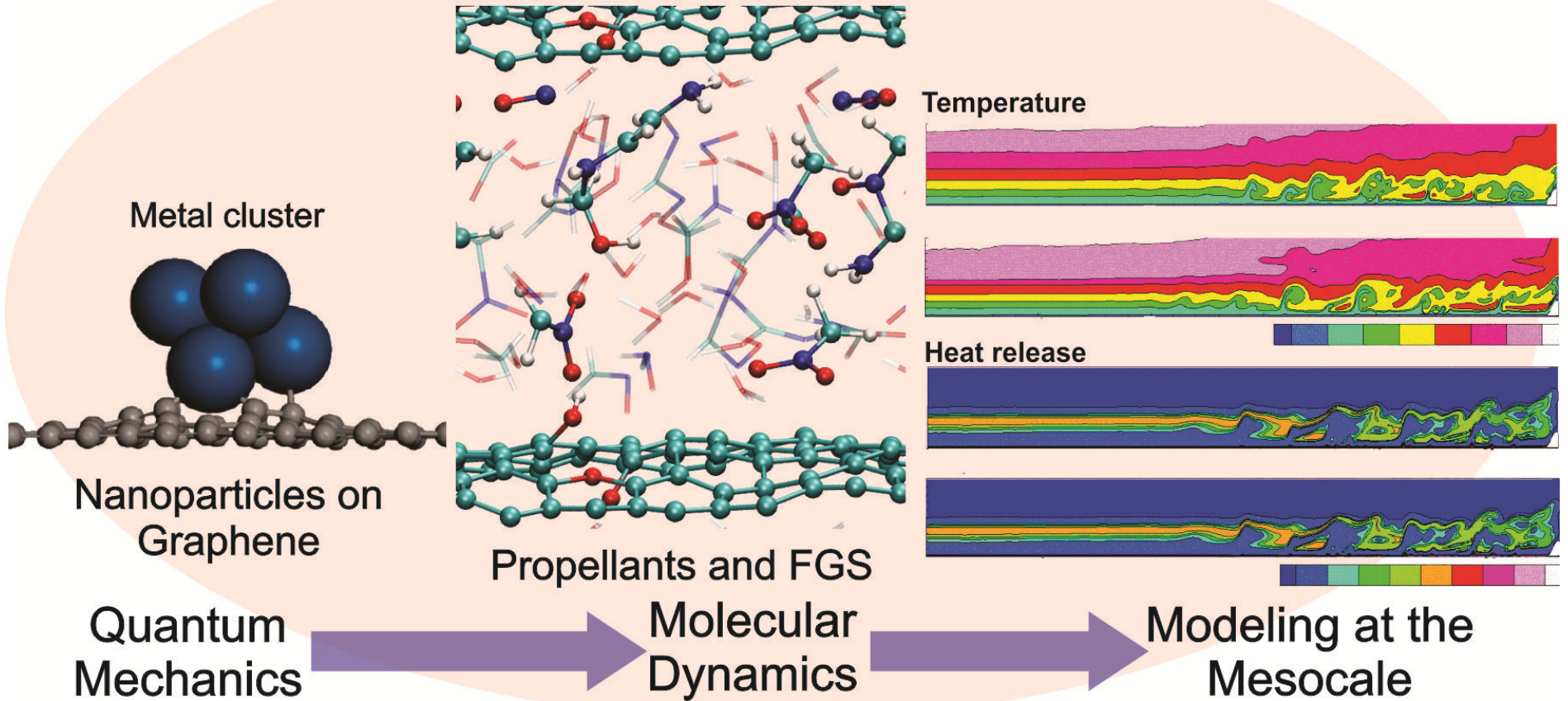
H. Li, et al. *J. Am. Chem. Soc.* (2005)



AFOSR/MURI
August 9, 2012

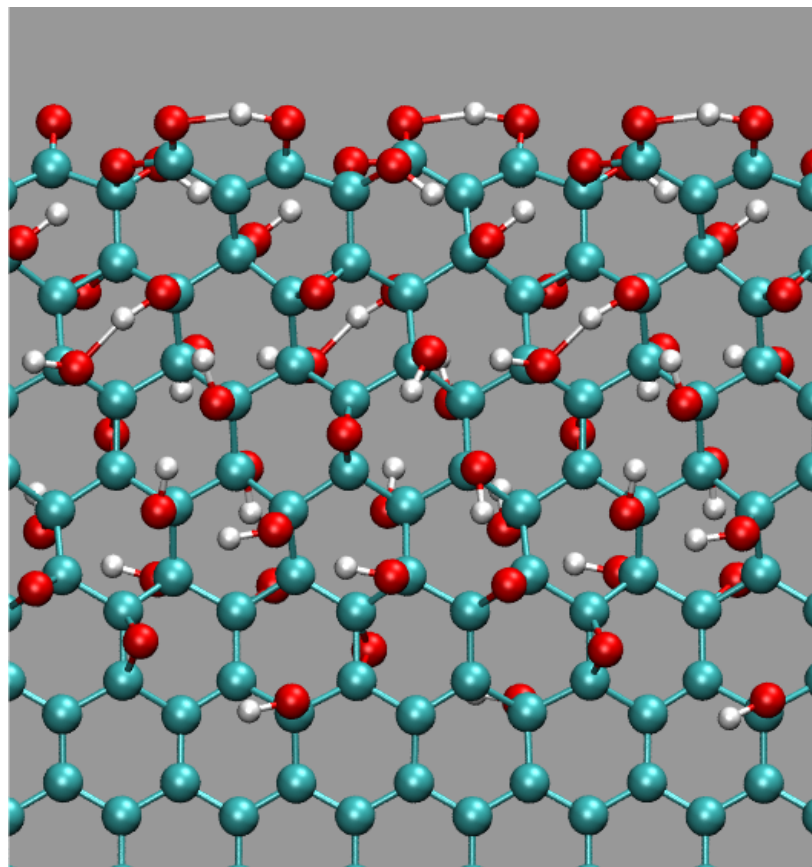
Modeling

Car, Selloni, Yang



AFOSR/MURI
August 9, 2012

Graphene Oxide Grows from the Edge

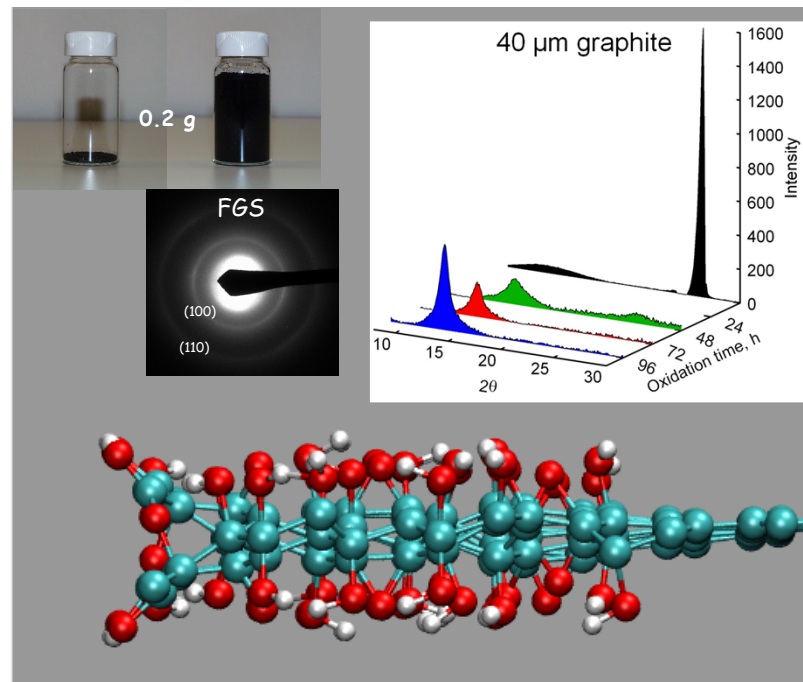


Model: $C_8H_4O_{6.2}$ with $OH:O=2:1$

Experiment: $C_8H_{2.54}O_{3.91} \sim C_8H_{4.61}O_{6.70}$

Nakajima et al. *Carbon* **26**, 357 (1998)

Hontora-Lucas et al. *Carbon* **33**, 1585 (1995)



As graphite oxidizes, the 0.34 nm XRD peak disappears and the 0.6-0.7 nm GO peak appears (above). Complete elimination of the native graphite peaks occur at a C:O ratio of 2:1.

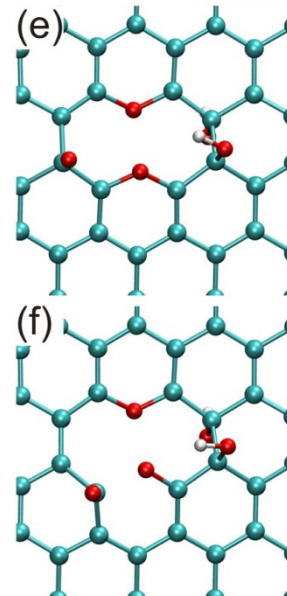
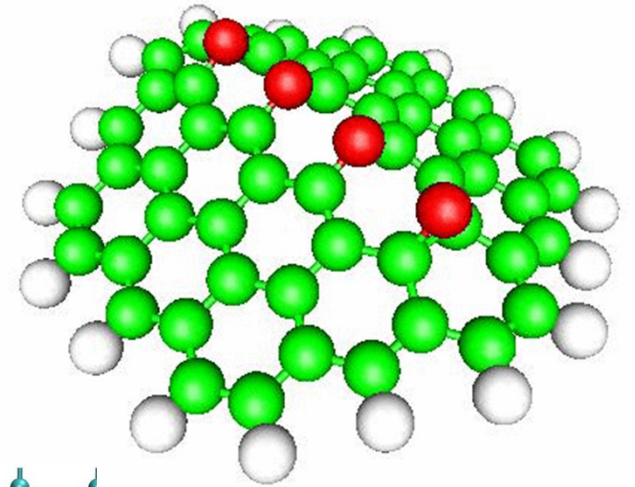
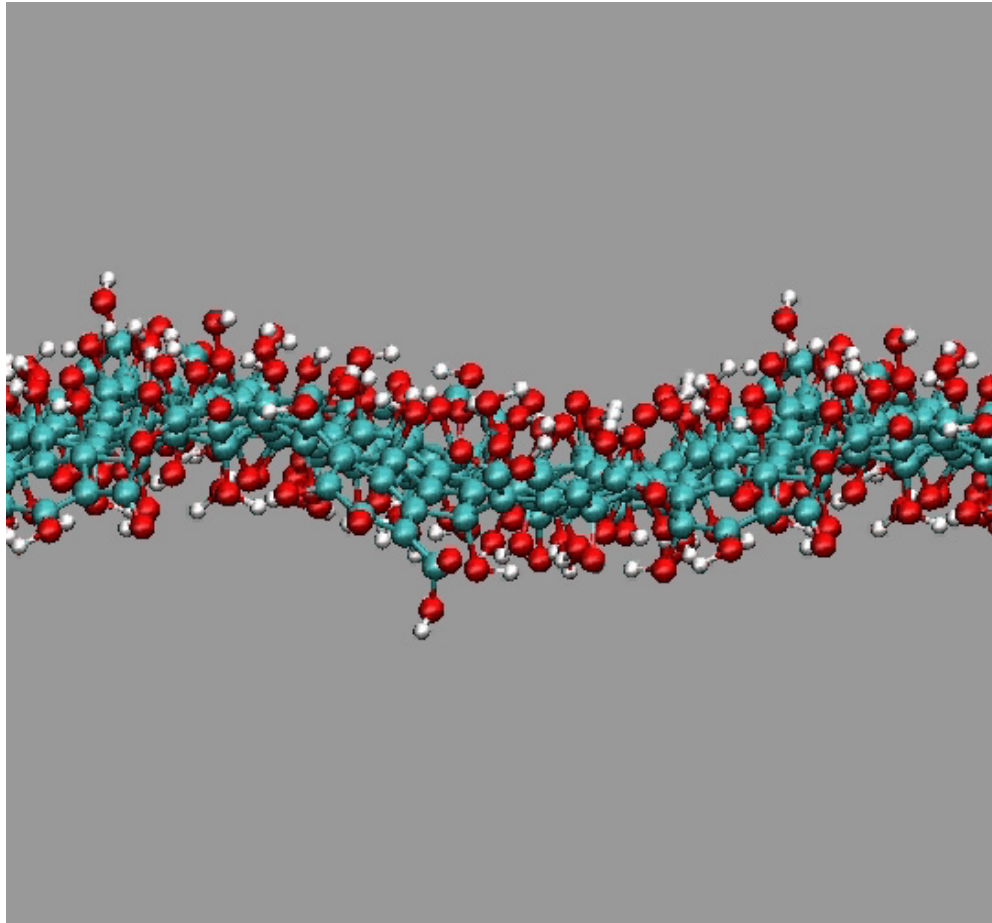
M.J. McAllister, et al., IAA, Chem.

Materials **19** 4396 (2007)



AFOSR/ARRA

Drying, Decomposition, and Vacancies



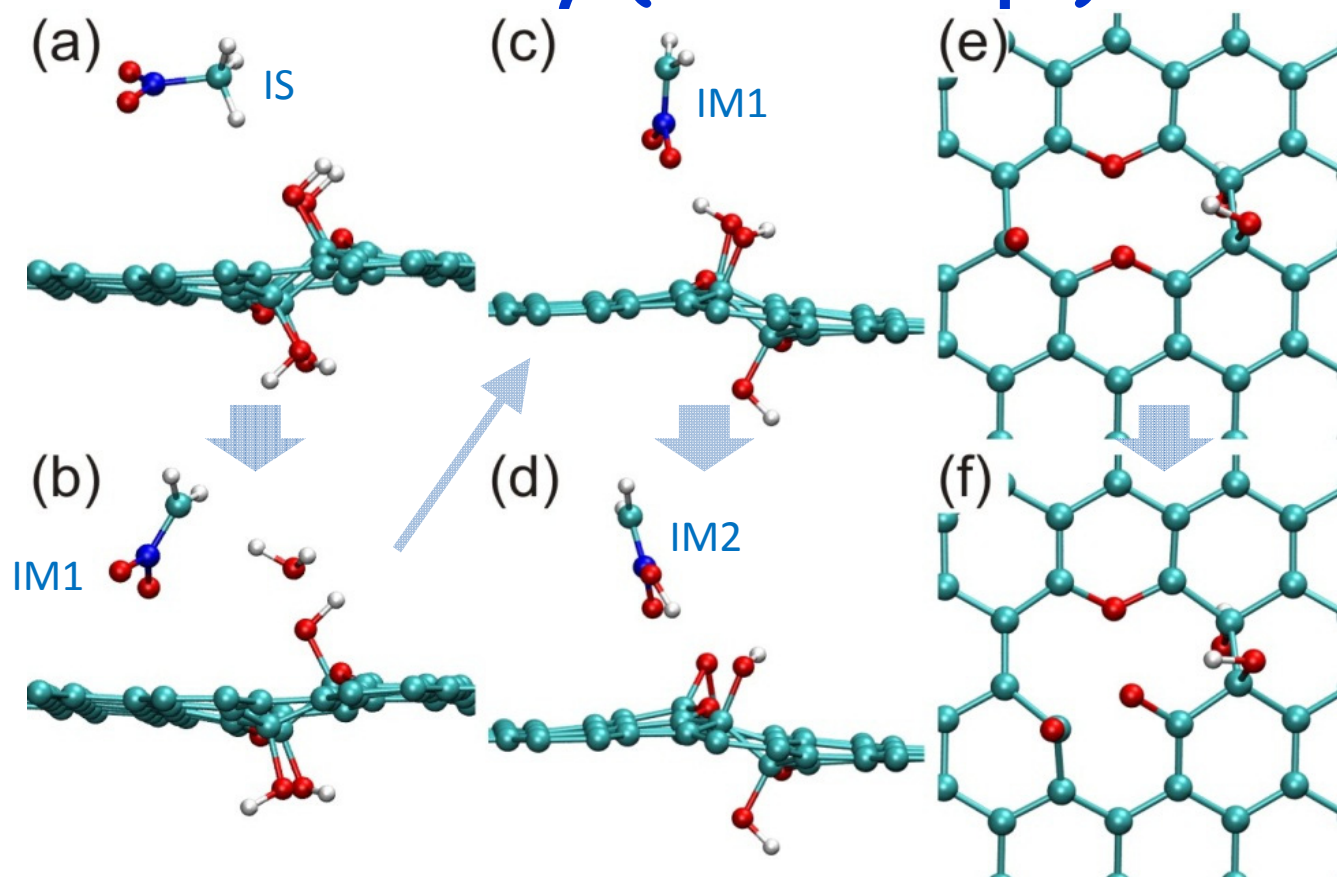
AFOSR/MURI
August 9, 2012

Thermal Decomposition of Nitromethane

- DFT (T=0K) calcs & ab-initio molecular dynamic simulations (T=2400K)
 - Pristine graphene
 - very weak interactions, no decomposition
 - Chemically modified graphene (CMG): no defects with hydroxides and epoxides groups
 - H-bonding to hydroxides \rightarrow $\text{CH}_2\text{NO}_2^- + \text{H}_2\text{O}$
 - Energetically favorable (~ 19 kJ/mol) but **NOT CATALYTIC**
 - FGS with decorated divacancy (2 ethers + 4 hydroxyls)
 - **CATALYTIC**: reaction sites on FGS regenerated
 - Energetically favorable (overall energy release ~ 200 kJ/mol)



Reaction of a NM with Functional Groups@ Vacancy (initial steps)

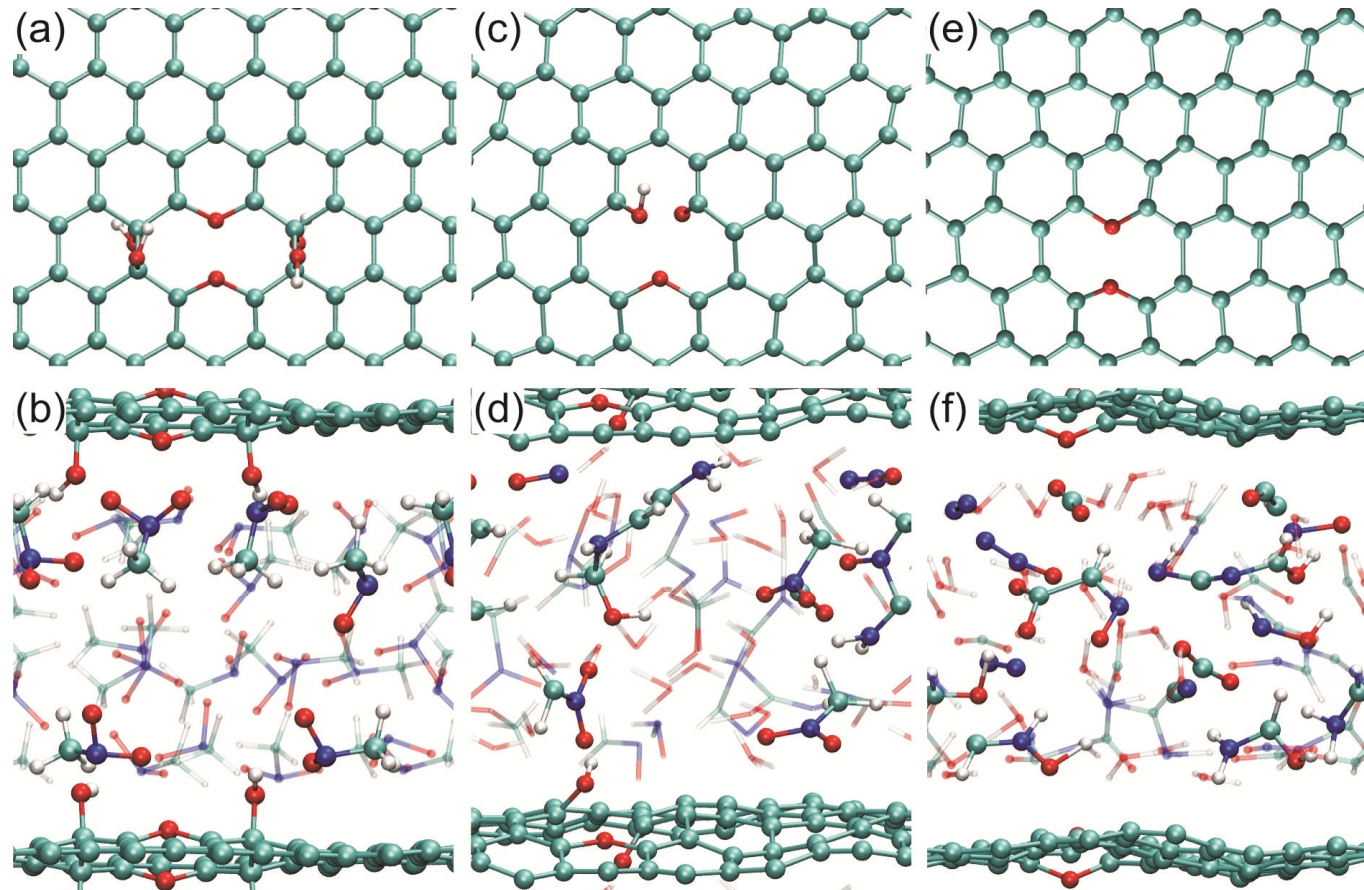


- (a) and (b): NM (IS) donates a proton to a hydroxyl around the divacancy, which leads to the formation of CH_2NO_2^- (IM1) and a water molecule. IM1 ~ 56 kJ/mol higher in energy than IS.
- (c) and (d): CH_2NO_2^- ion accepts a proton (CH_2NOOH ; IM2) from a hydroxyl around the vacancy, leaving one oxygen atom. IM1 \rightarrow IM2 slightly exoenergetic (~ 5 kJ/mol; $E_a \sim 3$ kJ/mol)
- (e) and (f): This oxygen diffuses toward an ether, which results in the formation of two carbonyls. $E_a \sim 4$ kJ/mol, but the energy gain is significant: ~ 92 kJ/mol, with a net energy gain of ~ 41 kJ/mol.



Liquid NM + FGS: Catalysis at Vacancies

$T = 2400 \text{ K}$
 $\rho = 1900 \text{ kg/m}^3$

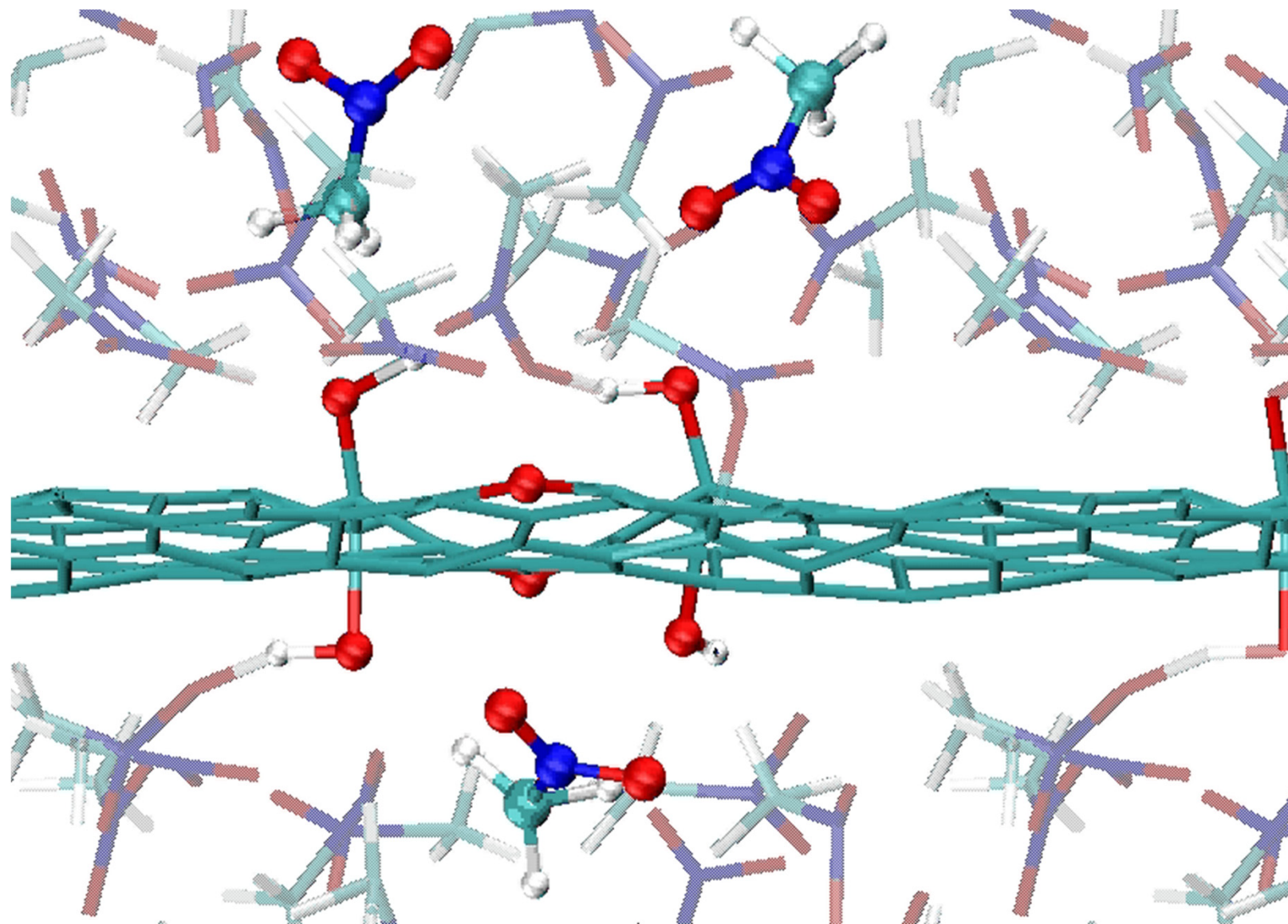


- (a) and (b) initial configuration (divacancy decorated by 2 ethers and 4 carbonyls);
- (c) and (d) after 10 ps;
- (e) and (f) final configuration. In the lower panels, a few intermediates or decomposition products are highlighted. White, red, and cyan balls (bonds) represent hydrogen, oxygen, and carbon atoms, respectively.



AFOSR/MURI
August 9, 2012

$\rho = 1900 \text{ kg/m}^3$; $T = 2400\text{K}$; $\tau = 0.92 \text{ ps}$



$t_0 = 0$
2 ethers,
4 hydroxyls

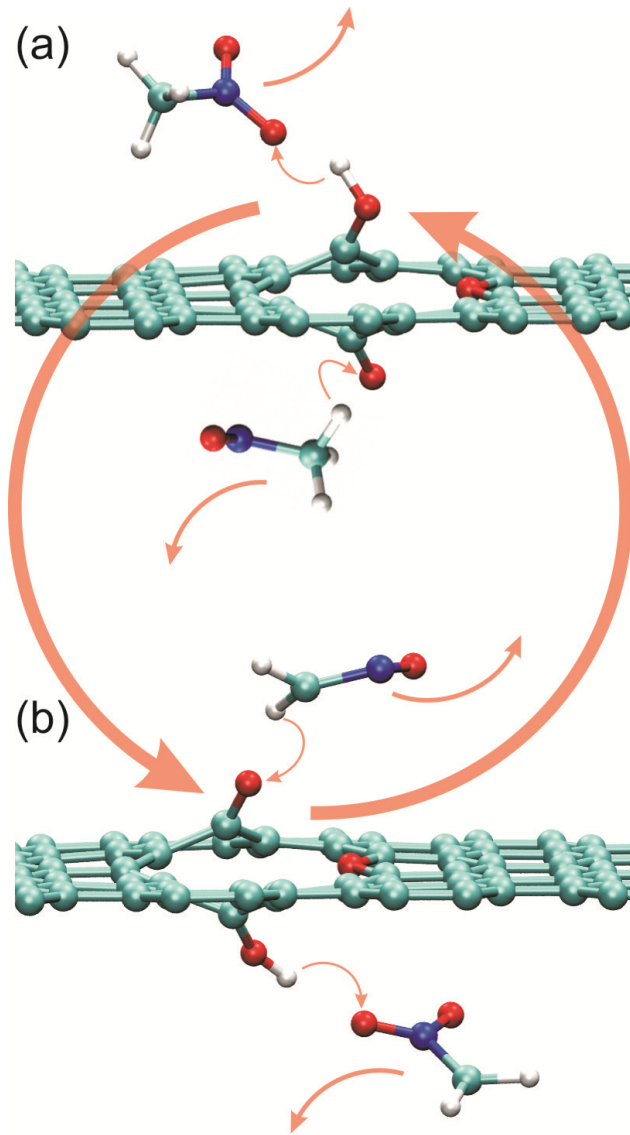


$t_f = 0.92 \text{ ps}$
2 carbonyls,
1 ether



AFOSR/MURI
August 9, 2012

FGS Catalysis



- Catalytic role of FGS essential to transform the NM molecules into more reactive intermediates
 - Once formed, reactions continue within the fluid
- Fast decomposition:
 - After ~ 14 ps, complete transformation into different species
 - Main combustion products are H_2O , CO_2 , and N_2
- Protonation, deprotonation and oxidation reactions promoted by FGS



AFOSR/MURI
August 9, 2012

Summary

- Develop synthesis methods to construct hierarchically structured nanocomposite fuels using functionalized graphene sheets as (i) nucleation templates and stabilizer for energetic particles, polymeric nitrogen molecules, embedded nitrogen; and (ii) carbocatalysts
- Employ quantum mechanical modeling to understand the fundamental mechanisms of energetic functions. High surface area graphene networks



AFOSR/MURI
August 9, 2012



Integration of Nanoenergetic Composite Ingredients/Mixtures and Reaction Characterization

R. A. Yetter, S. F. Son, S. Thynell and L. J. Groven
Penn State and Purdue Universities



AFOSR/MURI

Bottom Up vs. Top Down

Bottom Up

- Potential to precisely control structure of fabricated material
- Scaling and cost is often challenging

“Aluminum Clusters Exhibit Multiple Personalities”

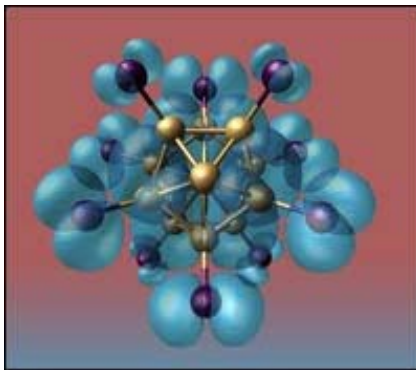
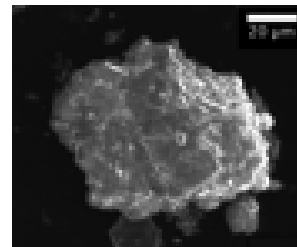


Image: D.E. BERGERON/P.J. ROACH/A.W. CASTLEMAN/N.O. JONES/S.N.KHANNA

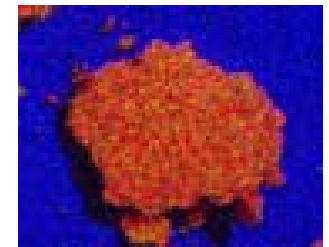
- Approaches can be synergistic
- In both cases, reaction characterization is critical

Top Down

- Precise control is generally not possible, but microstructure can be tailored
- Scaling and cost can be advantageous
- Demonstrated ability to tailor reactivity of Al particles with MA nanoscale inclusions



SEM image (left) and EDS elemental map (right) of Al-PTFE composite particles (Aluminum-red, Fluorine-green, Carbon-blue).



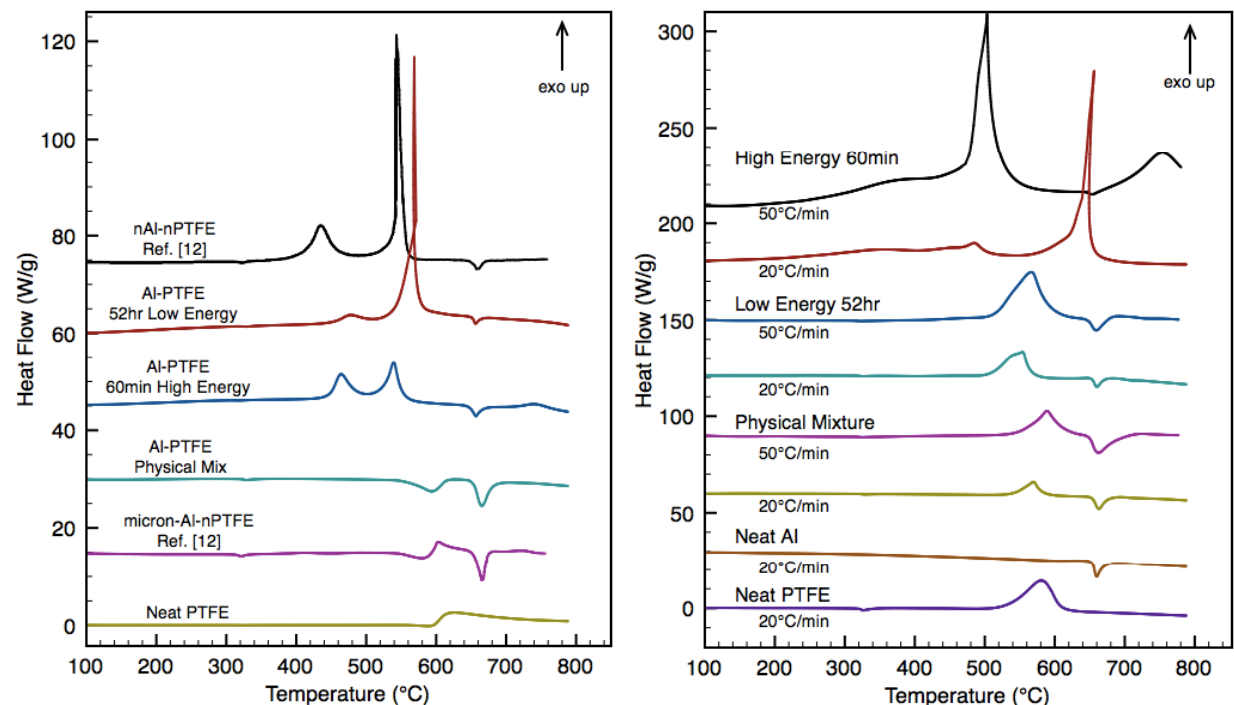
AFOSR/MURI
August 9, 2012

Disrupted Al Ignition Via Nanoscale Inclusions

- Mechanical activation can result in microscale fuel particles with well-distributed FC and reaction properties are tailorable with milling parameters

Use of fluorine in solid propellants could result in an increase of performance (Geisler, 1982)

Fluoropolymers with piezoelectric properties can be considered also to consider switchable (smart/functional) properties



DSC heating of Al-PTFE (70-30 wt.%) MA composites at 10°C/min in argon (left) and in O₂-Argon (20 vol.%) (right). features.



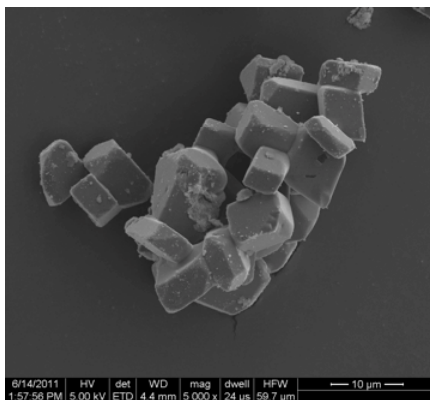
AFSOR



AFOSR/MURI
August 9, 2012

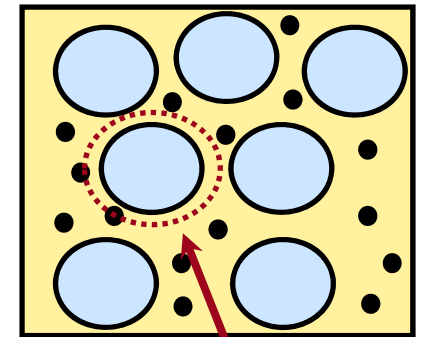
Encapsulation of Nanoscale Particles in AP

- Replacing nanoscale particles for micron powders results in rheology and mechanical issues
- If nanoscale particles are captured (encapsulated) WITHIN micron scale crystalline ingredients formulation issues could be avoided
 - More intimate & uniform mixing could improve catalytic and combustion rate
 - Dramatic decrease of diffusion scale

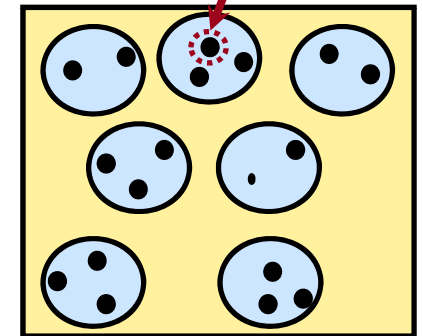


- 92% capture and ~5x decrease in surface area

Reese et al., submitted to PEP, 2012



Diffusion length scales



AFSOR

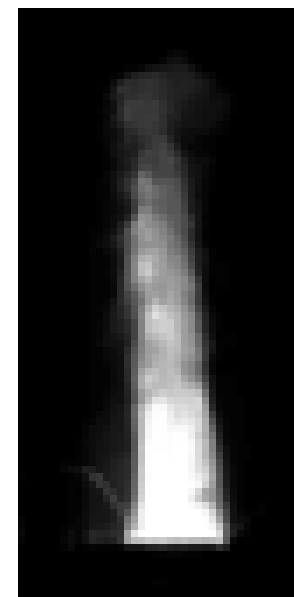
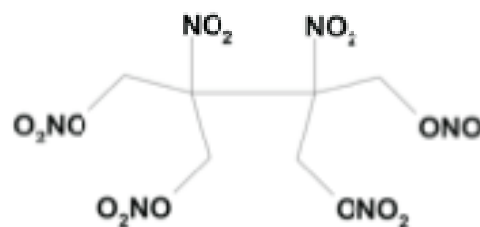


AFOSR/MURI
August 9, 2012

Integrating Nanoscale Particles

Another System

- New melt castable nitrate ester (SMX) desensitized with NC is a high performance (predicted 260s Isp) low smoke propellant
 - Can introduce decorated graphene or cluster composites into SMX/NC
- Also, encapsulation of nanoparticles in AP using crash crystallization has been demonstrated



AFOSR/ARDEC



Janesheski, Groven, and Son, APS 2011

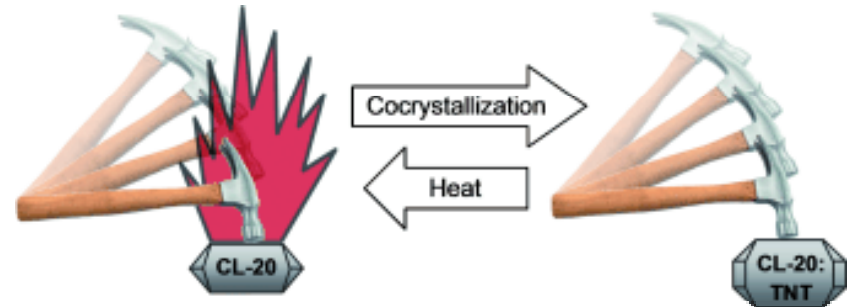


AFOSR/MURI
August 9, 2012

Smart and Functional

How can "switching" be designed in?

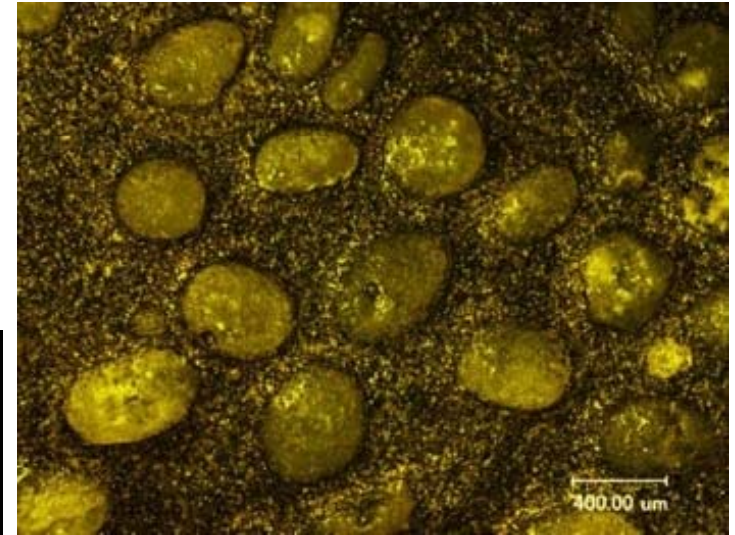
- Bolton and Matzger (2011) developed co-crystallized TNT and CL-20
 - Insensitive co-crystallized form then activated by heat to return it to its high-sensitivity form
- Bunker and Karnes (2004) fabricated coated Fe nanoparticles that activate with temperature
- Piezoelectric fluoropolymers have been formulated in reactives that can be sensitized with charge (Janesheski et al., 2011)
- Similar approaches to the previous work will be explored with our nanoscale composites



Integrating Nanoscale Particles

Propellant Formulations

- Decorated graphene, cluster composites, and MA materials can be added to liquid propellants or formulated into solid propellants

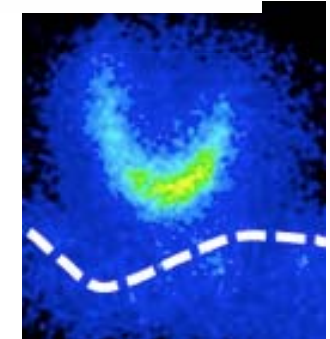
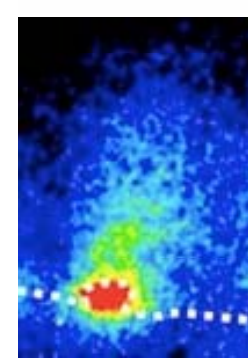
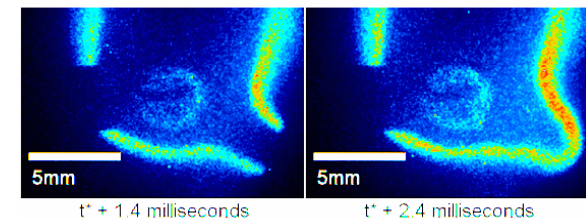
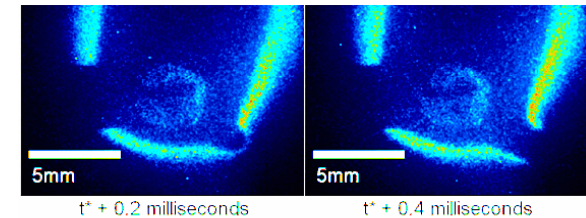
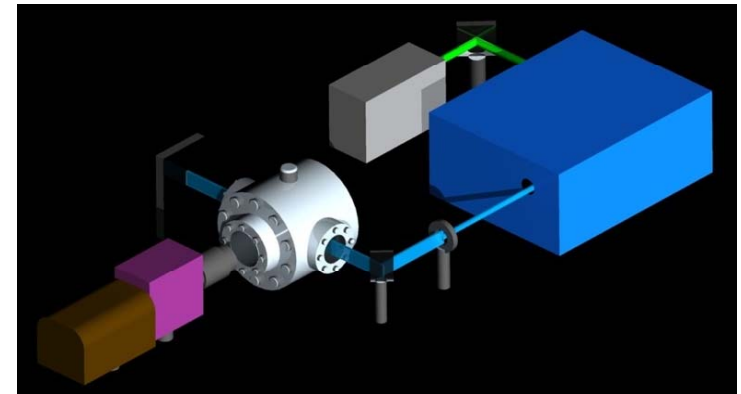


AFOSR/MURI
August 9, 2012

Performance, Aging, Sensitivity, and Processability

Performance

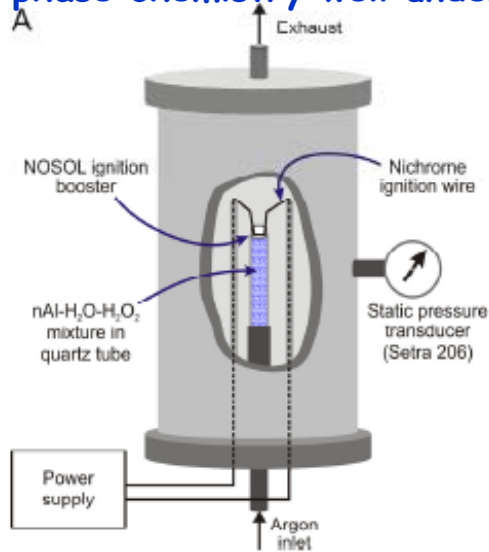
- Combustion characterization (Burning rates of strands or droplets, ignition thresholds, spectroscopic temperature measurement, agglomerate size, high speed visible imaging and OH PLIF)
- Thermal (DSC/TGA, calorimetry, heat capacity, conductivity, fast thermolysis)
- Characterize piezoelectric reactivity properties and other “switching” approaches
- Later in the program, small rocket motors or combustion chamber experiments could be considered



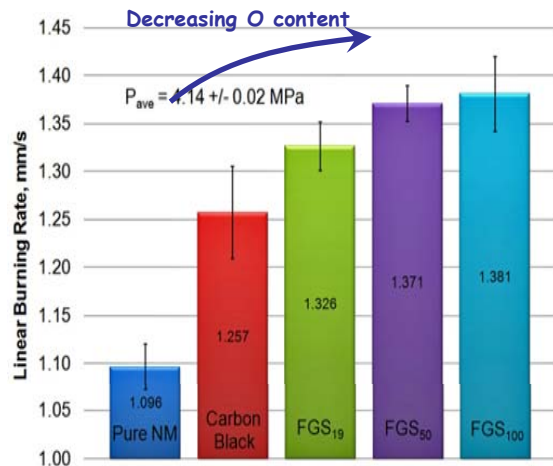
Examples of Analysis and Performance

Liquid Strand Burner: Addition of FGS to Nitromethane

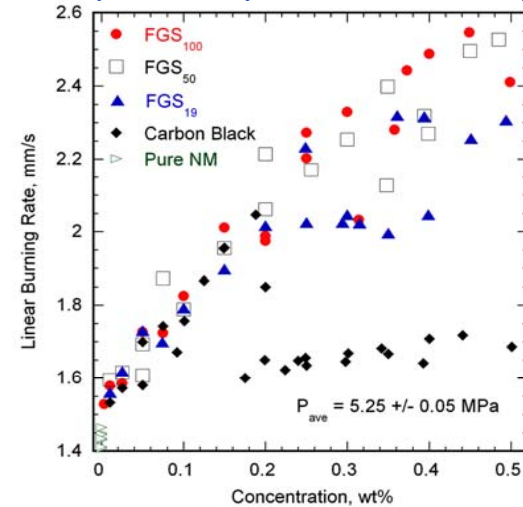
NM gas-phase chemistry well understood; liquid-phase chemistry not important at low pressures



Solids loading ~ 0.05 wt%



Yetter

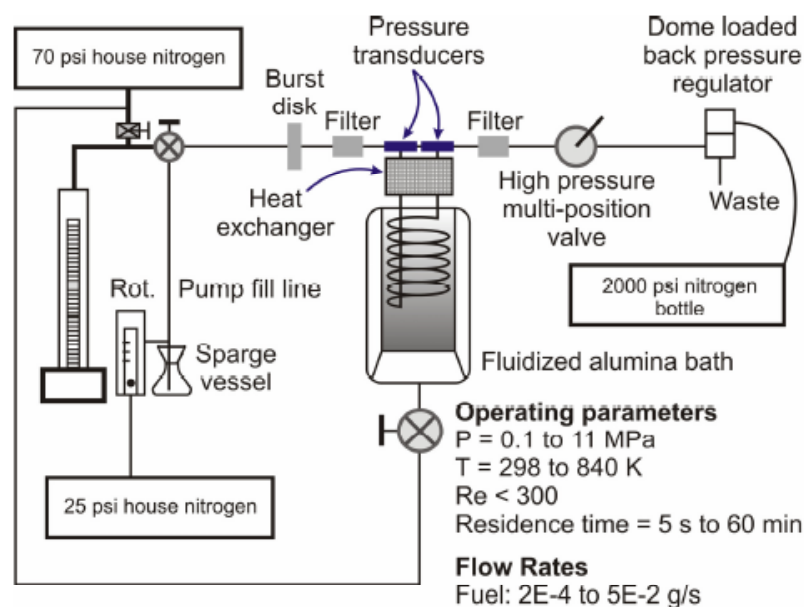


- More reduced FGS is a better accelerant than carbon black or FGS of low C/O (mol/mol).
- Lower deflagration pressure-limit with carbon additives.
- Reduced performance of carbon black and FGS₁₉ at ~0.2wt% may be due to particle aggregation at liquid/vapor interface, preventing passage of particles into vapor phase.
- At low FGS concentrations, the loss of surface defects/surface area lowers the burning rate.

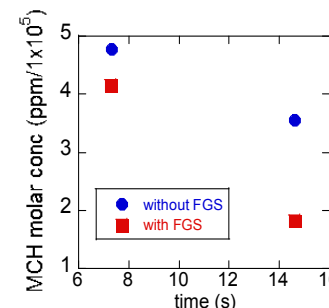
AFOSR/ARRA

Examples of Analysis and Performance

MCH (Methylcyclohexane, Toluene, Hydrogen) Liquid Sub/Supercritical Reactor



- MCH was ~32 % more decomposed with 0.005wt% FGS than without FGS at above conditions.



- Identified components in gaseous products and condensed phase: similar to those without FGS; however, methane (39% increase), ethane (41% increase), ethylene (18% increase), propylene (25% increase), propane (43%) all increased.

Liquid /Particle Mixtures: 0.005wt% FGS in MCH

Reactor Temperature	819.8±1.7 K ($Tr = 1.4$)
Reactor Pressure	651.9±3.2 psig ($Pr = 1.3$)
Reactor Coil Length	6.4 m
Pump flow rate	0.5 mL/min
Reynolds Number	844
Residence time	14.9 sec

Global Kinetic Parameters

Fuel/Additive	E_a (kJ/mol)	A (s^{-1})	R^2
MCH w/FGS19 50 ppm	56.99	4.61E+13	0.99
MCH Alone	73.47	2.38E+17	0.98

Fast Thermolysis of Individual Ingredients and Mixtures (Thynell)

Scientific Issues

Limited understanding of initiation of energetic materials and their interaction with nano-sized materials:

- initiation of decomposition of an individual ingredient can be quite different compared to mixtures of different ingredients,
- increased pressure increases phase change temperatures producing increased role of secondary condensed-phase reactions.
- Example: RDX and TAGzT mixture: RDX begins to decompose at $\square 265^{\circ}\text{C}$ and TAGzT at $\square 240^{\circ}\text{C}$, whereas their mixtures show significant interaction at $\square 200^{\circ}\text{C}$ using fast thermolysis.
- Studies with individual nanocomposite structures and integrated propellants.

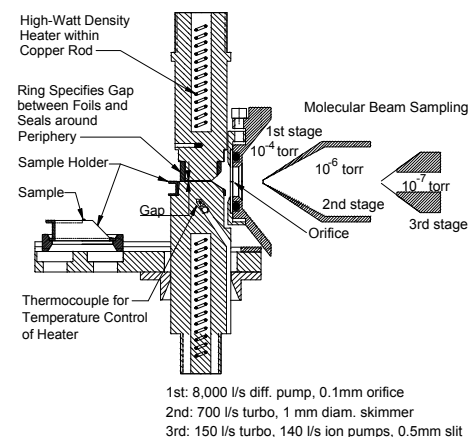
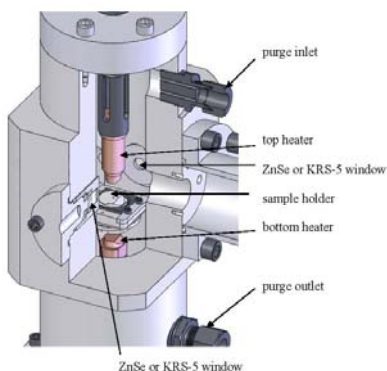
Compliments T-Jump TOF MS (UMD) by extension to high pressures and FTIR analysis.

Anticipated Findings

- Identification of sites on molecules where initiation of decomposition occurs
- In-depth knowledge of intermolecular initiation sites between different molecules
- Information of thermal stability of individual ingredients versus mixtures
- Role of externally applied pressure on initiation, secondary reactions, and release of molecules into the gas phase

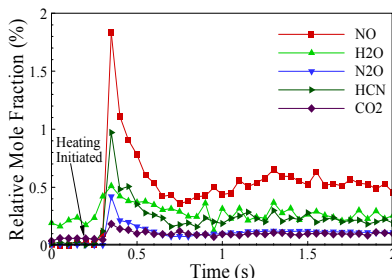
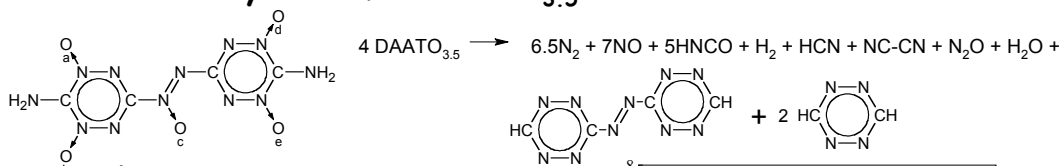
Method of Approach

- FTIR and ToF MS coupled with fast thermolysis (heating rate 2,000K/s) to probe gas-phase species
- FTIR spectroscopy to probe temporal changes in condensed-phase species.

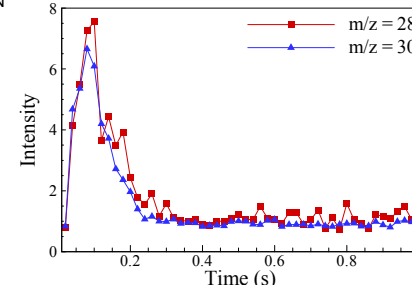


1st: 8,000 l/s diff. pump, 0.1mm orifice
2nd: 700 l/s turbo, 1 mm diam. skimmer
3rd: 150 l/s turbo, 140 l/s ion pumps, 0.5mm slit

Preliminary Data for DAATO_{3.5}

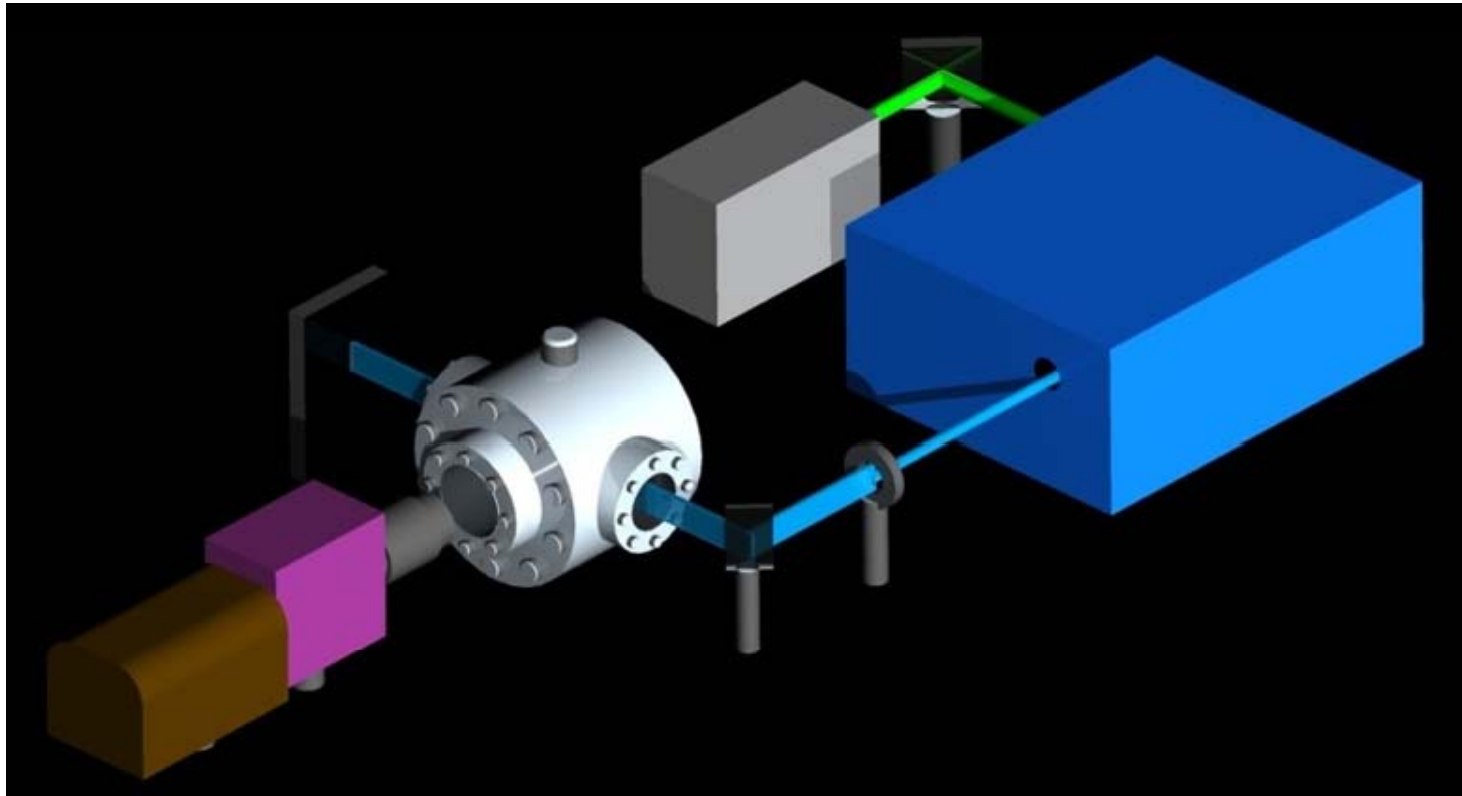


Species evolution of DAATO_{3.5} at 295°C and 1 atm N₂, generated from FTIR



Species evolution of DAATO_{3.5} at 295°C and 1 atm He/Ar generated from ToFMS.

High Speed OH PLIF



- Sirah Credo dye laser pumped with an Edgewave Nd:YAG at 5 kHz
- Up to 0.4 mJ per pulse, 7.8 ns FWHM duration
- Excites $Q_1(7)$ transition of the OH $A^2\Sigma^+ - X^2\Pi$ electronic system near 283.2 nm
- 1-1 and 0-0 band fluorescence detected near 309 nm



AFOSR/SMART

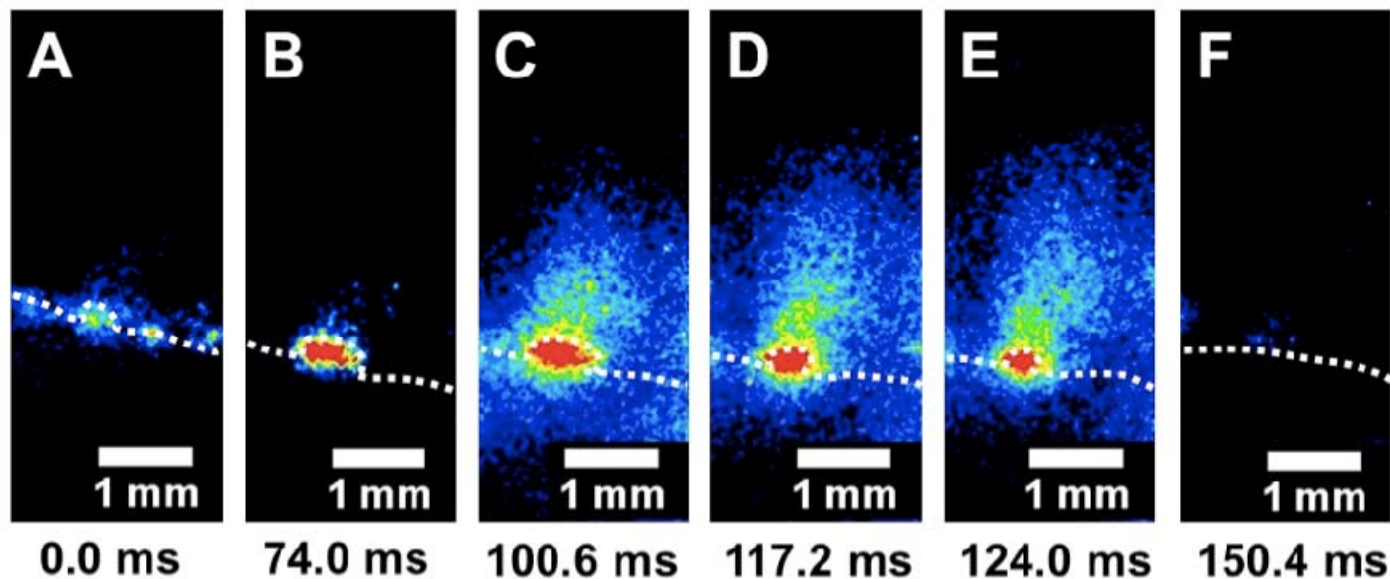


AFOSR/MURI
August 9, 2012

Final Diffusion Flame can be Observed

We've looked at effects of pressure, added catalysts, binder type
Can quantify flame structure affects by the addition of our nanostructured composites

HTPB/AP



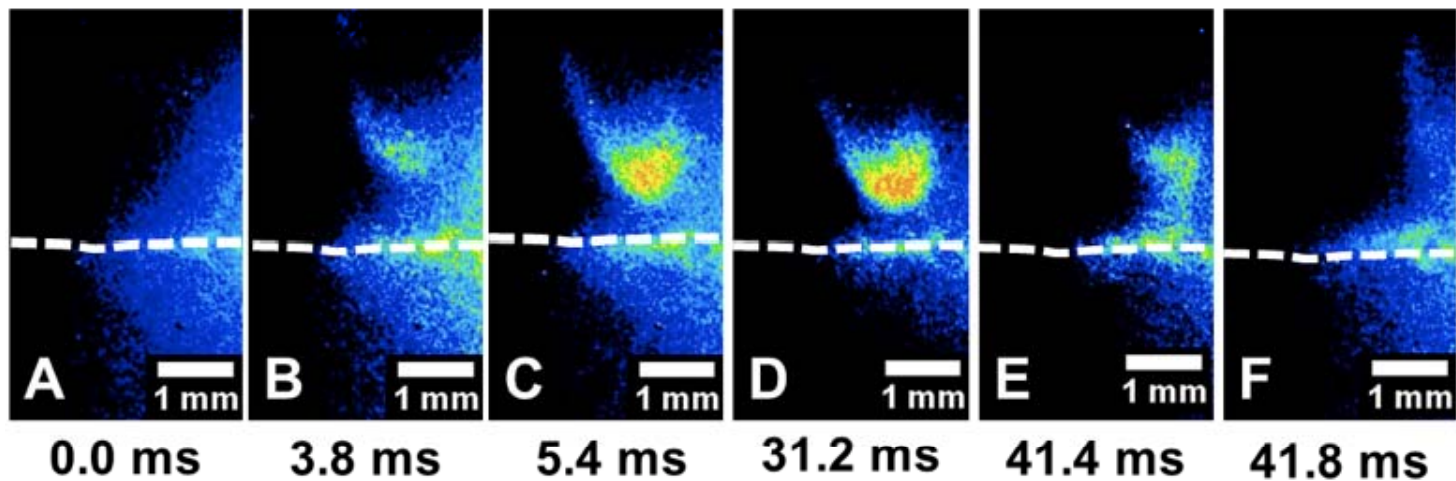
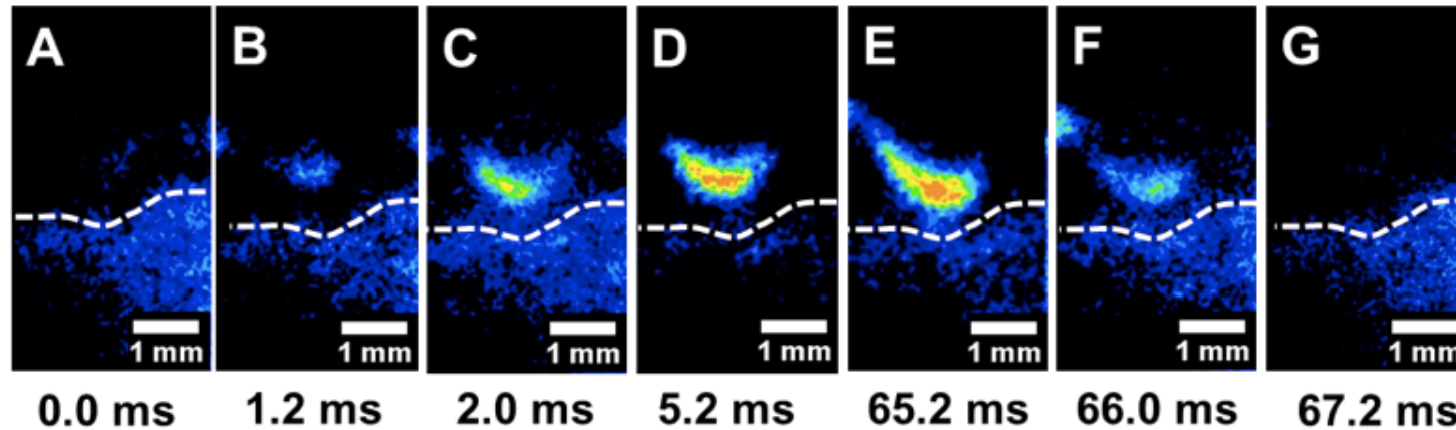
- At lower pressures, the AP protrudes (and fluoresces)
- The final diffusion flame is qualitatively similar to models



AFOSR/MURI
August 9, 2012

Final Diffusion Flame can be Observed

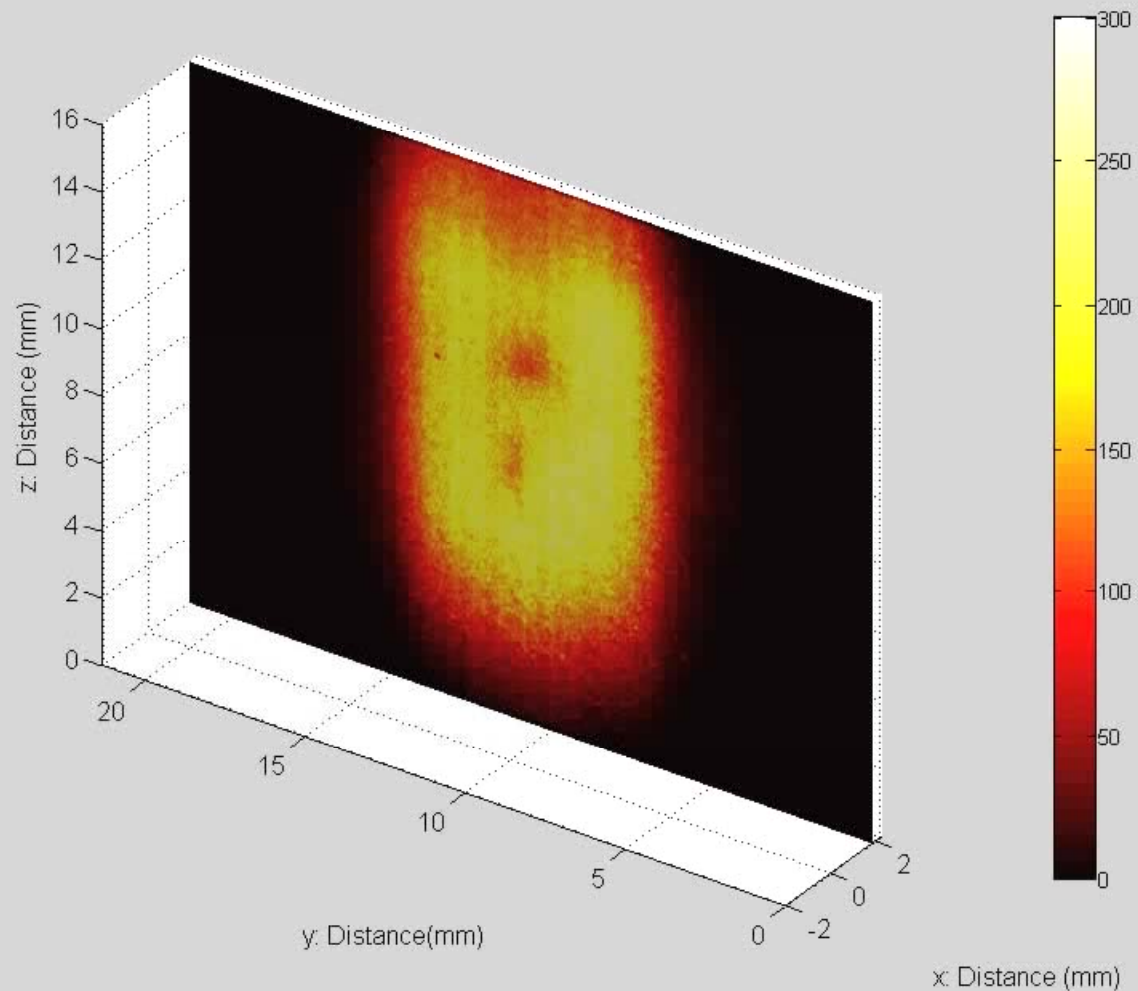
Now, > 6 atm the final diffusion flame surprisingly different from lower pressures (PBAN is similar to HTPB)



3D Time-Varying PLIF

- Using a rotating mirror 3D, time-varying data can be obtained

Laser freq = 5000Hz
galvo freq = 250Hz
sweep distance = 4.33mm
time = $t^* + 0.0$ ms
isosurface threshold = 80

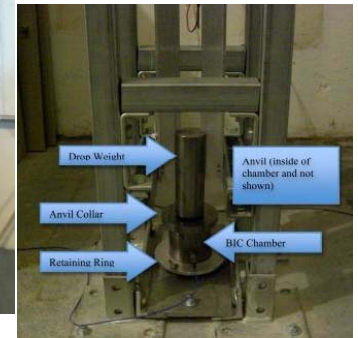


AFOSR/MURI
August 9, 2012

Performance, Aging, Sensitivity, and Processability to be Quantified

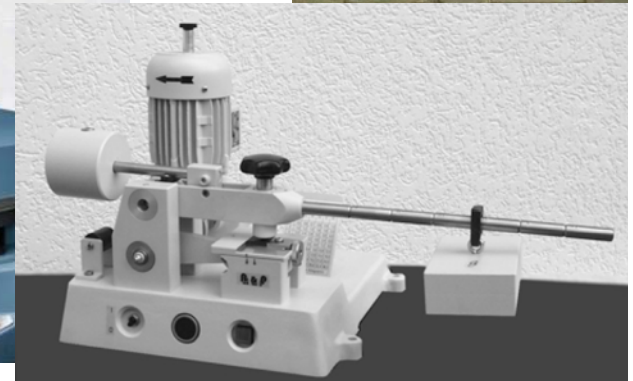
Aging

- Accelerated aging of particles and fabricated materials via controlled elevated temperature and humidity



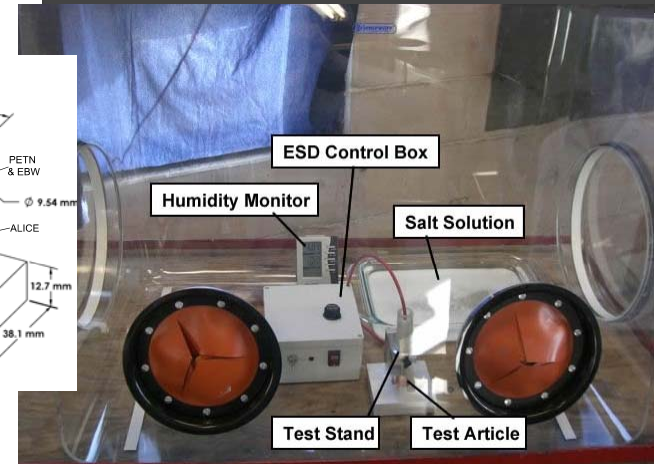
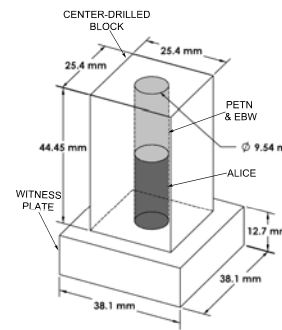
Sensitivity

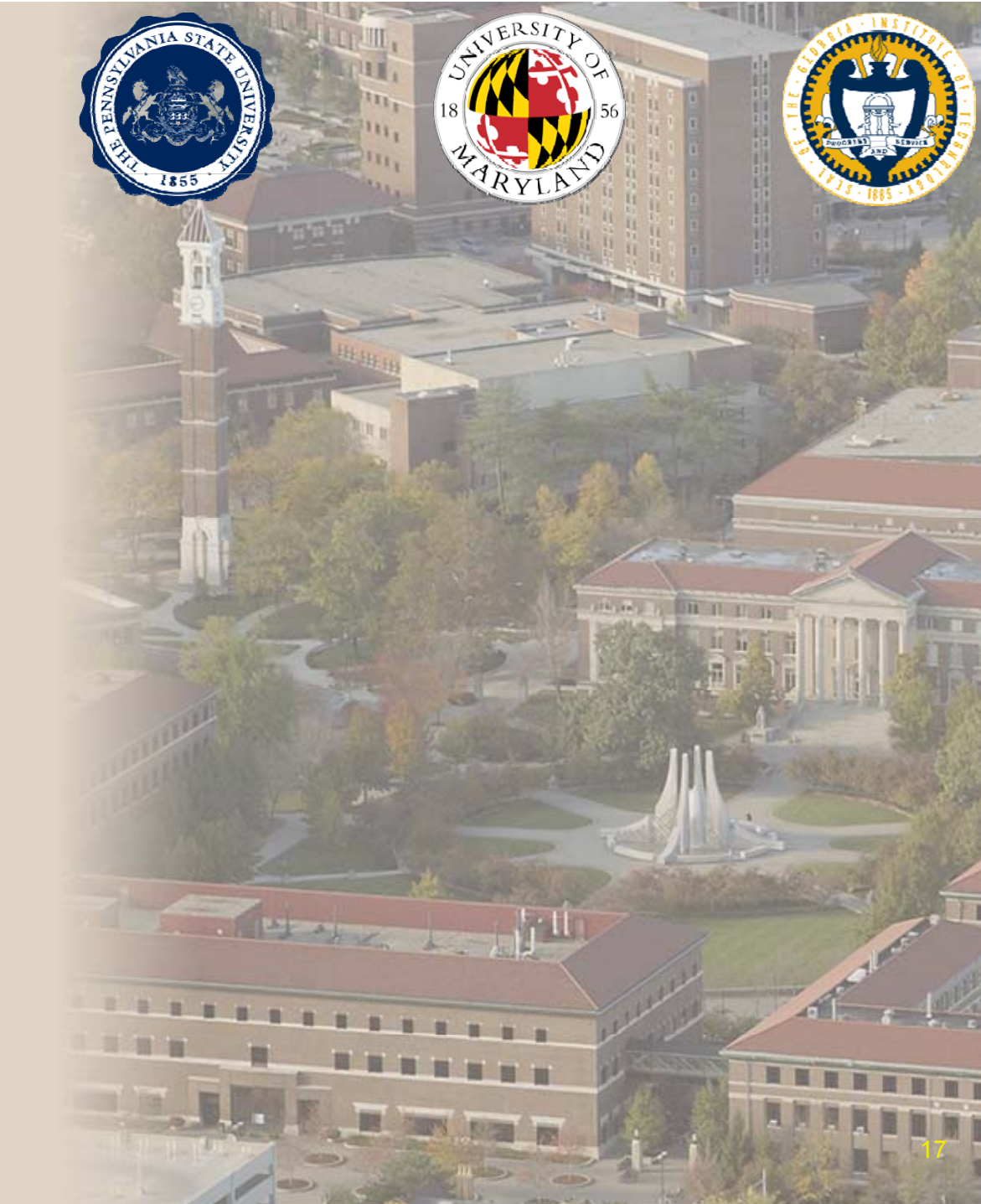
- Thermal, friction, ESD, shock, and impact



Processability

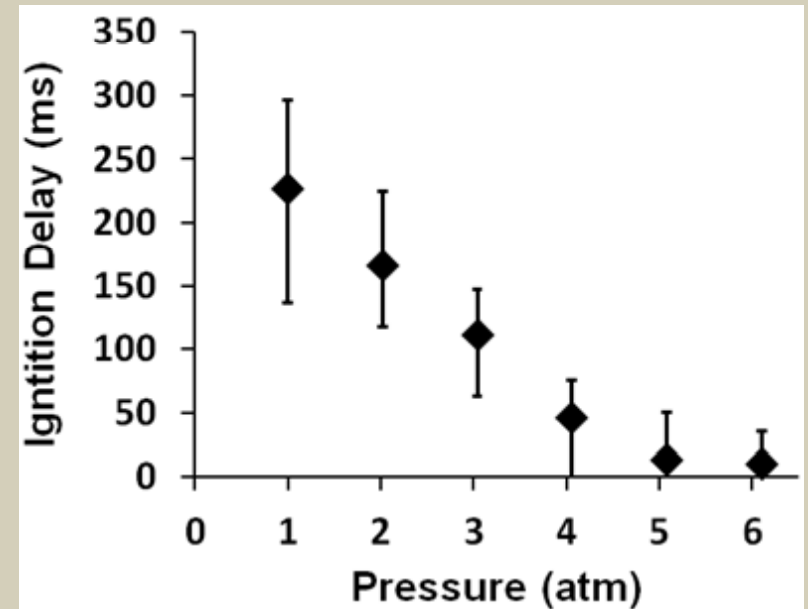
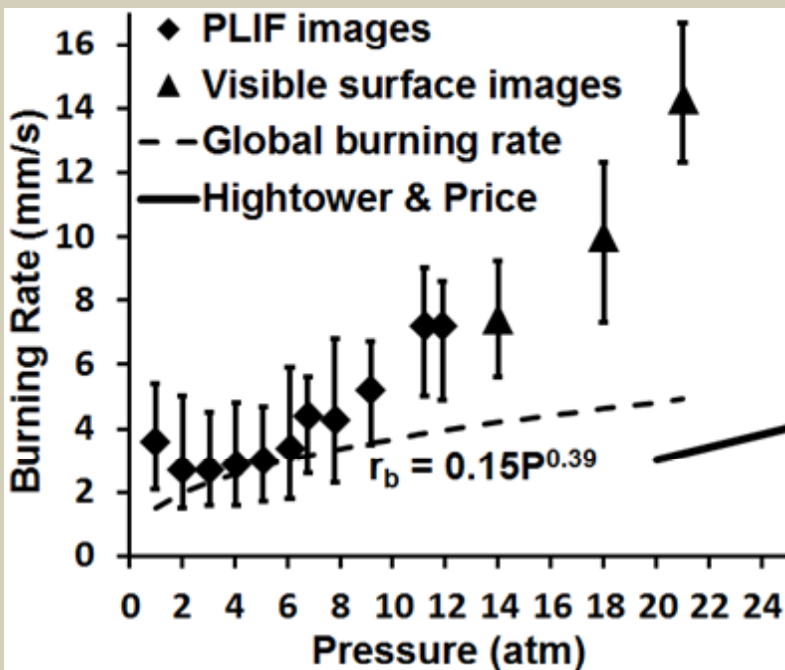
- Viscosity of mixed solid propellant





Crystal Burning Rates and Ignition Delay

- AP particles reach the surface and can exhibit an ignition delay
- Ignition delay was not measurable above 6 atm

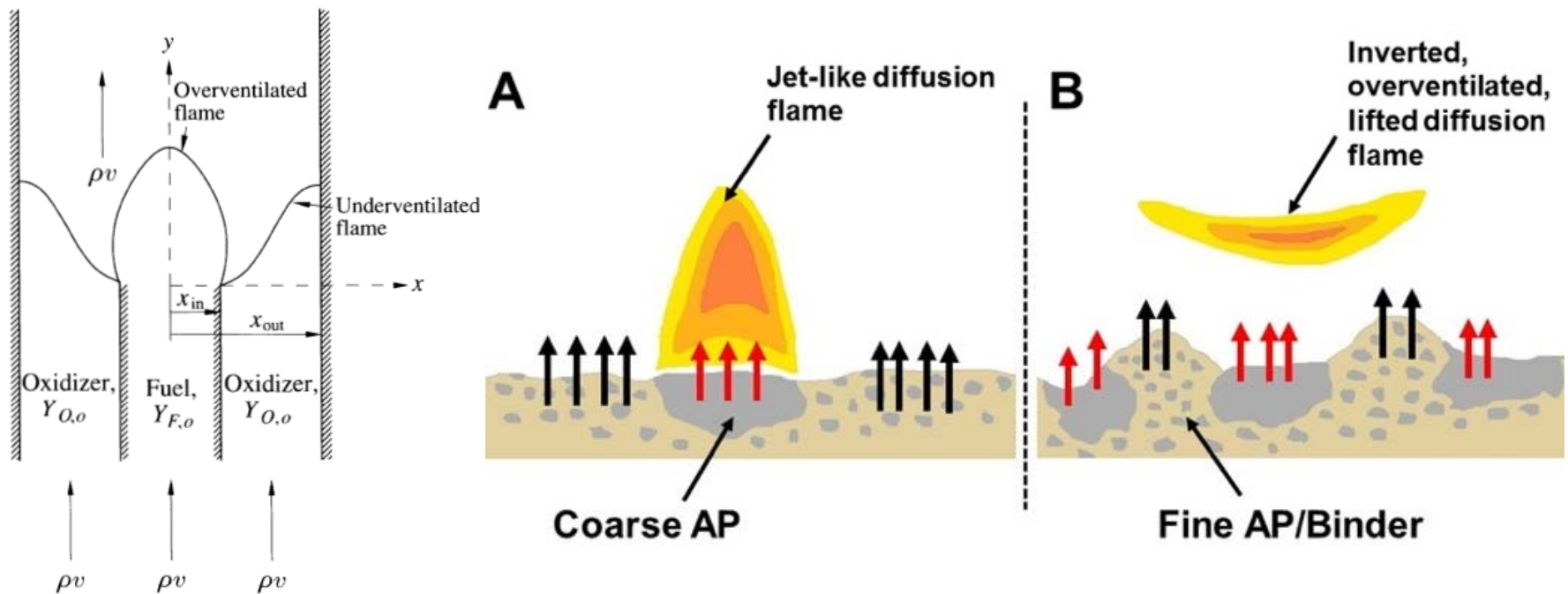


- Coarse AP burned near the low pressure deflagration rate up to 5-6 atm, then abruptly increases
- The effects of additives on the flame details can now be quantified



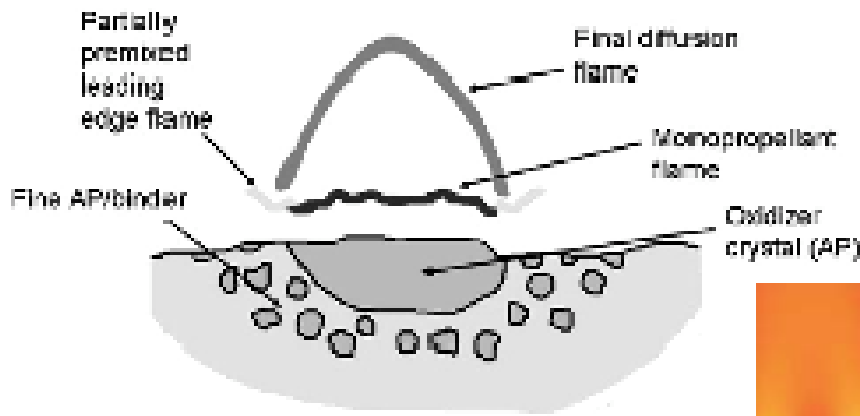
Final Diffusion Flame can be Observed

- Why does the flame structure change?
- At higher pressures the coarse particles burn faster than the surrounding fines/binder
- This blows the flame off the surface (lifted) and for a brief time there is excess oxygen (overventilated)



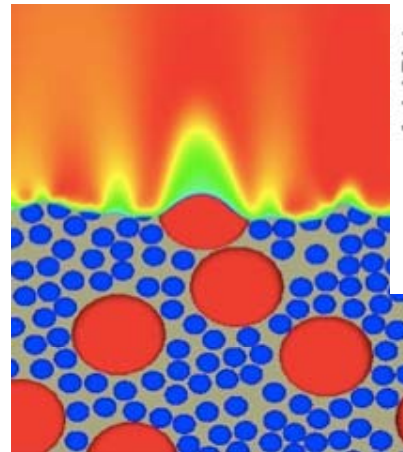
High Speed OH PLIF of AP Composites

Since the 1960s models have been made for AP propellant combustion, but no direct quantification of flame structures

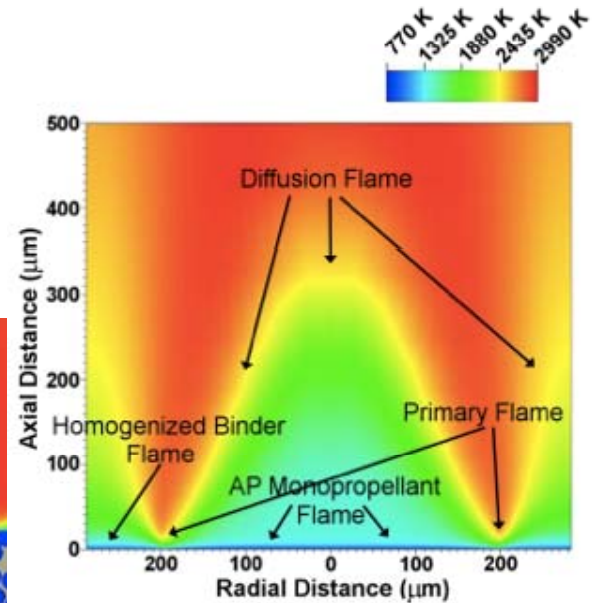


BDP model schematic (Beckstead & others)

These are inverted (or inverse) diffusion flames



Simplified chemistry with complex surface (Jackson and co-workers)



Detailed chemistry model with simplified surface (Gross and co-workers)

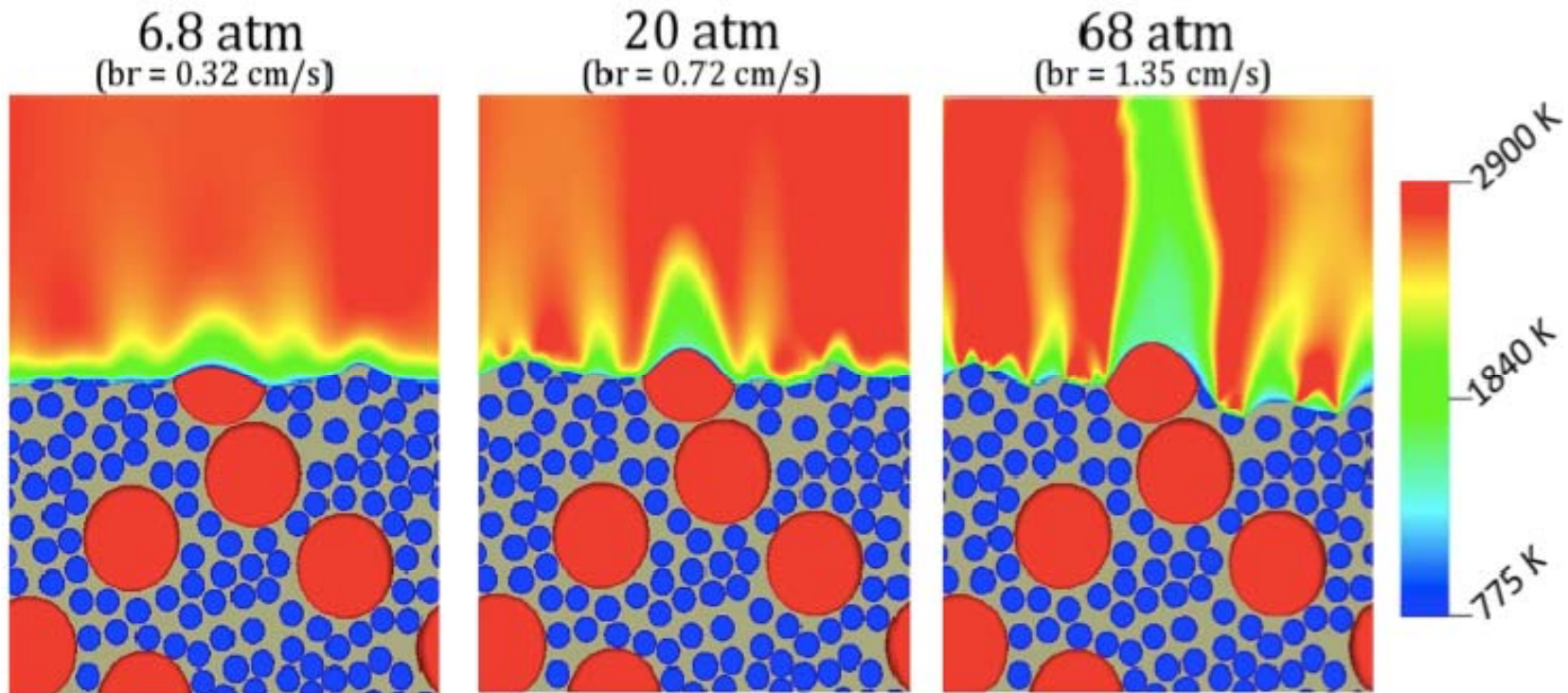
Massa, T.L. Jackson, J. Buckmaster, F. Najjar, Journal of Fluid Mechanics 581 (2007) 1-32.

M.L. Gross, M.W. Beckstead, Combust. Flame 157 (2010) 864-873.



AFOSR/MURI
August 9, 2012

Simulation Does Not Predict This



ROCFIRE code simulation above a simulated propellant grain at various pressures

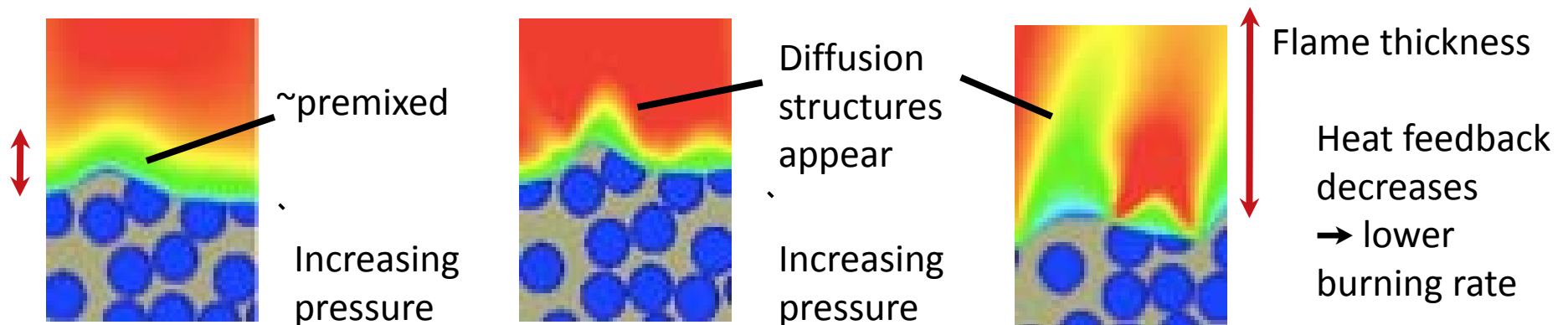
We are collaborating with Jackson and Gross to correct modeling



AFOSR/MURI
August 9, 2012

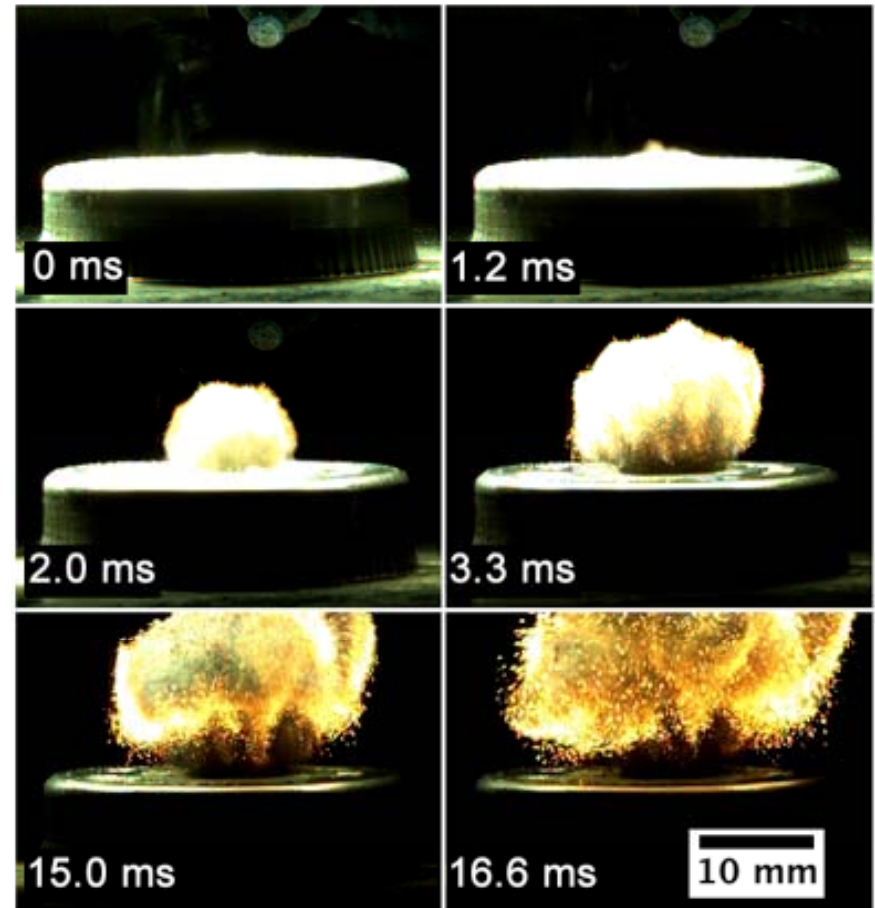
Why is the modeling so wrong?

- At low pressures, the flame above fine AP crystals, to a good approximation, is homogeneous/premixed
- Mixing time is longer than flame/reaction time scales
- Jackson and co-workers treat the fine AP/binder as a homogeneous/premixed flame (i.e., they do not resolve fine AP)
- At higher pressures, the “premixed” flame is closer to the surface
- Adequate mixing time is not available and thicker diffusion flame structures dominate, resulting in burning rates that are slower than predicted using a homogeneous/premixed flame



Disrupted Al Ignition Via Nanoscale Inclusions

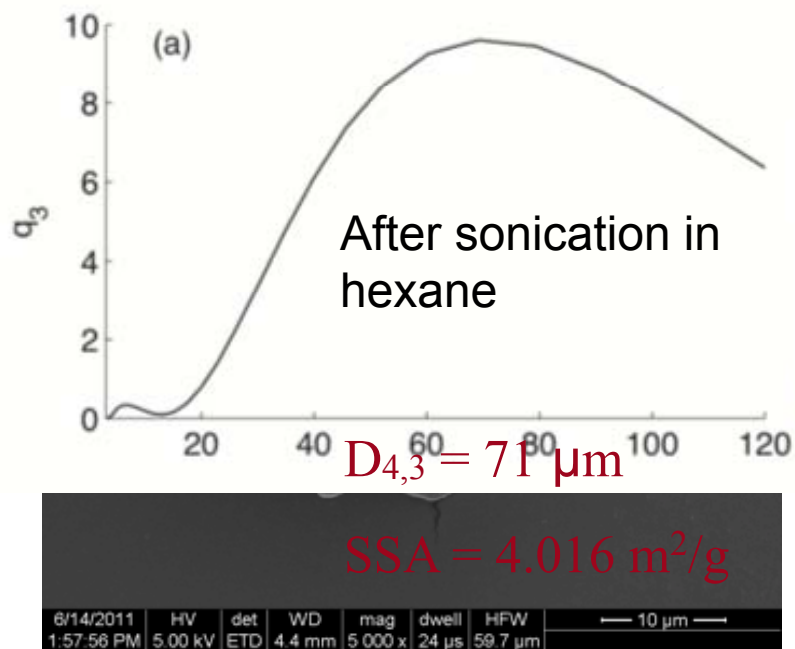
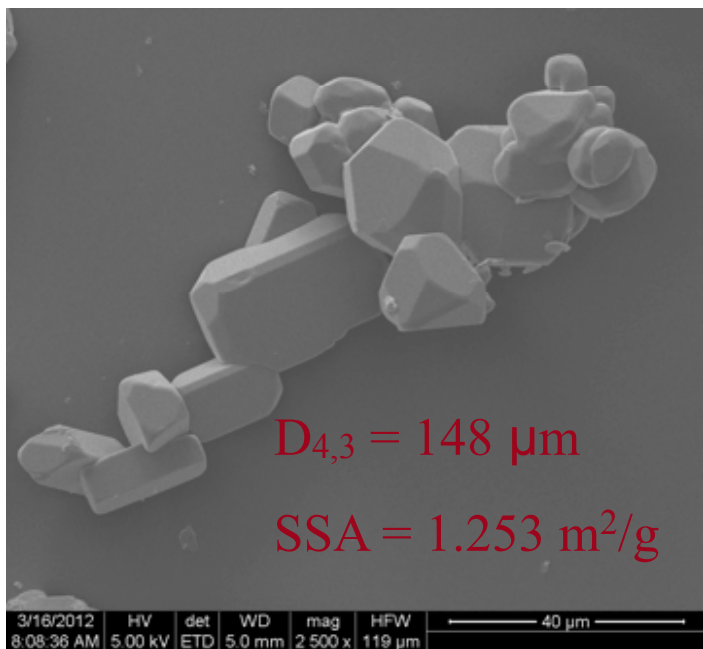
- Al/PMF (poly(carbon monofluoride)) can be made so easy to ignite that it can be ignited by a camera flash



AFOSR/MURI
August 9, 2012

Encapsulation of Nanoscale Particles in AP

Fe₂O₃/AP system studied most, but some nAl/AP Ethyl acetate-acetone antisolvent-solvent system
Successful capture is dependent on antisolvent-to-solvent ratio
Faster crash -> better



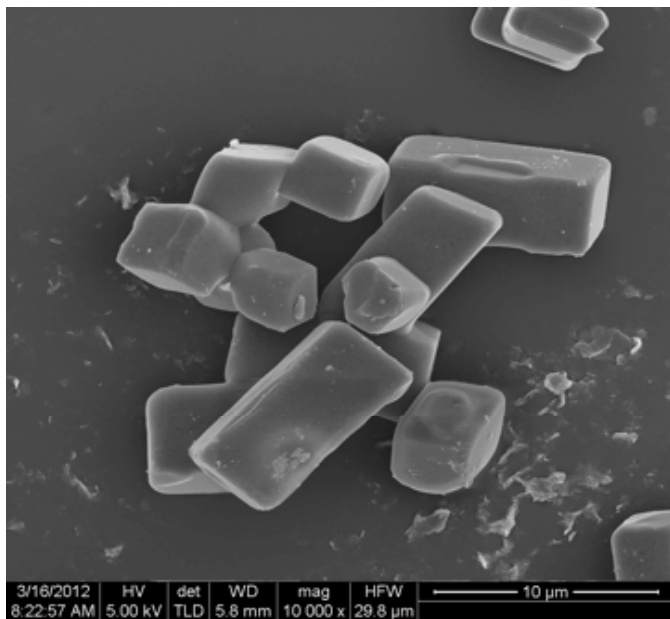
- Scanning electron microscopy of (left) 0.5:1 acetone/ethyl acetate ratio (slow crash) AP, (b) 0.5:1 AP + 1 wt% Fe₂O₃ particles



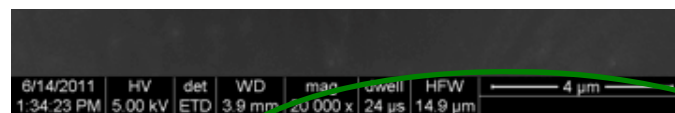
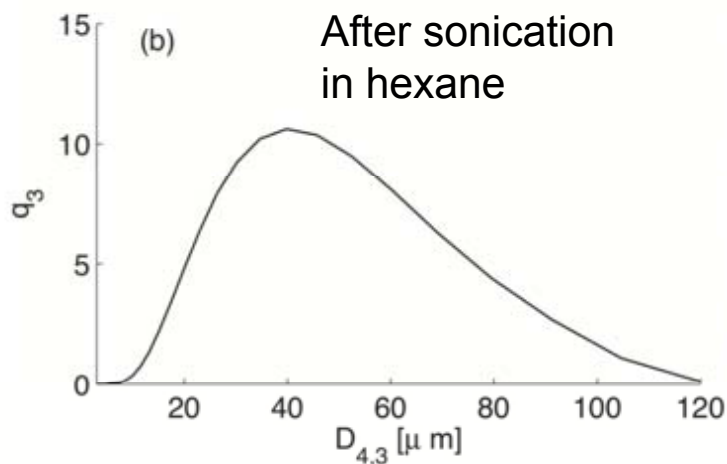
AFOSR/MURI
August 9, 2012

Encapsulation of Nanoscale Particles in AP

$D_{4,3} = 56 \mu\text{m}$ $SSA = 1.087 \text{ m}^2/\text{g}$



$D_{4,3} = 25 \mu\text{m}$ $SSA = 2.596 \text{ m}^2/\text{g}$



Crashed AP, then add 1% $\text{Fe}_2\text{O}_3 \rightarrow D_{4,3} = 14 \mu\text{m}$ $SSA = 11.25 \text{ m}^2/\text{g}$

- Scanning electron microscopy of (left) 3:1 acetone/ethyl acetate ratios (fast crash) AP, (right) 3:1 (fast crash) AP + 1 wt% Fe_2O_3 particles.



AFOSR/MURI
August 9, 2012